Università degli Studi di Ferrara

DOTTORATO DI RICERCA IN
FARMACOLOGIA E ONCOLOGIA MOLECOLARE

CICLO XXVII

COORDINATORE Prof. Cuneo Antonio

BDNF delivery strategies in an experimental model of temporal lobe epilepsy.

Settore Scientifico Disciplinare BIO/14

Dottorando

Dott. Falcicchia Chiara

Tutore

Prof. Simonato Michele

Anni 2012/2014

TABLE OF CONTENTS

Chapter 1. INTRODUCTION

1.1 EPILEPSY

1.1.1 Definition

In October 2012, with *Fact sheet n.999*, the World Health Organization (WHO) has defined epilepsy as "a chronic disorder of the brain characterized by recurrent seizures. Seizures are brief episodes of involuntary shaking which may involve a part of the body (partial) or the entire body (generalized) and are sometimes accompanied by loss of consciousness."
Epilepsy, in general, includes a number of neurological disorders of the central nervous system due to an excessive and hypersynchronous discharge of particular groups of neurons. Different parts of the brain can be the site of such discharges. Seizures can vary from the briefest lapses of attention or muscle jerks, to severe and prolonged convulsions. Seizures can also change in frequency, from less than one per year to several per day.

The word *epilepsy* derives from the Greek verb *epilambanein*, meaning *to be seized, to be overwhelmed by surprise*. This etymology is due to a characteristic feature of this disease, that is, the unpredictability of its seizures. Because of its strong social impact, due to the unpredictability and the violence of the symptoms and to his considerable spread among the population, through the centuries epilepsy has been described and defined in different ways based on knowledge and superstition.
Hippocrates, around the 4th century B.C., was among the first describing epilepsy as an ordinary, and not magical, pathology, with origins in the brain. Since then, several other definitions and approaches alternated in time to describe and treat epilepsy, resulting in the most peculiar and sometimes ludicrous ways to face the problem.
For the first clinical definition of epilepsy, it is necessary to wait 1870, when the neurologist John Hughlings Jackson defined a seizure *"an occasional sudden, excessive, rapid and local discharge of grey matter of the central nervous system."*

Today, it is well known that epilepsy is not a single condition, but a diverse family of disorders, having in common an abnormally increased predisposition to seizures. The International League Against Epilepsy and the International Bureau for Epilepsy define epilepsy as *"a disorder of the brain characterized by an enduring predisposition to generate epileptic seizures and by the neurobiologic, cognitive, psychological, and social consequences of this condition. The definition of epilepsy requires the occurrence of at least one epileptic seizure"* (Fisher et al, 2005).

1.1.2 Epidemiology

Epilepsy affects more than 50 million people worldwide (World Health Organization, 2005), with an estimated 2–3 million living in the United States (Hirtz et al., 2007), 6 million in Europe (World Health Organization, 2010), and at least 40 million in the developing world (World Health Organization et al., 2005), which makes this disease one of the most common neurological disorders in the world.

Incidence of epilepsy is higher in children (0-14 years) and in elderly (>60 years) than in adult individuals (15-59 years). The mean incidence rates of epilepsy in these age groups are, respectively: 82,2/100000 per year – 39,7/100000 per year – 34,7/100000 per year; the total incidence rate is 47,4/100000 per year. Incidence rate for age-specific epilepsy distribution is significantly different. A non significant trend to higher incidence of epilepsy in males compared to females has been reported, showing respectively mean incidence rates of 50,7/100000 per year and 46,2/100000 per year (Kotsopoulos et al, 2002; McHugh and Delanty, 2008). Incidence seems to be higher in males due to the greater exposure to risk factors that cause symptomatic epilepsies. Generally, the median seizure-specific incidence rates are higher for partial (34,4/100000 per year) than for generalized seizures (19,6/100000 per year), but this difference is not significant.

1.1.3 Classification of epileptic seizures

In 1989, the *International League Against Epilepsy* (ILAE) published the International Classification of epilepsies. In the paper, two possible etiological dynamics are presented:

a) *primary or idiopathic etiology:* brain disorder of unknown cause. In fact, most idiopathic epilepsy syndromes are presumed to be due to a genetic cause, but in most cases the specific genetic defect is not known and a family history of epilepsy may not be present.

b) *secondary or symptomatic etiology* with an identifiable lesion in the brain that triggers seizures, like a brain tumor, stroke, viral and bacterial encephalopathies, or other neurological disorders.

Epileptic seizures are divided into two major groups, depending on the site of initiation: partial-onset and generalized-onset seizures **(Fig. 1)**.

Partial-onset seizures refers to a specific and localized origin of the seizures. The symptoms depend on the function of that specific area. If the seizure does not alter consciousness it is known as simple partial. Partial seizures that cloud consciousness are known as complex partial seizures.

Generalized seizures refer to a general involvement of both brain hemispheres in the origin of the seizures. This kind of seizures is usually much more dramatic, given that many of the brain functions are affected at the same time. In many of these types of seizures, the subject will not have any recollection of the seizure afterwards. Generalized seizures may be initiated by a partial-onset seizure (secondarily generalized seizures).

Some seizures, such as epileptic spasms, are of an *unknown type* (Engel, 2006).

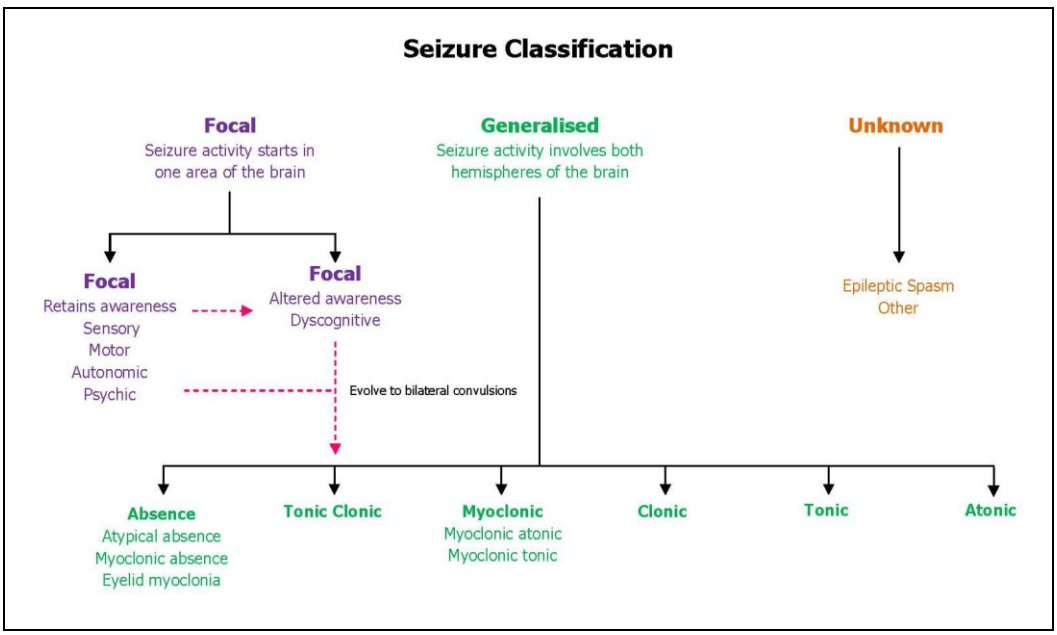

Figure 1: Classification of epileptic seizures.

1.1.4 Treatment

Epilepsy treatment is symptomatic, mainly aiming to control seizure recurrence, and only surgery can be sometimes curative. No currently available drug is capable of preventing epileptogenesis. Since the introduction of bromide as an antiseizure drug in 1857, there has been an impressive expansion of therapies that are clinically effective in decreasing the frequency and severity of seizures in people with epilepsy. This class of symptomatic treatments is widely referred to as ‘‘antiepileptic drugs’’ (AEDs).

AEDs target different biological substrates such as voltage-gated Na^+ channels (e.g. phenytoin and its derivatives), the GABA system (e.g. barbiturates or benzodiazepines) and voltage-gated Ca^{2+} channels (ethosuximide) **(Table 1)**.

NAME	MECHANISM OF ACTION	TRATMENT	ADMINISTRATION	SIDE EFFECTS
Carbamazepine	Regulates sodium channel permeability	Drug of choice for partial seizures. Used also in partial and generalized convulsive seizures.	400-2400 mg	Its common side effects include drowsiness, headaches and migraine, motor coordination impairment and/or upset stomach. Carbamazepine decreases tolerance to alcohol. Less common side effects include cardiac arrhythmias, blurry or double vision and/or the temporary loss of blood cells or platelets (in rare cases can cause aplastic anemia). Additionally, carbamazepine may exacerbate pre-existing hypothyroidism. There are also reports of auditory side effects.
Clobazam	Increases GABA action	Effective on partial seizures	10-40 mg, in association with other AEDs.	Common side effects are ataxia, somnolence, diplopia, dysarthria and rarely gelastic seizures and urticaria rashes.
Oxcarbazepine	See Carbamazepine	See Carbamazepine	600-3000 mg	Oxcarbazepine causes dizziness, drowsiness, blurred or double vision, fatigue and may cause headache, nausea, vomiting and stomach pain, diarrhea, constipation and dry mouth. It can also cause hyponatremia. Concentration loss is also reported to be a frequent side effect. Skin sensitivity to sunlight also may increase.

Levetiracetam	Binds a presynaptic molecule implicated in neurotransmitter release	Used for the treatment of partial seizures and secondarily or idiopathic generalized epilepsies	500-1000 mg, two or three times per day	Side effects include: hair loss; pins and needles sensation in the extremities; anxiety and psychiatric symptoms ranging from irritability to depression; and other common side effects like headache and nausea. It is generally well tolerated but may cause sleepiness, weakness, dizziness, and infection. In children, the most common side effects are sleepiness, accidental injury, hostility, irritability, and weakness.
Tiagabine	Increases GABA action maintaining GABA at synaptic level for longer time.	Used for the treatment of partial seizures and secondarily generalized	30-50 mg, in association with other AEDs.	Its side effects include confusion, difficulty speaking clearly/stuttering, mild sedation, and, in doses over 8 mg, paresthesia in the body's extremities, particularly the hands and fingers.
Gabapentin	Decreases glutamate release	Used for the treatment of partial and secondarily generalized seizures	900-2400 mg, in association with other AEDs.	Most common side effects include dizziness, drowsiness, and peripheral edema (swelling of extremities). Children 3–12 years of age were observed to be susceptible to mild-to-moderate mood swings, hostility, concentration problems, and hyperactivity. Rare side effects are represented by cases of hepatotoxicity. Gabapentin should be used carefully in patients with renal impairment due to possible accumulation and toxicity. It has a carcinogenic potential.
Lamotrigine	Regulates sodium channels	Used for the treatment partial and secondarily generalized seizures, it is also effective for treatment of many kinds of primary or idiopathic generalized seizures	50-600 mg, in association with other AEDs.	Common side effects include headache, dizziness and insomnia. Other side effects may include acne and skin irritation, vivid dreams or nightmares, night sweats, body aches and cramps, muscle aches, dry mouth, fatigue, memory and cognitive problems, irritability, weight changes, hair loss, changes in libido, frequent urination, nausea, and other side effects. In very rare cases, lamotrigine has caused the development of a dangerous rash called Stevens-Johnson syndrome (or SJS).
Phenobarbital	Potentiates the effects of GABA on $GABA_A$ receptors	Still used as AED. It is used to treat generalized convulsive seizures, myoclonus and partial seizures. It is also used in childhood febrile seizures	50-300 mg once a day	Sedation and hypnosis are the principal side effects of phenobarbital. Central nervous system effects like dizziness, nystagmus and ataxia are also common. In elderly patients, it may cause excitement and confusion, while in children it may result in paradoxical hyperactivity.

Phenytoin	Regulates sodium channel permeability	Effective in treating partial and generalized convulsive seizures, particularly partial convulsive seizures.	100-600 mg per day, per os. Intravenous administration is used when patient is in status epilepticus.	At therapeutic doses, phenytoin produces nystagmus, At toxic doses, patients experience sedation, cerebellar ataxia, and ophthalmoparesis, as well as paradoxical seizures. Idiosyncratic side effects are rash and severe allergic reactions. Phenytoin may cause atrophy of the cerebellum when administered at chronically high levels. Phenytoin predisposes patients to megaloblastic anemia and gingival hyperplasia. Phenytoin is a known teratogen and suggested to be carcinogenic. Phenytoin has been known to cause drug-induced Lupus and other dangerous or even fatal skin reactions, such as Stevens-Johnson syndrome and toxic epidermal necrolysis.
Topiramate	Modulates voltage dependent sodium channels.	Used for the treatment of partial and secondarily generalized seizures. It is also effective for treatment of many kinds of primary or idiopathic generalized seizures.	200-600 mg, in association with other AEDs.	The most often reported side effects are tiredness, pins and needles in the fingers and toes, dizziness, lowered sense of feeling in the skin, difficulty with language, nausea, diarrhea, indigestion, dry mouth, weight loss, decrease in appetite, drowsiness, forgetfulness, difficulty with concentration or attention, difficulty in sleeping (insomnia), anxiety, mood swings, depression, changes in taste and vision disorders. Rare side effects are blood clots, blurring of vision and eye pain, reduced sweating and metabolic acidosis.
Valproate	Potentiates GABA inhibitory activity and modulates sodium channel permeability.	Effective for all kind of seizures, it represent the drug of choice for primary generalized seizures and for benign epilepsy with partial seizures	600-3000 mg	Common side effects are dyspepsia and/or weight gain. Less common are fatigue, peripheral edema, dizziness, drowsiness, hair loss, headache, nausea, sedation and tremors. Valproic acid also causes hyperammonemia, which can lead to brain damage. Rarely, valproic acid can cause blood dyscrasia, impaired liver function, jaundice, thrombocytopenia, and prolonged coagulation times. Valproic acid may also cause acute hematological toxicities, cognitive dysfunction and reversible pseudo-atrophic brain changes. It is known as a teratogen.

Table 1: Anti-Epileptic Drugs.

The choice among the different AEDs depends on the semiology of the disease and the management of the treatment is correlated to the containment of seizures: some patients reach the goal by a monotherapy, some others, unfortunately, require polytherapy with the use of two or more AEDs. Monotherapy is desirable because it decreases the likelihood of adverse effects and avoids drug-drug interactions. Other important concerns are the risks related to the potential for teratogenicity, which may limit the use of effective antiseizure medications in women of child bearing potential (AESBSC and ILAE, 2012).

In spite of the numerous AEDs available, several patients are refractory to pharmacological treatments and continue to experience seizures. Indeed, of those who develop epileptic seizures 47% will be controlled with the first AED prescribed, 32% with the second AED, and 9% with the third. Fourth and subsequent AEDs have at most a 5% chance of bringing remission (Duncan, 2007). This leaves around 30% of individuals that have no chances to control their seizures by pharmacological approaches. Therefore it is of central importance to develop new drugs able to contain seizures or even to prevent epileptogenesis. This latter goal could be reached not only by empirical experimentation of new chemical compounds, but also by increasing our knowledge of the complex basis of the pathology.

When drug treatments result ineffective and patients experience refractory seizures, other medical approaches may be applied. These alternative treatments include surgery, vagus nerve stimulation, ketogenic diet.

Epilepsy surgery is an effective and safe alternative form of therapy for selected patients with intractable partial epilepsy. Determining the suitability of the surgical treatment and the best approach always requires a full assessment, which includes video-electroencephalogram (EEG) monitoring, neuropsychological examination, and structural magnetic resonance imaging. In some patients it may be necessary to perform functional imaging tests and intracranial electrode recordings. These tests make it possible to locate the epileptogenic zone. The best surgical results are obtained in patients with small epileptogenic lesions, which can be totally resected. Nevertheless, in many patients in whom complete control is not achieved after surgery, the improvement in seizure control also has a positive impact on their quality of life (Villanueva et al, 2007). Surgery usually reaches 90% of success in healing focal epilepsy.

Intractable epilepsy may also be treated by *vagus nerve stimulation* (VNS). VNS consists of two electrodes embedded in a silastic helix that is wrapped around the cervical vagus nerve. The stimulator is always implanted on the left vagus nerve in order to reduce the likelihood of adverse cardiac effects. The electrodes are connected to an implantable pulse generator (IPG) which is positioned subcutaneously either below the clavicle or in the axilla. The IPG is programmed by computer via a wand placed on the skin over it. In addition, extra pulses of stimulation triggered by a hand-held magnet may help to prevent or abort seizures (Sakas et al., 2007). Pilot study results demonstrated significant reduction in the frequency, intensity, and duration of seizures with chronic, intermittent VNS (Labar et al, 1998). Follow up studies report a mean of 50-60% success for VNS when associated to normal pharmacological treatment (Abubakr and Wambacq, 2008; Milby et al, 2008).

VNS seems also to progressively increase its effectiveness in seizures containment in time (Ardesch et al, 2007; Milby et al, 2008). Very few are the side effects of this practice, comprising hoarseness of voice, cough and sometimes weight loss; most of them are very mild and bearable for patients.

Ketogenic diet represents another side treatment for intractable refractory epilepsy and for epilepsy at large. The efficacy of the diet is independent of the type of seizure and is effective for both generalized and partial seizures at varied ages. The ketogenic diet has been widely used as a treatment for drug-resistant childhood epilepsy since the first reports of its beneficial action in seizure control. Although the exact mechanism of action is still unclear, the high fat and restricted carbohydrate content of the diet is thought to mimic the biochemical response to starvation, when ketone bodies become the main fuel for the brain's energy demands. The diet has been shown to be effective in retrospective and prospective observational studies: more than half of children who were treated showed a greater than 50% reduction in seizures, and many were seizure free after only 3 months (Neal et al., 2008).

The diagnosis of epilepsy is essentially based on a detailed history of the clinical manifestations such as onset and course of the crisis, duration and frequency of the same, as well as any concomitant causes and analysis of the EEG pattern. An isolated seizure does not imply a diagnosis of epilepsy, as it can occur in normal people, such as in children aged less than five years during fever above 38°C (benign seizures). Occurrence of seizures without massive provocation is therefore an essential factor for the diagnosis. In practice, it is often impossible to fulfill this criterion, because information about a patient's seizures is usually anamnestic and the EEG is mostly interictal. Thus the diagnosis of epilepsy is not as easy as it might seem at first sight.

Among epileptic syndromes, temporal lobe epilepsy (TLE) is the most common in adults, and affects at least 20% of all patients with epilepsy.

1.1.5 Temporal Lobe Epilepsy

Temporal lobe epilepsy (TLE) was defined in 1985 by the ILAE as a condition characterized by recurrent seizures originating from the medial or lateral temporal lobe. Mesial temporal lobe epilepsy (mTLE) arises in the hippocampus, parahippocampal gyrus and amygdale, lateral temporal lobe epilepsy (lTLE) arises in the neocortex on the outer

surface of the temporal lobe of the brain. TLE is frequently associated with hippocampal sclerosis, reactive gliosis and synaptic rearrangement (Thom et al., 2009).

Seizures may involve only one or both lobes, giving rise to simple partial, complex partial or secondarily generalized seizures. About 40 to 80% of people with TLE also perform repetitive, automatic movements (called automatisms), such as lip smacking and rubbing the hands together. As seizures usually involve areas of the limbic system that control emotions and memory, some individuals may have problems with memory, especially if seizures have occurred for more than 5 years. However, these memory problems are almost never severe. Seizures occur often after an initial insult like an infection, stroke or trauma, vascular malformation or prolonged febrile seizures; a genetic cause is less frequent. Between the initial insult and the onset of the crisis, a latency period called "epileptogenesis" occurs, with changes in structure and physiology of the brain tissue (**Fig. 2)**.

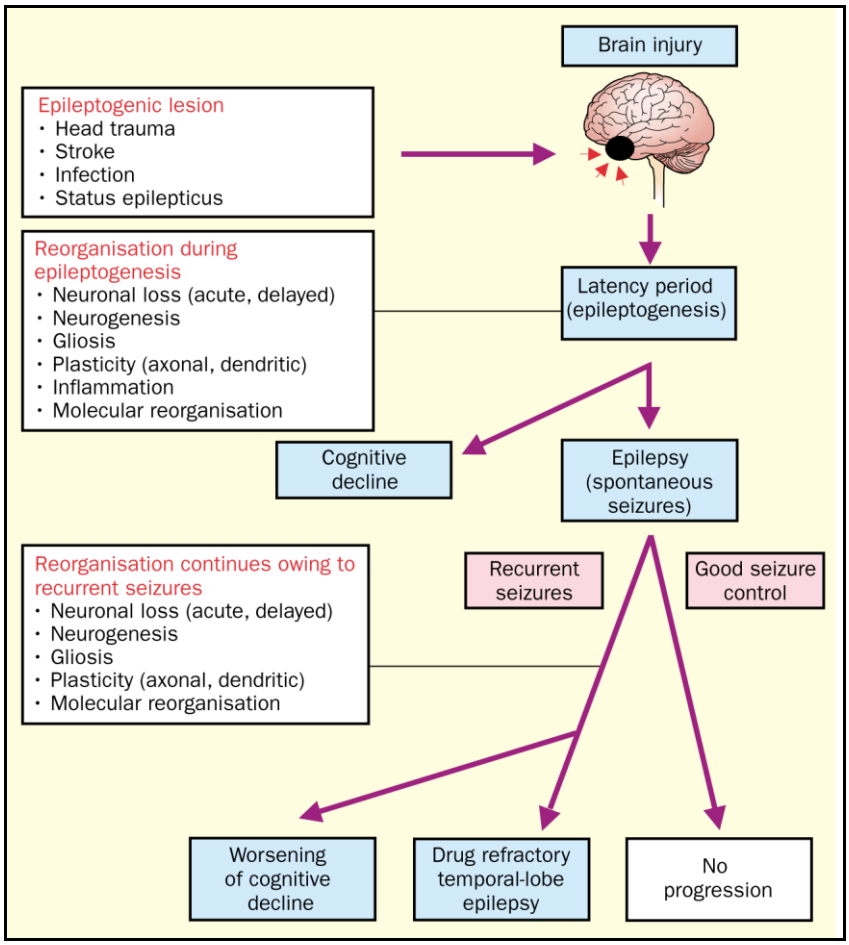

Figure 2: Epileptic process in symptomatic temporal-lobe epilepsy (Pitkänen, 2002).

Existing AEDs are used to control seizures, but up to 40% of patients will fail to respond (Kwan and Brosie, 2000). This is particularly true of TLE, the most pharmacoresistant of the epilepsies, where continuation of seizures contributes to ongoing problems with work and social activity, as well as increased personal health risks. For some individuals, neurosurgical resection of the temporal focus is often the only remaining course, while many others are deemed unsuitable for surgery. Furthermore, current AEDs have little influence on the underlying pathophysiology and there has been little success in directly targeting the underlying molecular processes (Pitkänen and Lukasiuk, 2011). Status epilepticus (SE), or perhaps even brief, recurring seizures can precipitate neuronal loss and contribute to density/volume decline in patients (Fujikawa et al., 2000). Such decline is associated with other comorbidities, including depression. Given these admissions, the cell and molecular processes underlying epilepsy and epileptogenesis constitute a high research priority. For this, animal models are of central importance.

1.1.6 Experimental models of TLE

The study of epilepsy cannot be performed only in humans because of several different reasons, from ethical issues to practical inapplicability, from unavailability of controls to high costs of human research. Epilepsy models for studying epilepsy are principally used for three reasons:

1. to understand basic mechanisms underlying the pathology;
2. to devise new approaches for diagnosis;
3. to test new drugs or new therapies.

Of course, uncovering the basic mechanisms underpinning the disease will help develop new diagnostic, therapeutic and preventive approaches. Models of epilepsy are the best instruments on which innovative experimental approaches for diagnosis and therapies can be tested. Human studies can give a big support, but preliminary data are normally retrieved from in vitro and in vivo experiments.

Epilepsy models should be created or prepared in order to faithfully reproduce the diversity of human epileptic conditions. Therefore, several different models have been developed. On the other hand, some experimental approaches model only some of the manifestation of epilepsy (epilepsy equivalent) allowing only the investigation on a particular symptom and

not on the whole complex picture. In any event, this gives the opportunity to study an aspect of the disease.

Induced models of epilepsy consist in the application of chemical, electrical or damaging insults on a healthy brain, in order to transform that brain in an ill one, capable to display features of the epilepsy in study.

Chemical model of epilepsy	**GABA**	Pentylentetrazole
		Bicuculline
		Picrotoxin
		Glutamic Acid Decarboxylase (GAD) inhibitors
		Beta carbolines and convulsant benzodiazepine Ro 5-3663
		GHB (gamma-hydroxy-butyrate)
	Excitatory Amino-Acid	Kainic acid
		Quisqualic acid/alfa-amino-3Hydroxy-5-Methyl-4-Isoxasole Propionic acid
		N-Methyl-D-Aspartic acid (NMDA)
		Homocysteine, homocysteic acid
	Acetylcholine related substances	Pilocarpine and litium-pilocarpine
	Other drugs	Strycnine
		Aminophylline
		Insulin induced hypoglycemia
		Ay-9944
	Inhalants	Fluorothyl
	Topical application	Metals (cobalt, zinc, antimony, aluminia cream, iron
		Antibiotic (penicillins and cephalosporins)
		Tetanus toxin
Electical model of epilepsy	Electroshock seizures	
	Local electrical stimulation	
	Electrical kindling	
	Self sustaining status epilepticus by Perforant Path stimulation	
	Self sustaining status epilepticus by Amigdala stimulation	
	Focal status epilepticus by perforant path stimulation in anesthetized rats	
	Continuous hippocampal stimulation	
Lesion model of epilepsy	Cortical freeze lesion model	
	Antiproliferative agents (5-azacytidine, methyl-mercury, nitrosureas and carmustine)	
	Methylazoxymethanol acetate (MAM) model	
	In-Utero irradiation as a model of cortical dysplasia	
	Hypoxia-induced seizures and hypoxic encephalopathy in neonatal period	
	Lateral fluid percussion brain injury	
	Chronic Partial Cortical Isolation model	
	Head Trauma: haemorrhage-Iron Deposit	
	Stroke	
Others	Complex febrile seizures – experimental model in immature rodents	
	Infection induced seizures	Model of neurocysticercosis
		Model of herpes virus infection
	Rasmussen's encephalitis model	

Table 2: Induced model of epilepsy (classification based on the tools used to develop the models).

For TLE, the pilocarpine model is an highly isomorphic model, described for the first time in 1983 by Turski and colleagues (Turski et al., 1983). In this model, administration of

pilocarpine induces a status epilepticus (SE) characterized by tonic-clonic generalized seizures, followed by a latent period of seizures free behavior and by a chronic period, with the occurrence of spontaneous recurrent seizures (SRSs).

In detail: within 5 minutes from the injection, animals begin to be motionless, display oro-facial movements, salivation, eye blinking, twitching of vibrissae and yawning. Discontinuous seizures are initially observed, and then about 60% of the animals develop SE (Cavalheiro et al., 1991). All behavioral changes are correlated with a high voltage, fast electroencephalographic (EEG) activity that appears to originate in the hippocampus and to propagate to the amygdala and the neocortex (Turski et al., 1983).

SE spontaneously remits 5-6 hours after pilocarpine administration but is generally stopped at 2-3 hours with anticonvulsant drugs such as diazepam. In the following 1-2 days, animals may experience some occasional, self-limiting generalized seizures of less than 1 min duration (Mazzuferi et al., 2010).

The duration of the latent period that follows varies in function of the dose of pilocarpine (Liu et al., 1994), the duration of SE (Lemos and Cavalheiro, 1995; Fujikawa, 1996, Biagini et al., 2006, Goffin et al., 2007), the strain and age of the animal (Biagini et al., 2006; Goffin et al., 2007). Cavalheiro et al. (1991) identified a mean duration of 14.8 days. During the latent phase, tissue rearrangements related to epileptogenesis occur (Dalby and Mody, 2001; Pitkänen and Sutula, 2002).

The chronic period follows epileptogenesis and, as previously mentioned, is characterized by the appearance of spontaneous recurrent seizures. Severity of seizures can be scored using a scale developed in 1972 by Racine (Racine, 1972) and recently revised (Veliskova, 2006). The scale is reported in **Table 3**. It uses numbers from 1 to 6 to define seizure classes: the first three stages are representative of partial seizures, stages from 4 to 6 are representative of generalized ones. SRSs begin as partial seizures and become secondary generalized. The recurrence of seizures is almost regular throughout the lifetime of the animal and appears in a clustered manner, in cycles peaking every 5-8 days or more (Goffin et al., 2007; Arida et al., 1999). Seizures frequency is higher during the diurnal period (Arida et al., 1999), with an incidence of 67% (Arida et al., 1999; Goffin et al., 2007). In 90% of the cases, the EEG during seizures is characterized by a dysrhythmic activity that starts in the hippocampus and spreads to the neocortex, usually lasting less than 60 seconds (Cavalheiro et al., 1991).

Classes	*Features*	
1	Staring and mouth clonus	***Partial***
2	Automatisms	
3	Monolateral forelimb clonus	
4	Bilateral forelimb clonus	***Generalized***
5	Bilateral forelimb clonus with rearing and falling	
6	Tonic-clonic seizures	

Table 3: Racine's classification of seizures. Scores from 1 to 3 are representative of partial seizures, the last three of generalized ones

Pilocarpine exerts its effects by binding M1 muscarinic receptors, resulting in alterations in Ca^{2+} and K^{+} current (Segal, 1988). The high concentration of intracellular Ca^{2+} promotes the release of glutamate from presynaptic termini that, in turn, provokes SE. Once activated, seizures are subsequently maintained by activation of NMDA receptors. Glutamate, acting on AMPA/KA receptors, allows the entrance of Na^{+} into the cells and, as a consequence, the Mg^{2+} ion that blocks NMDA receptor is removed. Excessive activation of NMDA receptors leads to a massive entrance of Ca^{2+} into the postsynaptic cells and induces excitotoxic effects and cell death.

Recent observations have shown that activation of cholinergic neurons may not be the only factor triggering pilocarpine SE. Marchi et al. (2007a, b) suggested that pilocarpine induces an early focal damage to the blood-brain barrier (BBB) in regions highly sensitized to cholinergic agonists, and this may contribute to the development of seizures, facilitating the entrance into the brain of blood-borne factors (e.g. K^{+}).

Moreover, a peripheral activation of the immune system has been hypothesized to play a role, because high levels of serum IL-1β have been found after injection of pilocarpine. High concentrations of the pro-inflammatory cytokine is known to cause sudden rapid changes in excitability of both inhibitory and excitatory neurons (Yang et al., 2005).

As reviewed by Curia et al. (2008), age, strain, gender, dose, association with other drugs to reduce mortality or collateral effects, are variables that have to be carefully controlled to obtain a reliable model of the pathology. The lack of a standardized protocol has led some investigators to criticize this model. However, it continues to be used in many laboratories because easy, rapid and highly homologous to the human disease, involving the same

mechanisms and brain areas and displaying the same pattern of responsiveness to AEDs observed in TLE patients.

1.2 EPILEPTOGENESIS

Many acquired epilepsies have an identifiable cause, such as head trauma, an episode of status epilepticus (SE), a stroke, or a brain infection (Pitkanen and Sutula, 2002). It is thought that these insults set in motion a cascade of neurobiological events that, in time, will lead to the occurrence of spontaneous seizures and to the diagnosis of epilepsy. This phenomenon is termed "epileptogenesis". In other words, epileptogenesisis is the process by which a previously normal brain becomes epileptic. The cellular alterations underlying epileptogenesis include neurodegeneration, neurogenesis, axonal damage or sprouting, dendritic remodeling, gliosis, recruitment of inflammatory cells into brain tissue, angiogenesis, alterations in extracellular matrix, and acquired channelopathies (**Fig. 3**).

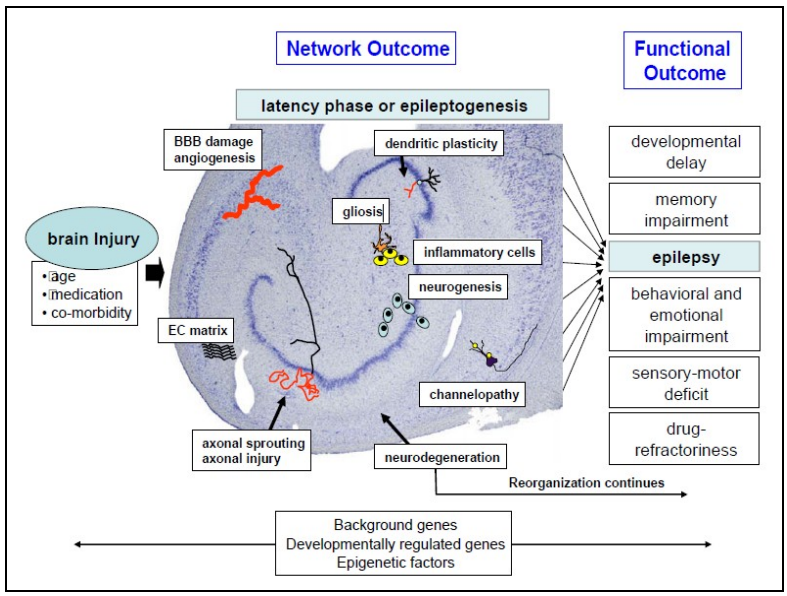

Figure 3: cellular alterations occurring during the epileptogenic process (Pitkänen and Lukasiuk, 2009).

Importantly, recent experimental and patient data suggest that molecular and cellular changes triggered by an epileptogenic insult can continue to progress after the epilepsy diagnosis, even though they might qualitatively and quantitatively differ at various phases of the epileptic process (Pitkänen and Lukasiuk, 2011). These neurobiological data raise

the question of whether the term "epileptogenesis" should be extended to also include disease progression (Pitkänen, 2010). Thus, not only the prevention or delay of epilepsy but also seizure modification (less frequent or shorter seizures, milder seizure type, change from drug-resistant to drug-responsive) and cure would be considered to be clinically relevant endpoints for antiepiletogenesis studies (Pitkänen and Lukasiuk, 2011).
The seizure-free period between an epileptogenic insult and the first spontaneous seizure is referred to as the "latent period" and may last from weeks to years. Epileptogenesis may depend on genetic and/or acquired mechanisms. Genetic influence is thought to be strongest in idiopathic epilepsies, whereas mechanisms of circuitry reorganization after a brain insult are more extensive in acquired epilepsies. However, the functional consequences of a brain injury always depend on the genetic background (Pitkänen and Lukasiuk, 2009).

1.2.1 Genetic and epigenetic mechanisms of epileptogenesis

Over 13 genes associated with human epilepsy have been identified so far and at least 33 single gene mutations in mice have been linked to an epileptic phenotype.

Benign familial neonatal convulsions (BFNC), generalized epilepsy with febrile seizures plus (GEFS+) and autosomal dominant nocturnal frontal lobe epilepsy (ADNFLE) are three idiopathic diseases in which gene mutations code for mutated voltage-gated or ligand-gated channels. In particular, mutations in BFNC were identified in genes for potassium channels, KCNQ2 and KCNQ3 (Singh et al., 1998; Biervert et al., 1998). These mutations are responsible of a loss of function that leads to a decrease in size of the potassium current. It has been suggested that even a moderate reduction (20-25%) of function may be associated with epilepsy (Schroeder et al., 1998).
GEFS+ is associated with a point mutation in the genes coding for the β-subunit (SCN1B) or for the α1-subunit (SCNA1A) of a voltage-gated sodium channel (Wallace et al., 1998; Escayg et al., 2000). *In vitro* studies suggest that the mutation results in defective inactivation of the sodium channel, which could lead to failure to limit the sustained repetitive firing of a depolarized neuron (McNamara, 1999).

ADNFLE begins clinically in childhood and patients have brief, nocturnal seizures with motor features. Mutations affect genes coding for nicotinic cholinergic receptors (Steinlein et al., 1997; Phillips et al. 1998) and result in decreased Ca^{2+} flux through the receptor, which may lead to a reduction in the amount of GABA released from presynaptic terminals, and trigger seizures via synaptic disinhibition (Kuryatov et al., 1997).

PME (progressive myoclonus epilepsies) is a group of rare single-gene epilepsies characterized by myoclonus, generalized tonic-clonic seizures and progressive neurological dysfunction mainly in the form of dementia and ataxia (Berkovic et al., 1986). Among these, the Unverricht-Lundborg disease (ULD) and the Lafora disease (LD) are the best characterized. Genetic mutations lead to deficit of two proteins, cystatin B and laforin respectively, that result in epilepsy (Acharya, 2002).

Other changes in gene expression occur without affecting the DNA sequence but by chemical modification of DNA or chromatin: these include DNA methylation and alterations in the methylation or acetylation status of histones. These mechanisms are termed *epigenetic*. Seizure or SE-induced histone modifications have been reported for the promoters of a number of genes, including those involved in neuronal plasticity such as c-fos, c-jun and CREB (Sng et al., 2006). Recently, it has been proposed that aberrant promoter methylation is an important pathogenic mechanism underlying epileptogenesis. Specifically, increased levels of promoter methylation was shown in surgically-resected specimens from patients with TLE (Kobow and Blumcke, 2011). Deacetylation of histones at the GluR2 promoter leads to decreased gene expression, resulting in facilitation of epileptogenesis (Sanchez et al., 2001). A greater understanding of these mechanisms may open new therapeutic windows for difficult-to-treat epilepsies. In addition, epigenetically active pharmacologic compounds may be recognized as novel anticonvulsant (and, potentially, antiepileptogenic treatments), which may rapidly advance to clinical application (Kobow et al., 2012).

1.2.2 Acquired postinjury mechanisms

In addition to SE, various other types of brain insults, such as traumatic brain injury (TBI), stroke and tumors, can trigger the epileptogenic process. The common trait of all these

insults is the ability to induce a specific set of cellular alterations. Although these cellular alterations may be different in different models and in different patients, commonly identified features include neurodegeneration, neurogenesis, gliosis, neuroinflammation, axonal sprouting, dendritic plasticity, angiogenesis and changes in the extracellular matrix. These alterations are accompanied by a variety of molecular changes that can lead, in addition to epilepsy, to other functional impairments such as developmental delay or memory, emotional and behavioral impairment (Pitkänen and Lukasiuk, 2009).

1.2.2.1 Neurodegeneration

Areas damaged in TLE typically include the hippocampus, but may also extend to extrahippocampal regions, such as the entorhinal and pyriform cortices or the amygdala. The severity of the seizures directly determines the extent of brain damage (Ben-Ari and Dudek, 2010).

The hippocampal circuitry is fundamental for information processing, as disorders affecting this brain region result in impaired cognitive functions. The normal hippocampus consists of subfields. The dentate gyrus (DG), a tightly packed layer of small *granule cells*, and a series of *Cornu Ammonis* (CA) areas: CA4 (inside the DG), CA3, a very small zone called CA2, CA1. The CA areas are all characterized by densely packed pyramidal neurons. The areas that follow CA1 in the neuronal pathway that runs across the hippocampus are the subiculum two ill-defined areas called the presubiculum and parasubiculum, a transition to the cortex proper (the entorhinal area of the cortex).

The intrahippocampal circuitry consists of a trisynaptic excitatory pathway. First, perforant path axons from the entorhinal cortex (EC) project to the granule cells in the outer molecular layer (ML), next the mossy fiber axons of the granule cells innervate the pyramidal cells in the CA3 area, then the Schaffer collateral axons of CA3 pyramidal cells project to the pyramidal cells in the CA1 area (**Fig. 4**). Each of these subareas also contains complex intrinsic circuitry and extensive longitudinal connections. Further, mossy fibers and the perforant path also innervate GABAergic neurons and glutamatergic mossy cells in the hilus, which project to granule cells. Within the hippocampus, the flow of information from the EC is largely unidirectional, with signals propagating through a series of tightly packed cell layers: DG, CA3, CA1, then the subiculum, then out of the hippocampus and back to the EC.

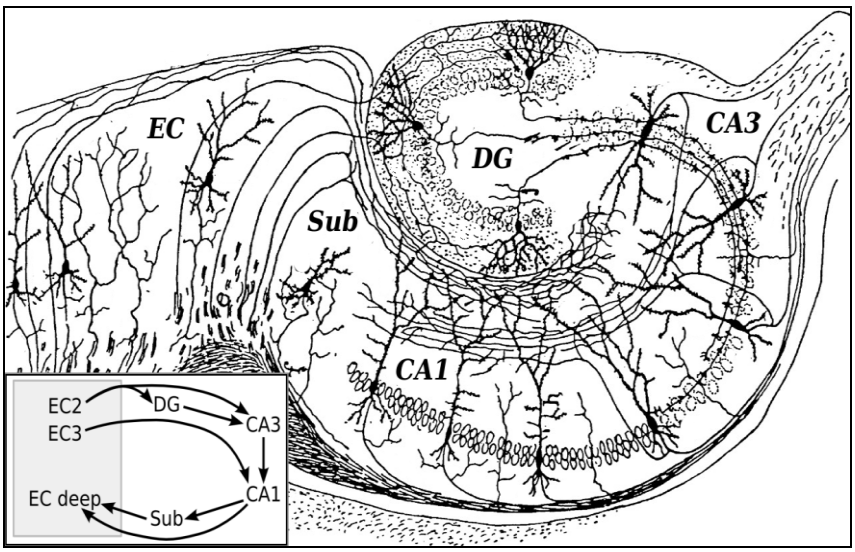

Figure 4: Schematic representation of hippocampal circuitry.

In an epileptic hippocampus, several degenerating cells are identified in CA1 and CA3 pyramidal cell layer and in the hilus, with milder damage in CA2 pyramidal layer and in granule cells. During the last decades, several studies on the human epileptic temporal lobe tissue have shown that these pathophysiological changes are not identical in all patients (Blumcke et al., 2013). This pattern is also reproduced in several animal models, including the pilocarpine model: pronounced cell loss in these regions, accompanied by edema, is observed 3 days after the injection of the alkaloid (Paradiso et al., 2009). The molecular mechanisms that underlie the development of hippocampal sclerosis are still unclear, although some studies suggest that alterations in gene expression in the hippocampus may play a role (Van Gassen et al., 2008). However, cell death is believed to be the initiating event that leads to an excitatory neuronal circuitry and to epileptic seizures (Bhowmik et al., 2014).

1.2.2.2 Neurogenesis

Abnormal hippocampal neurogenesis has emerged as another important feature of TLE. Neurogenesis is a process of generation of new neurons in the central nervous system through division of neural stem cells (NSCs) and neuronal differentiation of newly born cells. Although most of the neurogenesis occurs during development, certain regions of the brain maintain neurogenesis throughout life. These include the subgranular zone (SGZ) of the DG in the hippocampus and the subventricular zone (SGZ) lining the lateral ventricles (Kuruba et al., 2009). Within the DG, progenitors that divide throughout life are found in a 50-100 μm zone just beneath the layer of granule cells (hence SGZ) that also contains the

processes of adult neurons and glia (**Fig. 5**).

A great fraction of these new cells differentiate into granule cells of the DG, migrating up into the granule cell layer (GCL), extending dendrites into the dentate molecular layer, and projecting axons into the dentate hilus and CA3 stratum lucidum. Over time, these newly added granule cells incorporate into the functional hippocampal circuitry through establishment of granule cell specific afferent and efferent synaptic contacts.

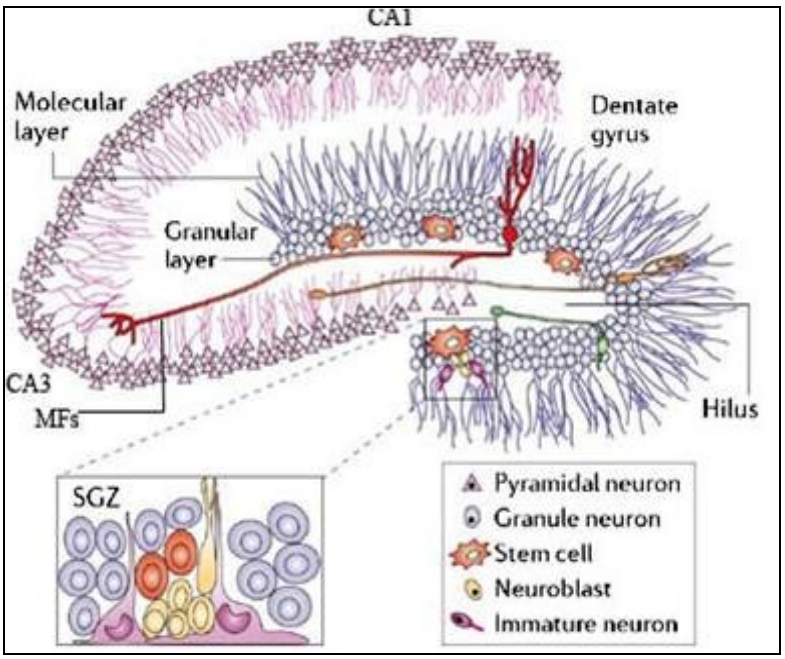

Figure 5

The extent of hippocampal neurogenesis in the adult brain is not static, as it responds to both physiological and pathological stimuli though the net result of a particular stimulus varies depending on the activation of positive or negative regulators. For instance, physical exercise or exposure to enriched environment positively enhances the amount of hippocampal neurogenesis through up-regulation of multiple positive regulators (Kuruba et al., 2009).

One of the most robust stimuli that increase neurogenesis appears to be seizures. Acute seizures or status epilepticus abnormally increase the amount of hippocampal neurogenesis and induce aberrant migration of a significant fraction of newly born neurons into the dentate hilus and in the molecular layer, as well as the projection of axons from newly-born neurons into the dentate molecular layer. Altogether, these events lead to a significant synaptic reorganization in the hippocampus (Ashok, 2014). The precise reasons for the aberrant migration of newly born cells are still being examined. A study supports the

involvement of reelin, a migration guidance cue that promotes appropriate migration of newly born neurons into the GCL. Since reelin is produced by interneurons that are typically lost in TLE, its deficiency after acute seizures is thought to favor ectopic, aberrant migration and integration of newborn cells into the dentate hilus (Gong et al., 2007). A contribution may derive also from an aberrant glial scaffold (probably due to gliosis) that may guide new neurons into the hilus and not toward the molecular layer (Shapiro et al., 2005). Studies in animal models revealing increased hippocampal neurogenesis in epilepsy are consistent with studies on tissues from patients in the early phase of TLE (Blümcke et al., 2001).

Another pathophysiological feature of the epileptic hippocampus that may be related to abnormal neurogenesis is granule cell dispersion (GCD) to the hilus and inner molecular layer, which is present in 40-50% of the patients (Kralic et al., 2005). Studies suggest that these aberrantly migrated granule cells are hyperexcitable and integrate abnormally (Gong et al., 2007).

1.2.2.3 Dendritic plasticity and changes in the extracellular matrix

Postinjury tissue remodeling is also characterized by the loss of dendritic spines, changes in their morphology and reduction of branches. These alterations may affect the availability of various receptor types as well as their stoichiometry and, thus, compromise the information flow from afferent inputs. Another important change in dendritic plasticity is correlated with neurogenesis. In epileptic conditions, newly generated granule cells present hilar basal dendrites (HBDs) that persist in the mature cells integrating into synaptic circuits and, being furnished with spines, probably contribute to additional recurrent excitatory circuits (Spigelman et al., 1998; Ribak et al., 2000). Moreover, in epileptic rats, HBDs are significantly longer and form a dense plexus in the hilus as compared to control animals in which the majority of the dendritic processes from newborn cells are orientated along the SGZ-GL border (Shapiro et al., 2005).

Alterations in postinjury remodeling of neuronal circuits are accompanied by changes in the extracellular matrix (ECM). A large number of enzymes contribute to ECM degradation and rearrangement, in particular the tissue-type and the urokinase plasminogen activator (tPA and uPA), their inhibitors TIMP-1 and -2, anf metalloproteinases appear to be involved (Lukasiuk et al., 2006).

1.2.2.4 Neuroinflammation and gliosis

It has become clear over the past two decades that the brain is immunologically active. The brain innate immune response to injury or excessive neuronal activity is orchestrated mainly by its resident microglial and astrocytic populations, but neurons also play a key role (Vezzani et al., 2013).

Several lines of evidence demonstrate a link between the activation of inflammatory pathways and neurodegenerative diseases, including epilepsy. Interesting, inflammatory reactions occur not only in epileptic disorders characterized by an inflammatory pathophysiology, but also in TLE or in tuberous sclerosis, raising the possibility that inflammation may be a common factor contributing or predisposing to the occurrence of seizures and cell death, in various forms of epilepsy with different etiologies. Increased markers of inflammation have been found in plasma and cerebrospinal fluid after recent tonic-clonic seizures and in brain tissue obtained from patients surgically treated for drug-resistant epilepsies (Crespel et al., 2002; Peltola et al., 2002). Inflammatory processes are not only present in the chronic epileptic brain but some of these pathways are also upregulated following an epileptogenic injury, and they often persist during the latent phase that precedes spontaneous recurrent seizures. This evidence has generated the testable hypothesis that brain inflammation, in addition to its established contribution to ictogenesis, may play a role in the development of the epileptogenic process (Vezzani et al., 2013). However, the role of neuroinflammation is controversial. Some authors consider immune reactions in the CNS a protective, adaptive and beneficial endogenous response – similar to the classic response to infection. This is supported by the evidence that released cytokines can induce the synthesis of growth factors that can promote repair of the CNS (Elkabes et al., 1996) or stimulate antioxidant pathways (Wilde et al., 2000). Moreover, activated glial cells can operate as scavengers, removing potentially harmful debris. Neurons as well as astrocytes are affected by the initial insult and recurrent seizures. Following stressful stimuli, astrocytes upregulate the glial fibrillary acidic protein (GFAP) and its cell body and processes show hypertrophy. This process is called reactive gliosis and is present in several acute and chronic CNS diseases. Further, the organization of astrocytes in non-overlapping spatial domains can be lost during recurrent seizures, which could worsen pathophysiology (Oberheim et al., 2008).

1.2.2.5 Mossy fibers sprouting (MFS)

Mossy fiber sprouting has been the subject of extensive research and controversy since it was first described more than two decades ago. The hypotheses concerning this phenomenon are based largely on evidence derived from Timm staining of the inner molecular layer of the dentate gyrus in humans and animal models that have undergone injury-induced epileptogenesis (Dudek et al., 2004). Axonal plasticity is associated with synaptic activity and, therefore, the ability of recurrent epileptic bursts to induce sprouting of axonal branches is not surprising. One hypothesis has been that neuronal injury leads to the formation of new axon collaterals of dentate granule cells (i.e., mossy fiber sprouting), which form recurrent excitatory synaptic connections with other granule cells whose proximal dendrites are in the inner molecular layer of the dentate gyrus (Pitkänen and Sutula 2002; Sutula, 2002).

MFS has been observed in many experimental models (Nadler, 2009), and also in the hippocampus of surgical patients with various forms of epilepsy (Mathern et al., 1996). In the epileptic hippocampus, granule cells have been found to produce basal dendrites that extend into the hilus, an additional target for recurrent mossy fiber synapses (Ribak et al., 2000). Furthermore, many granule cells born during epileptogenesis and presenting aberrant features, such as basal dendrites and ectopic migration in the hilus (Parent et al., 2007), receive innervation from other granule cells and contribute to the formation of a reverberating network (Nadler, 2009).

It has been hypothesized that, at least in the initial phases of epileptogenesis, the prevalent target of sprouted mossy fibers may be inhibitory basket cell interneurons, which would provide a homeostatic compensatory mechanism for restoration of inhibition (Cross & Cavazos, 2009). Nonetheless, because sprouted mossy fibers increase excitatory monosynaptic connections between granule cells, it is likely that the aberrant MFS contributes to the maintenance of chronic TLE (Santhakumar et al., 2005). However, it is a subject of contention whether the frequency and severity of spontaneous seizures in chronically epileptic animals are directly proportional to the extent of aberrant MFS. Reports from human TLE and some animal models of epilepsy suggest that there is no direct link between the total number of lifetime seizures and the density of MFS (Pitkanen et al., 2000). In contrast, reports from other animal models of TLE suggest increased seizure frequency with an increase in the density of MFS (Buckmaster and Dudek, 1997). Thus, studies in diverse animal models of TLE are needed to understand these issues fully.

Other proposed hypotheses are that new excitatory synapses are formed with dormant basket cells, although only the pyramidal-shaped basket cells have dendrites in the inner molecular layer (Freund et al., 1996), and that mossy fibers in the inner molecular layer arise from newly born granule cells (i.e., neurogenesis), rather than sprouting of existing granule cells (Parent et al., 1999).

1.3 AIMS

1.3.1 Overview

The primary aim of this thesis was to explore unconventional strategies for clinical application of temporal lobe epilepsy. The heart of the work has been to develop new delivery systems to block or to enhance the BDNF signal, with the aim of exploring the usefulness of BDNF as a therapeutic target. These strategies include the injection in the pathologic brain area of HSV-1 based amplicon vectors capable to silence BDNF expression and the implantation in the epileptogenic area (the hippocampus) of an encapsulated cell biodelivery (ECB) system filled with cells capable of producing and secreting BDNF.

The other aim of the thesis was to explore the implication of GABA in models of acquired and genetic epilepsy. First, we studied the alterations of GABA release in the ventral hippocampus of rats at different time points after status epilepticus. Second, we studied the loss of cortical GABA terminals in Unverricht-Lundborg disease, the most common progressive myoclonic epilepsy.

The rationale for these studies is briefly summarized below.

1.3.2 Implication of BDNF in epilepsy

As described above, BDNF is a neurotrophic factor belonging to the neurotrophin family that exerts multiple effects in the brain including regulation of neurogenesis, of cell death, of plastic modification of synaptic contacts, of neuronal excitability. BDNF has been

reported to exert contrasting effects in epilepsy. For example, BDNF signal reduction has been reported by many to retard epileptogenesis (Kokaia et al., 1995; Binder et al., 1999; Xu et al., 2004; He et al., 2004) and, along the same line, BDNF exacerbates seizure activity in epileptic hippocampi in vitro (Scharfman, 1997; Scharfman et al., 1999). However, BDNF may also exert beneficial effects (Palma et al., 2005; Paradiso et al., 2009). Thus, the involvement of BDNF in epilepsy has earned interest in scientific community because of this dual aspect: a pro- ("bad") and/or an anti- ("good") epileptic effect (Simonato et al., 2006). One mechanism that may underlie these contrasting effects may be the precise regulation of its local availability, because BDNF can be synthesized locally in distinct cellular domains and thereby induce different and maybe opposite effects at a very local scale (Chiaruttini et al., 2008).

1.3.3 Implication of GABA in epilepsy

The involvement of excitatory and inhibitory amino acids in the generation and spread of epileptic seizures has been well documented by many (see for example Ben-Ari, 2006; Werner and Covenas, 2011). The fundamental concept is that augmented activity of the excitatory amino acids glutamate and aspartate and impaired activity of the inhibitory amino acid GABA may be responsible for seizure generation. Less clear is how the impairment of GABA signaling is generated: loss of GABA neurons, reduction of GABA release, reduction of GABA effectiveness at its receptors (Sierra-Paredes and Sierra-Marcuno, 2007). In any event, the role of GABA must be central, as many drugs potentiating GABA transmission are effective antiseizure agents (Treiman, 2001).

Unfortunately, little is known on the dynamic changes in the GABAergic system in the natural course of TLE and in its progression towards pharmaco-resistance. In the epileptic tissue, seizures are not generated in a normal circuit but in a profoundly rewired network (Cossart et al., 2005), and only some aspects of the alterations specifically affecting the GABA system have been identified. For example, a substantial loss of glutamic acid decarboxylase (GAD) mRNA-containing (i.e. GABAergic) neurons has been found in the hilus of dentate gyrus (Obenaus et al., 1993) and in the stratum oriens of CA1 (Houser and Esclapez, 1996). A reduced number of specific GABAergic neurons, including parvalbumin (Drexel et al., 2011; Kuruba et al., 2011) and somatostatin-positive

interneurons (Paradiso et al., 2009; Sun et al., 2007), has been found in the epileptic hippocampus. Moreover, repetitive activation leads to profound post-synaptic $GABA_A$ receptor desensitization (run-down) in the human epileptic tissue (Ragozzino et al., 2005) and in chronically epileptic rats (Palma et al., 2007; Mazzuferi et al., 2010), indicating an impairment of post-synaptic GABA responses.

Chapter 2. BDNF

2.1 NEUROTROPHIC FACTORS

Involvement of neurotrophic factors (NTFs) in epilepsy have earned particular interest in the scientific community because of their dual aspect: a pro- ("bad") and/or an anti- ("good") epileptic effect. In fact, it seems that some NTFs favor epileptogenesis or progression of epilepsy (or both) whereas others oppose these processes. Still other NTFs can exert both positive and negative effects (Simonato et al, 2006).

2.1.1 Neurotrophins

In the brain, NTFs play a crucial role in the control of neuronal plasticity and survival. The best studied NTFs are a family of molecules termed neurotrophins, a group of structurally related polypeptide growth factors (Murray and Holmes, 2011). The first neurotrophin was identified by the Nobel-prize winner Rita Levi-Montalcini and named "the" nerve growth factor (NGF). To date, six member of the family have been identified: NGF, brain-derived neurotrophic factor (BDNF), and neurotrophins (NT) 3, 4/5, 6 and 7 (the latter found only in fish; Götz et al, 1994). Based on their three dimensional structure **(Fig. 4)**, neurotrophins are classified as part of the cysteine knot superfamily due to a distinct structure, formed by cystein residues, involved in a double loop formed by two disulphide bonds penetrated by a third disulphide bond, known as the cysteine knot (McDonald et al., 1991). The N- and C-termini are highly variable in both sequence and structure. In particular, the high variability in the N-terminus region is thought to be essential for determining receptor binding specificity (Kullander et al., 1997).

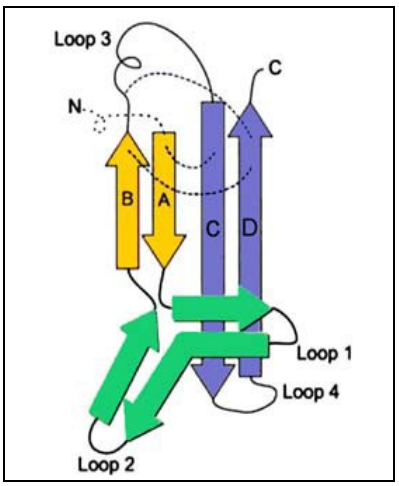

Figure 4: Schematic representation of the neurotrophin molecule. Dashed blue lines represent the three disulfide bonds of the cysteine knot. The N terminus is disordered in the unbound structures and is shown by a dashed line (Butte et al., 2001).

Neurotrophins activate one or more of the high-affinity tropomyosin-receptor kinase (Trk) receptors (Binder and Scharfman, 2004; McAllister et al., 1999) as well as the low-affinity p75 neurotrophin receptor (p75NTR; Curtis et al., 1995). The influence of neurotrophins spans from developmental neurobiology to neurodegenerative disorders. In addition to their effects on neuronal cell survival, neurotrophins can also regulate axonal and dendritic growth and guidance, synaptic structure and connections, neurotransmitter release (Chao, 2003), differentiation in the developing nervous system (Binder and Scharfman, 2004; McAllister et al., 1999), and synaptic plasticity. Levels of the different neurotrophins change in a predictable manner in relation to specific stages of embryonic development. It is well established that the overall levels of neurotrophins determine the balance between cell survival and apoptosis during development. In turn, neural activity has profound effects on the levels of neurotrophins (Chao, 2003).

The different neurotrophins share approximately 50% amino acid homology and they are initially synthesized as precursors (pro-neurotrophins) of approximately 240-260 amino acids, which are cleaved to produce the mature proteins (Mowla et al., 2001). Pro-neurotrophins are cleaved intracellularly by furin or pro-convertases at a highly conserved dibasic amino-acid cleavage site to release carboxy-terminal mature proteins. The mature proteins of 118-129 amino acids, which are about 12 kDa in size, form stable, non-covalent dimers, and are normally expressed at very low levels during development. The amino-terminal half (or pro-domain) of the pro-neurotrophin is believed to be important for the proper folding and intracellular sorting of neurotrophins. Once synthesized, neurotrophins

can be sorted into either a constitutive or a regulated secretory pathway, and sorting seems to be regulated by efficiency of protease processing (Mowla et al., 1999). Different neurotrophins show binding specificity for particular receptors. NGF binds preferentially to tyrosine receptor kinase A (TrkA); BDNF and NT4 to TrkB; and neurotrophin 3 (NT3) to TrkC **(Fig.5)**.

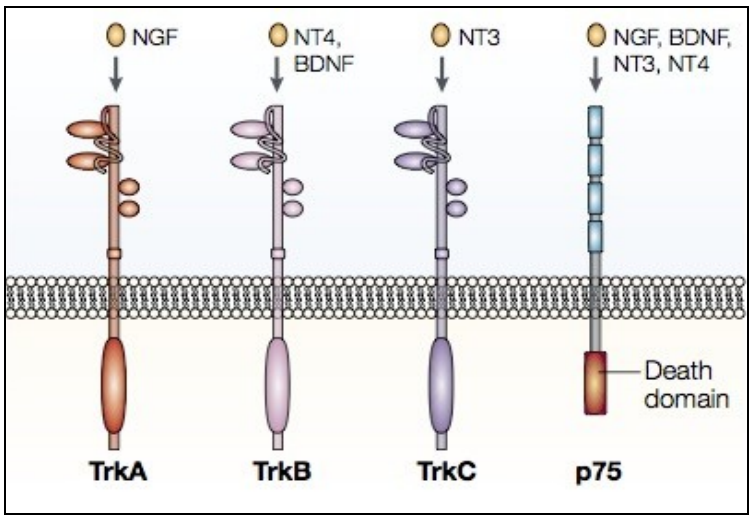

Figure 5: Schematic models of Trk and p75 receptor activation (Chao, 2003).

A selective binding to these different receptors permits the transduction of very different signals. It is not excluded a direct interaction that allows fine tuning and cross talk.

Trks are transmembrane glycoproteins of approximately 140 kDa. Trk proteins have four domains: an intracellular tyrosine kinase domain, a single trans-membrane region, an extracellular neurotrophin-binding domain consisting of two cysteine-rich regions separated by a leucine-rich repeat, and two IgG-like domains near the plasma membrane. Neurotrophins bind to the second IgG-like domain, induce receptor dimerization and trigger tyrosine kinase activity (Roux et al., 2002). As stated above, each neurotrophin preferentially binds to a particular Trk: NGF activates TrkA, BDNF and NT-4/5 activate TrkB while NT-3 binds preferentially to TrkC. In addition, the interaction of neurotrophins with their receptors might be influenced by the splicing variants of Trk receptors (Bucci et al., 2014). Truncated forms of the TrkB and TrkC receptors, which lack the tyrosine kinase domain, are unable to dimerize and are thus considered to be dominant negative modulators of Trk signaling, in contrast with their full-length counterparts (Eide et al., 1996).

When neurotrophins bind to Trk receptors, they lead to Trk dimerization and phosphorylation of specific tyrosine residues in the cytoplasmic domain, initiating signaling cascades. These phosphorylated tyrosine residues act as docking sites for adaptor proteins that propagate neurotrophin signals (Huang et al., 2003). Trk receptors can activate three major pathways: Ras, phosphatidylinositol 3-kinase (PI3K) and phospholipase C-γ1 (PLC-γ1) signal transduction pathways (Kaplan et al., 2000; Pawson et al., 2000; **Fig.6**). The Ras pathway induces the differentiation of neurons and neurite growth, while the second pathway mediates the survival functions of the neurotrophins. Finally, the phosphorylated tyrosine in the C terminus recruits phospholipase C-γ (PLCγ) which, in turn, catalyzes the cleavage of the substrate PIP2 to DAG and IP3, with DAG inducing activation of PKC and IP3 leading to release of Ca^{2+} from internal stores. The latter pathway seems to play an important role in neurotrophin-mediated neurotrophin release (Canossa et al., 1997) and in synaptic plasticity. It has also been reported that the PLC-γ track regulates the neuron-specific intermediate filament protein, peripherin (Loeb et al., 1994).

These three signal transduction pathways are also activated by the binding of mature neurotrophins to heterodimers formed by one monomer of Trk and one of p75NTR (**Fig.6**).

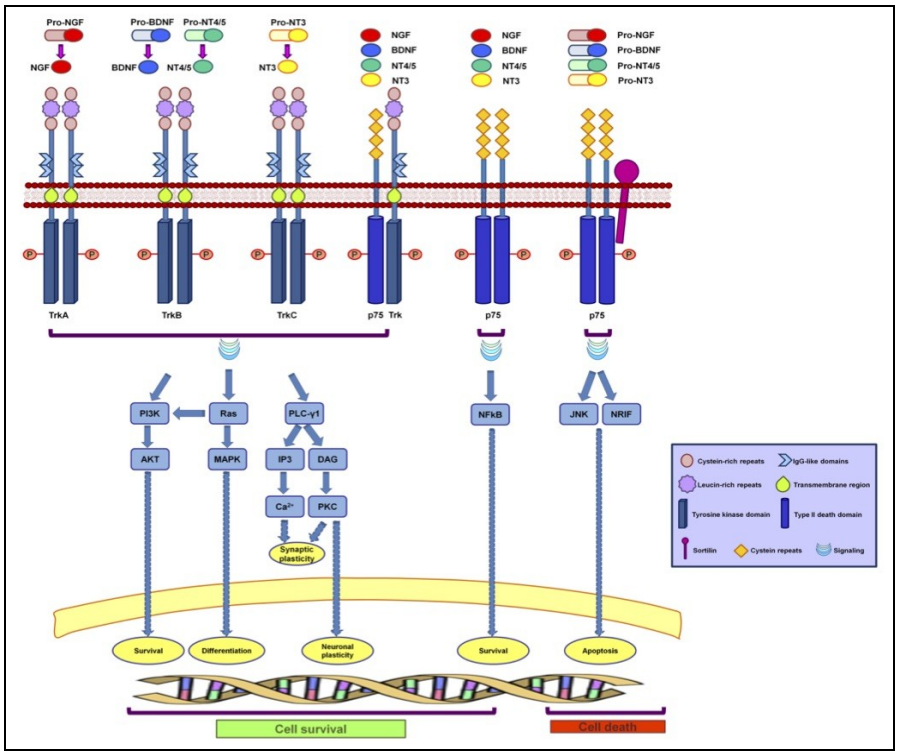

Figure 6: Signal transduction pathways activated by the neurotrophins.

p75NTR, a trans-membrane glycoprotein receptor of approximately 75 kDa, is a member of the tumor necrosis factor (TNF) receptor superfamily. Unlike the Trk receptors, p75NTR binds to all neurotrophins with approximately similar low affinity and to all pro-neurotrophins with high affinity (Bucci et al., 2014). In the extra-cellular domain of p75NTR, the four cysteine repeats participate in binding to neurotrophins, while in the intracellular domain there is a type II death domain similar to those present in members of the TNF family (Lee et al., 2001). Binding to the p75NTR receptor has been shown to affect cell survival (Barret and Bartlett, 1994) and axonal outgrowth (Dechant and Barde, 1997), and to result in activation of NF-κB (Carter et al., 1996). p75NTR also interacts with a number of other receptors, and these interactions often modulate ligand binding as well as signaling and trafficking. p75NTR is frequently co-expressed and associated with Trk receptors and increases Trk's affinity for neurotrophins while reducing ligand-induced Trk receptor ubiquitination, thus delaying Trk receptor internalization and degradation (Makkerh et al., 2005).

Several variants of the p75NTR receptor have been identified, including soluble forms and truncated proteins lacking in the ability to bind neurotrophins (Dechant and Barde, 1997).

The precise role of these variants is unknown, but their presence may be functionally relevant.

The complexity of this multiple ligand, multiple receptor signalling system is made evident by the often-opposing actions of the neurotrophins; for example, Trk receptors are widely reported to promote cell survival and enhancement of the efficacy of synaptic transmission, while strong evidence exists in support of a role for p75 in mediating cell death and in functional impairment, as will be described in subsequent sections (Hennigan et al., 2007).

The expression of Trk receptors is dynamically regulated. In the CNS, TrkA is found at high density in basal forebrain cholinergic neurons (BFCNs). These neurons provide the major cholinergic input to the cerebral cortex and the hippocampus, and can be lost in neurodegenerative diseases like Alzheimer disease. TrkB is broadly expressed in the nervous system, which explains the multitude of actions it exerts (Lei et al., 2007). TrkC is typically expressed in the early phases of development (Tessarollo et al., 1993). The expression profile of P75NTR is also highly regulated, showing a down-regulation during postnatal development (Bothwell, 1995) and a rapid induction after injury, such as nerve lesion or seizures (Roux et al., 1999). This confirms the link between p75 receptor and cell death in pathological situations.

2.1.1.1 BDNF

BDNF is the most represented member of the neurotrophin family in the adult brain. The BDNF protein consists of a non-covalently linked homodimer and contains a signal peptide following the initiation codon and a pro-region containing an N-linked glycosylation site. It is initially produced as a proneurotrophin (pro-BDNF, ~30 kDa) that a protease cleaves to the mature form (~14kDa; Binder and Scharfman, 2004). In addition to the mature form, pro-BDNF is also biologically active.

The BDNF gene in humans has been mapped to chromosome 11p but several BDNF transcripts can be generated in both humans and rodents (Liu et al., 2005, Liu et al., 2006). In the BDNF gene, seven exons encoding for the 5' untranslated region (5'UTR) are alternatively spliced to the eighth exon, which contains the coding sequence and the 3'UTR, giving rise to ten different mRNA transcripts (two exons have internal splice sites). Furthermore, because the 3'UTR contains two termination sites, each of these ten transcripts can have either a short or a long untranslated tail, providing the final

astonishing number of 20 different transcripts that encode an identical protein. All these BDNF mRNAs are expressed in the brain, but at different levels and not in all neurons. In addition, although some BDNF transcripts are widely expressed in many neurons, some splice variants (for instance, the one containing exon 1) can be found only in restricted neuronal populations (Simonato et al., 2006).

BDNF and its receptor trkB have a widespread distribution in the CNS (Merlio et al., 1993, Conner et al., 1997). Alternatively spliced forms of BDNF mRNA can remain in the cell soma or be targeted to the dendrites, where they can be locally translated into protein. It is thought that these dendritic forms have a crucial role in the potentiation of active synaptic contacts, whereas the somatic forms are implicated in cell survival and in differentiation of neuronal precursors (**Fig. 7i**). Moreover, mRNA translation yields the production of a pro-BDNF that might or might not be transformed into the mature form intracellularly. This is very important because, as described above, the pro- and the mature forms are thought to exert contrasting effects (**Fig. 7ii**). Pro-BDNF and mature BDNF synthesized in the cell body can remain in the soma (and modulate survival and differentiation through autocrine or paracrine mechanisms) or can be targeted to the axons or dendrites (or both), modulating synaptic efficacy. These latter actions can be coordinated with those produced by dendritically synthesized BDNF (**Fig. 7iii**). Released pro-BDNF can also undergo a high-affinity interaction with p75NTR receptors or can be transformed into mature BDNF by extracellular proteases (**Fig. 7iv**). Mature BDNF can finally bind to receptors with high (TrkB) or low affinity (p75; **Fig.7v**).

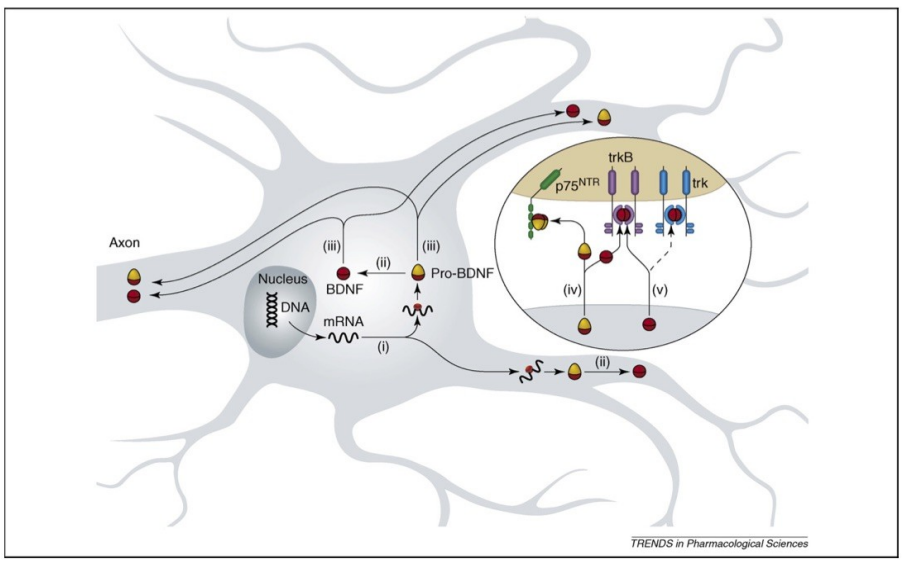

Figure 7: Mechanisms underlying possible effects of the BDNF (Simonato et al., 2006). See text for description.

2.1.2 BDNF and epilepsy

As described above, the BDNF protein may exert contrasting effects depending on its different subcellular sites of action (soma, dendrites, axons). These contrasting effects may explain contradictory findings in the epilepsy field, for example that BDNF may favor or oppose epileptogenesis (Simonato et al., 2006). Thus the therapeutic potential of BDNF for epilepsy is still controversial (Koyama and Ikegaya, 2005; Kuramoto et al., 2011; Simonato et al., 2006). There are several reports supporting the notion that BDNF might aggravate epilepsy. Scharfman et al. (2002b) found that intrahippocampal infusion of BDNF provokes seizures in rats. Overexpression of BDNF in transgenic mice also increases excitability (Croll et al., 1999). Furthermore, intraventricular infusion of BDNF accelerates kindling development (Xu et al., 2004). On the other hand, other reports suggest that BDNF had antiepileptic effects. Infusion of BDNF delays the development of kindling according to other authors (Reibel et al., 2000a). Viral vector-mediated supplementation of BDNF attenuates epileptogenesis in the pilocarpine model (Paradiso et al., 2009).

Taken together, the data presented depict a complex situation, in which BDNF seem to favor development and progression of epilepsy but, at the same time, might produce anti-seizures effects in the chronically epileptic brain. How these effects are orchestrated remains unclear (Simonato et al., 2006). Because BDNF can produce functionally contrasting effects in the context of epilepsy, depending on the stage of progression of the disease, understand these mechanisms in depth could be instrumental for the development of new therapeutic strategies. One hypothesis could be that different splice variants, endowed with different cell site destinations and different functional effects, may be produced at different stages of the diseases (Chiaruttini et al., 2008).

2.2 BDNF DELIVERY STRATEGIES

2.2.1 Generalities

The development of effective NTF-based therapies has been hindered in large part by the inability to deliver them across the blood brain barrier (BBB) to the target site in a stable, controlled, and continuous manner (Rubin et al., 1999). Several approaches are under investigation for direct, local delivery of these compounds to the desired brain target, but each strategy has its own advantaged and disadvantages (Emerich et al., 2014).

Direct brain infusion. A catheter implanted into the brain is attached to a pump to control the rate and timing of infusion. Surgery is invasive, pumps are prone to leakage, protein stability can be poor, immunological responses can block protein function, and distribution from the site of injection may be inadequate (Tatarewicz et al., 2007).

Cell-based delivery. Cells engineered to produce trophic factors are injected into the brain, where they can migrate to increase diffusion of the desired factor into the brain tissue. This approach may permit anatomical integration between the host and transplanted cells and good cell viability and neurochemical diffusion may be achieved. However, migration is uncontrolled and cells cannot be retrieved (Huang et al, 2012).

Biomaterial-based drug delivery. Molecules can be incorporated into injectable or implantable biomaterials to provide sustained local targeted delivery to the brain. These approaches do not currently provide long-term delivery, necessary for chronic CNS diseases (Orive et al, 2009).

Gene therapy approaches. A viral vector containing the gene that expresses a factor is injected into the brain causing the local neurons to produce the factor. This approach can achieve localized factor production but there is no any way to regulate expression (Marks et al, 2010).

Cell encapsulation. There are generally two categories for cell immunoisolation by encapsulation, micro- and macro-, each with some benefit and limitations (Emerich et Winn, 2004). Microencapsulation permits use of allo- and xeno-grafts without immunosuppression and thin wall and spherical shape are optimal for cell viability and neurochemical diffusion. These same capsules are, however, mechanically and chemically

fragile and cannot be retrieved once implanted within the brain parenchyma. Macrocapsules also permit the use of allo- and xeno-grafts without immunosuppression, provide good cell viability and neurochemical diffusion, have good mechanical stability, and can be retrieved if needed or desired. Multiple implant sites may be required for optimal benefits (Emerich et al, 2014).

In the frame of this thesis, we exploited two distinct approaches to down-regulate and to up-regulate BDNF levels locally in the epileptic hippocampus. (1) A type of herpes simplex virus-1 (HSV-1) based vectors called amplicons (section 2.2.2) were used to host the BDNF gene in antisense, in order to down-regulate BDNF levels. (2) An encapsulated cell biodelivery device (section 2.2.3) was loaded with cells engineered to produce and secrete BDNF to up-regulate its levels.

2.2.2 HSV-1 based amplicon vectors

Viral-derived vectors are the most promising gene transfer tools due to the fact that viruses are naturally occurring molecular devices that have evolved to ensure targeted gene delivery and efficient expression in most cell types (Epstein, 2009).

HSV-1-based vectors have the capacity to deliver up to 150 Kb of foreign DNA to the nucleus of most proliferating and quiescent mammalian cells, making this family of vectors a very interesting tool for gene transfer and gene therapy. The uniqueness of HSV-1-based vectors stems from several properties: (1) the very large capacity to host foreign DNA; (2) the virus DNA does not integrate into the host cell DNA, implicating no risk of insertional mutagenesis; (3) the complexity of the virus genome, which contains approximately 40 genes that are not essential for virus replication and can therefore be deleted without disturbing virus production in cultured cells; (4) the capacity of HSV-1 to infect neurons and the ability to trans-synaptically spread from neuron to neuron in both anterograde and retrograde directions; (5) the capacity to establish a latent infections in neurons (Epstein, 2009).

Three different types of vectors can be derived from HSV-1 to exploit one or more of these properties (**Fig. 8**). Recombinant attenuated viruses are replication-competent vectors carrying mutations that restrict spread and lytic viral replication to cancer cells without causing major toxicity to the healthy tissues. Defective, replication-incompetent non-pathogenic recombinant vectors lack one or more genes essential for replication, but retain

many advantageous features of wild-type HSV-1, like the ability to express transgenes after having established latent infections in central and peripheral neurons. Amplicon vectors are defective, helper-dependent vectors that carry no viral genes and take advantage of the large carrier capacity of the virus particle to deliver long or multiple transgenic sequences (Epstein, 2005).

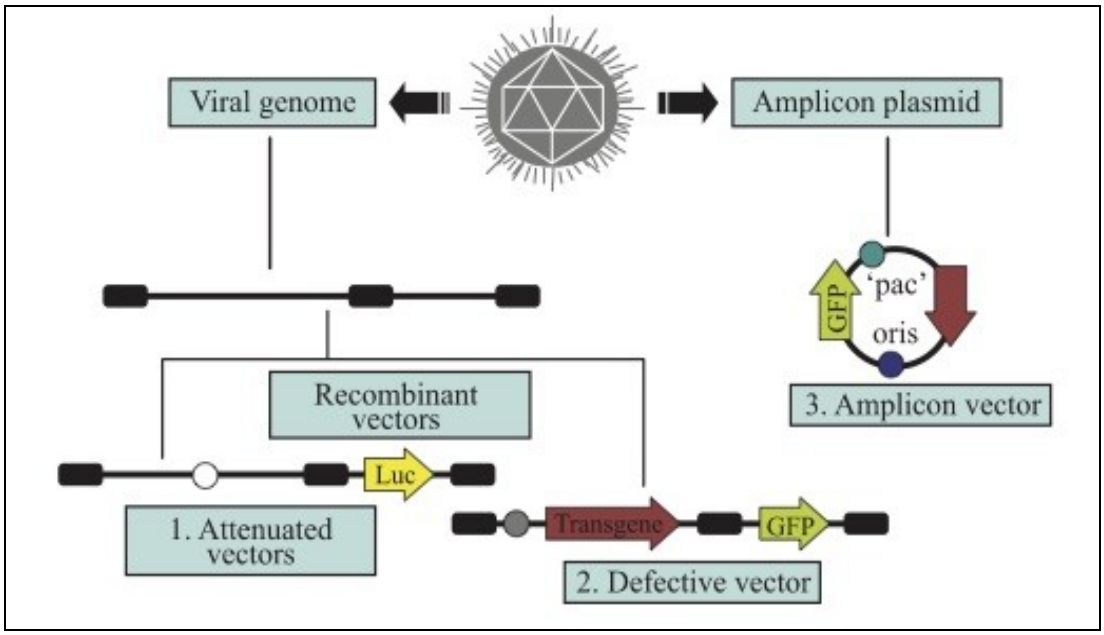

Figure 8: The three types of HSV-1-based vectors (Esptein, 2009).

Amplicon vectors (Spaete and Frenkel, 1982) are HSV-1 particles identical to wild- type HSV-1 from the structural, immunological and host-range points of view, but which carry a concatemeric form of a DNA plasmid, named the amplicon plasmid, instead of the viral genome (Epstein, 2005). An amplicon plasmid (**Fig.9A**) is a standard *Escherichia coli* plasmid carrying one origin of virus replication (*Ori-S*) and one packaging signal (pac or '*a*') from HSV-1, in addition to the transgenic sequences of interest (Spaete & Frenkel 1985, Deiss et al., 1986).

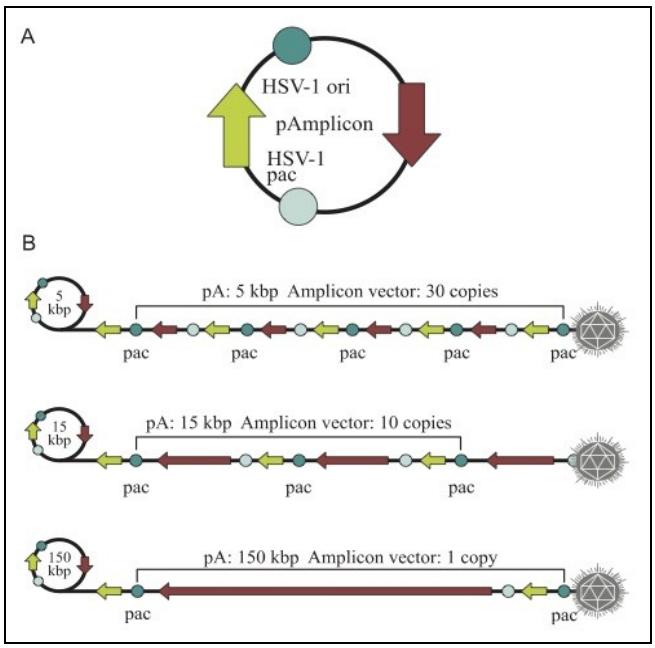

Figure 9: Amplicon plasmid and amplicon vectors (Epstein, 2009)

One major advantage of amplicons as gene transfer tools is the fact that they carry no virus genes and consequently do not induce synthesis of virus proteins. Therefore, these vectors are non-toxic for the infected cells and non-pathogenic for the transduced organisms. Furthermore, the absence of viral genes in the amplicon genome strongly reduces the risk of reactivation, complementation or recombination with latent or resident HSV-1 genomes. Amplicons are quite versatile tools due to the fact that, during their production, the genome replicates, like HSV-1, via a mono-directional, rolling circle-like mechanism, generating long concatemers composed of tandem repeats of the amplicon plasmid (Boehmer & Lehman 1997; **Fig. 9B**). Since infectious HSV-1 particles will always package approximately 150 Kb DNA (the size of the virus genome), the number of repeats that a particular amplicon vector can carry and deliver depends on the size of the original amplicon plasmid (Kwong & Frenkel 1984). Therefore, an amplicon plasmid of around 5 Kb will be repeated approximately 30 times in the amplicon vector, while a very large amplicon plasmid, carrying a 150 Kb genomic locus, will originate amplicon vectors carrying a single repeat of this sequence. This is important especially to get an efficient knock-down of the expression of the target gene. A second benefit that arises from the lack of viral genes in the amplicon vector is that most of the 150 Kb capacity of HSV-1 can be used to accommodate very large pieces of foreign DNA.

All of these features make the amplicon vectors one of the most powerful, interesting and versatile gene delivery platforms.

2.2.3 Encapsulated cell biodelivery (ECB) device

Encapsulated cell biodelivery (ECB) is an attractive alternative to more direct gene therapy methods and combines the potency of gene therapy with an implantable and retrievable device. This technology targets diseased neurons with therapeutic biological substances continuously produces and secreted by genetically engineered human cells enclosed within the implant (Emerich et al., 2014). Within the tip of the implant, a stably genetically engineered human cell line grows on a polymer scaffold behind a semipermeable hollow fiber membrane and continuously secretes a biologically active amount of the therapeutic protein directly into a localized region of the brain (Lindvall et Wahlberg 2008). ECB devices filled with genetically modified human cells to release gene products into the host tissue have the advantage of being a reversible treatment: the ECB devices can be removed from the brain with a relatively simple procedure and thereby terminate their effect. The cells in the ECB devices can have long-term viability when implanted into brain because the nutrients from the surrounding host tissue can penetrate the semipermeable membrane of the device while the gene products are released into the host tissue. Another advantage of ECB devices is that the encapsulated cells do not alter host cells or integrate into the host brain. Furthermore, the semipermeable membrane isolates the cells in the device from immune reactions against them in the host brain. Therefore, there is no need for immunosuppressant drugs (Nikitidou et al, 2013).

The active portion of the device consists of a 7 mm long semipermeable polyethersulfone (PES) hollow fiber membrane with an inner diameter of 500 μm filled with a poly vinyl alcohol (PVA) cylindrical matrix, which serves as support for the cells. The genetically engineered human cell line grows on this matrix (**Fig. 10**).

The technology is capable of making practically any cell derived therapeutic, including recombinant growth factors, peptides, and antibodies. The encapsulated cells provide long-term factor secretion from the implanted device (Nikitidou et al, 2013).

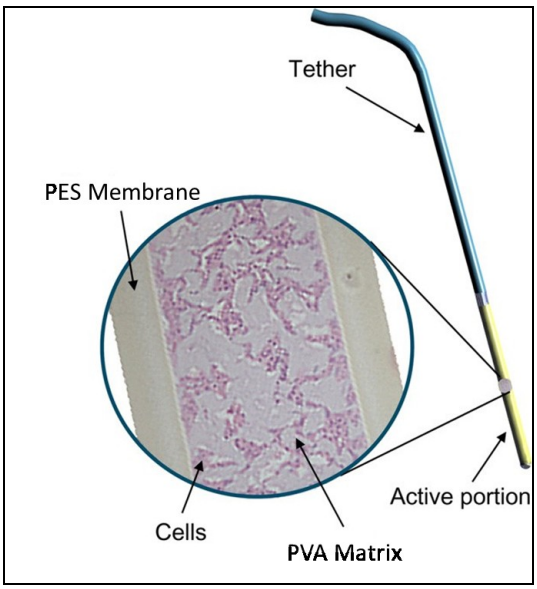

Figure 10: Schematic representation of ECB device (Lindvall andWahlberg, 2008).

2.3 SILENCING BDNF EXPRESSION WITH HERPES SIMPLEX VIRUS TYPE-1 BASED AMPLICON VECTORS IN AN EXPERIMENTAL MODEL OF TEMPORAL LOBE EPILEPSY

Silencing BDNF expression with Herpes Simplex Virus type-1 based amplicon vectors in an experimental model of temporal lobe epilepsy

Chiara Falcicchia,[1,2] Pascal Trempat,[1,2] Anna Binaschi,[1] Marilyne Labasque,[1] Paolo Roncon,[1] Marie Soukupova,[1] Hervé Berthommé[2] and Michele Simonato[1,3]

[1] *Department of Medical Science, Section of Pharmacology, Neuroscience Center, University of Ferrara and National Institute of Neuroscience, Ferrara, Italy;*
[2] *Bioviron, Univ. Claude Bernard-Lyon 1, Villeurbanne, France;*
[3] *Laboratory of Technologies for Advanced Therapy (LTTA), Technopole of Ferrara, Ferrara, Italy*

Running title:

Amplicons for silencing BDNF gene expression

Corresponding author:

Chiara Falcicchia
Department of Medical Sciences, Section of Pharmacology
University of Ferrara
Via Fossato di Mortara 17-19
44121 Ferrara, Italy
Tel: (+39) 0532 455345
Fax: (+39) 0532 455205
e-mail address: chiara.falcicchia@unife.it

Abstract

Brain-derived neurotrophic factor (BDNF) has been found to produce pro- but also anti-epileptic effects. Thus, its validity as a therapeutic target must be verified using advanced tools designed to block or to enhance the BDNF signal. The aim of this study was to develop tools to silence the BDNF signal. We generated Herpes simplex virus type 1 (HSV-1) derived amplicon vectors, i.e. viral particles containing a genome of 152 kb constituted of concatameric repetitions of an expression cassette, enabling the expression of the gene of interest in multiple copies. HSV-1 based amplicon vectors are non-pathogenic and have been successfully employed in the past for gene delivery into the brain of living animals. Amplicon vectors are thus a relevant and reliable choice for expressing a silencing cassette, which, in multiple copies, is expected to lead to an efficient knock-down of the target gene expression. Two BDNF silencing strategies have been developed. The first, antisense, has been chosen to target and degrade the cytoplasmic mRNA pool of BDNF, whereas the second, based on the convergent transcription technology, has been chosen to repress transcription at the BDNF gene. Both these amplicon vectors proved to be effective in down-regulating BDNF expression *in vitro*, in BDNF-expressing mesoangioblasts cells. However, only the antisense strategy was effective *in vivo*, after inoculation in the hippocampus in the pilocarpine model of temporal lobe epilepsy, in which BDNF mRNA levels are strongly increased. Interestingly, the knock down of BDNF levels induced with BDNF-antisense was sufficient to produce significant behavioral effects, in spite of the fact that it was produced in a part of a single hippocampus and not in the entire epileptogenic area. In conclusion, this study demonstrates a reliable effect of amplicon vectors in knocking down gene expression *in vitro* and *in vivo*. Therefore, this approach may find broad applications in neurobiological studies.

Keywords

BDNF, gene silencing, hippocampus, epilepsy

Introduction

The neurotrophin brain-derived neurotrophic factor (BDNF) is widely expressed in the brain, where it exerts a key role in neuronal survival, differentiation, and plasticity (Cohen-Cory et al., 2010; Yoshii and Constantine- Paton, 2010). BDNF is therefore viewed as a promising therapeutic target for CNS-related disorders, including epilepsy (Simonato et al., 2006; Simonato and Zucchini, 2010). However, an important issue that has limited developments in the direction of bringing therapies that target the BDNF system to the clinics has been the difficulty in delivering it to a specific and restricted brain region and thereby locally modulating its levels. Here, we present novel tools to pursue this aim: amplicon vectors derived from Herpes simplex virus type 1 (HSV-1) capable to down-regulate BDNF expression *in vitro* and *in vivo*.

HSV-1 amplicon vectors hold considerable promise as gene-transfer vehicles because of some unique features: (i) the very large capacity to host foreign DNA, (ii) the inability to integrate viral DNA into host chromosomes, that reduces the risk of insertional mutagenesis, (iii) the capacity to infect nervous system cells (Epstein et al., 2009). Finally, another attractive feature of amplicon vectors is that they carry and deliver a variable number of repeats of the transgene (Kwong & Frenkel 1984), which makes then particularly suited to get an efficient knock-down of a target gene through expression of multiple copies of the silencing transgene.

Two silencing strategies have been pursued in the frame of this study. The first, called “antisense”, has been chosen to target and degrade the cytoplasmic mRNA pool of BDNF via an RNA interference mechanism (Wang and Barr, 2005), whereas the second, based on the “convergent transcription technology” (Tran et al., 2003), has been chosen to repress the BDNF gene through chromatin remodeling.

Double-stranded RNAs (dsRNAs) induce a potent and specific post-transcriptional gene silencing by triggering the degradation of homologous target mRNAs. This form of gene suppression was first observed in the nematode worm *Caenorhabditis elegans* and termed RNA interference or RNAi (Paul et al., 2002). RNAi is therefore a biological process in which RNA molecules inhibit gene expression by causing the destruction of specific mRNA molecules in sequence-specific manner. Similarly, experimental introduction of antisense RNA into cells can be used in certain biological systems to interfere with the function of an endogenous gene (Fire et al., 1998).

The convergent transcription approach is based on the co-expression of sense and antisense RNA strands from independent expression cassettes or a divergent cassette in which a full-length cDNA sequence is positioned between two identical promoters (Wang et al., 2003; Lee et al., 2002), such that independent transcription from each promoter produces a pool of sense and antisense RNAs capable of forming long dsRNAs and undergoing processing to the effector siRNAs (Tran et al., 2003). The use of convergent transcription from opposing promoters to induce RNAi-mediated gene inhibition has been reported in trypanosomes and Drosophila (Shi et al., 2000; Giordano et al., 2002), as well as in yeast and mammalian cells, through a transcriptional gene silencing mechanism (Gullerova and Proudfoot, 2012). It has been predicted that the expression of up to 8% of human genes may be influenced by antisense RNA or antisense transcription (Chao-Chung et al., 2003; Shendure et al., 2002), suggesting that convergent transcription does occur with high frequency in the human genome (Tran et al., 2003).

The silencing effect of amplicon vectors has been assessed by examining their efficiency in down-regulating BDNF levels *in vitro*, in BDNF-expressing mesoangioblast cells, and *in vivo*, using a rat model of temporal lobe epilepsy (TLE) in which BDNF mRNA levels are strongly increased in the hippocampus.

Materials and Methods

Amplicon vectors

***Amplicon plasmids*.** For construction of the plasmid containing antisense BDNF (plasmid pAm2-BDNF-antisense-GFP), the XbaI-BamHI fragment containing the cytomegalovirus (CMV) promoter was cut from the pMA-RQ-CMV plasmid and cloned in the XbaI-BamHI sites of pAm-GFP, a plasmid expressing the green fluorescent protein (GFP) under control of the ICP22 promoter, to obtain the pAm-GFP-CMV plasmid. The BDNF fragment was cut from the plasmid pBSK-BDNF using EcoRI and cloned in the polylinker NheI blunt-end site of pAm2-GFP-CMV, flanked by the CMV promoter and a SV40 polyadenylation signal (Fig. 1A). To discriminate between cloning in sense and antisense orientation, 12 starter cultures, obtained after transformation of *E. Coli* high efficiency transformation competent bacteria, were digested with ScaI, PvuII and PstI, and run on agarose gel electrophoresis.

For construction of the BDNF convergent transcription plasmid (pAm-CT-BDNF-GFP), a new CMV fragment (HindIII/PmeI) was subcloned into the HindIII/EcoRV site of pAm-GFP-CMV, in the opposite direction compared to the other CMV promoter, obtaining the pAm-CT-GFP plasmid. The pAm-CT-BDNF-GFP plasmid was then obtained by cloning the EcoRI sticky-end in the EcoRV-digested pAm-CT-GFP plasmid, in order to put the BDNF sequence between the two CMV promoters (Fig. 1B). The pAm2-GFP plasmid was used as control amplicon (Fig. 1C).

Cell lines and virus. The cell lines employed in this study were the following: genetically modified mesoangioblasts producing BDNF and GFP (MABs-BDNF; Su et al.,

2012), Gli36 cells (a human glioblastoma cell line), Vero cells (African green monkey kidney epithelial cell line), Vero 4.42 cells (that express the HSV-1 immediate early genes ICP4, ICP27 and ICP42 required for helper virus replication) and Vero cells expressing the ICP4 and Cre genes. All cell lines were propagated in Dulbecco's minimum essential medium (DMEM, Lonza, Switzerland) supplemented with 10% fetal bovine serum (FBS, Invitrogen Gibco, USA), 100 U/ml penicillin and 100 mg/ml streptomycin (Invitrogen). Cells were maintained at 37°C in a humidified incubator containing 5% CO_2.

Amplicon production. Amplicon vectors were produced by transfecting 10 µg of each amplicon plasmid (pAm2-BDNF-antisense-GFP, pAm-CT-BDNF-GFP and pAm2-GFP) into Vero 4.42 cells using the jetPRIME reagent (Polyplus-transfection, France). Cells were superinfected the following day with the LaL□J helper virus at a multiplicity of infection (MOI) of 0.5 plaque forming units (pfu)/cell in medium M199 (Gibco) supplemented with 1% FBS and 1% penicillin/streptomycin. Three days later, cells were harvested and amplicon viral particles were extracted by several rounds of freeze/thaw and sonication. To calculate purity of the production, amplicon and helper particles were titrated to obtain transduction units (tu)/ml and pfu/ml. Several successive rounds of infections and productions were performed to obtain high quantity of amplicon particles and a final infection-production step was performed on a Vero cell line expressing the ICP4 and Cre genes to obtain a final high purity working stock.

Cell infection. Confluent MABs-BDNF cells seeded in 6-well plates were infected with the GFP-control, BDNF-antisense or CT-BDNF amplicon at MOI 5 or 20, and maintained at 34°C in DMEM with 10% FBS for 24, 48, 72 or 96 h. At each time point, cells were washed twice in PBS, then scraped and resuspended in 50 □L of lysis buffer (50 mM Tris-HCL pH 8, 150 mM NaCl, 1% NP-40) containing a protease inhibitor cocktail (Roche, Germany). The protein content of the lysates was evaluated by the

Bradford method using the Bio-Rad protein assay kit (Bio-Rad Laboratories, CA, USA).

Animals

Male Sprague-Dawley rats (240-260 g; Harlan, Italy) were used for in vivo experiments. They were housed under standard conditions: constant temperature (22-24ºC) and humidity (55- 65%), 12 h light/dark cycle, free access to food and water. Experiments involving animals were conducted in accordance with European Community (EU Directive 2010/63/EU), national and local laws and polices (authorization: D.M. 83/2009-B and D.M. 246/2012-B). All efforts were made to minimize animal suffering.

Amplicon infusion. Under ketamine and xylazine (43 and 7 mg/kg, i.p.) anesthesia, a glass needle connected to a perfusion pump was implanted in the right dorsal hippocampus using a stereotaxic apparatus for small animals, with the following coordinates: A −1.7; L −1.5; D +3.7 (Pellegrino and Cushman, 1979). Anesthesia was then maintained using isofluorane (1.4% in air, 1.2 ml/min). Two different doses of amplicon vector, $1x10^4$ tu and $5x10^5$ tu, were injected in a volume of 1 ul at a flow rate of 0.1 ul/min. Amplicon vectors (GFP-control, BDNF-antisense and CT-BDNF) were injected 5 days before pilocarpine administration.

Status Epilepticus. Pilocarpine was administered i.p. (340mg/kg), 30 min after a single injection of methyl-scopolamine (1 mg/kg, s.c., to prevent peripheral effects of pilocarpine), and the rats' behavior was monitored for several hours thereafter, using the Racine's scale. Within the first hour after injection, all animals developed seizures evolving into recurrent generalized convulsions (status epilepticus, SE). SE was interrupted 3 h after onset by administration of diazepam (10 mg/kg i.p.) and rats were killed by decapitation under light diethyl-ether anesthesia at three different time points: 3h, 6h and 24h after onset of SE. Brains were rapidly frozen in 2-methylbutane.

Histology

Rats were killed under deep isofluorane anesthesia. Brains were removed, immersed in 10% formalin for 48 h and then paraffin embedded. Serial section of 6 μm were cut with a Microtome (Leica RM2125RT, Germany). In all experiments, adjacent sections were used for different staining procedures.

Immunohistochemistry. Sections were dewaxed and rehydratated as described above. All antigens were unmasked using a commercially available kit (Unmasker, Diapath), according to the manufacturer's instructions. After washing in phosphate buffered saline (PBS), sections were incubated with Triton x-100 (Sigma; 0.3% in PBS 1×, room temperature, 10 min), washed twice in PBS 1×, and incubated with 5% BSA and 5% serum of the species in which the secondary antibody was produced for 30 min. They were incubated overnight at 4°C in humid atmosphere with a primary antibody specific for different cellular markers: GFAP (mouse polyclonal, Sigma) 1:100; IBA-1 (rabbit monoclonal, AbCam MA, USA) 1:200, GFP (rabbit polyclonal, Santa Cruz, Texas) 1:50. After 5-min rinses in PBS, sections were incubated with Triton (as above, 30 min), washed in PBS and incubated with a goat anti-mouse Alexa 594 secondary antibody (1:250, Invitrogen) for mouse primary antibodies, or with a goat anti-rabbit, Alexa 488 secondary antibody (1:250; Invitrogen) for rabbit primary antibodies, at room temperature for 3.5 hours. NeuroTrace (1:150) was included in the secondary antibody incubation. After staining, sections were washed in PBS, counterstained with 0.0001% DAPI for 15 min, and washed again. Coverslips were mounted using anti fading, water based Gel/Mount (Sigma).

Western Blot

Tissue sample extraction. The left and right dorsal hippocampi were dissected and processed to extract total RNA, genomic DNA and proteins using the RNeasy Lipid Tissue Mini kit (Qiagen, Germany). RNA extraction was performed following the manufacturer instructions. Proteins and genomic DNA were isolated after RNA extraction using the phenol phase. Briefly, genomic DNA was precipitated from the phenol phase with ethanol and pellets were washed with sodium citrate ethanol solution and stored in 75% ethanol at -80°C. After DNA precipitation, proteins were isolated from the supernatant ethanol-phenol by isopropanol precipitation. Proteins were then washed several times with 0.3 M guanidine HCl-95% ethanol solution before being air-dried and rehydrated in a Laemmli-like buffer (62 mM Tris-HCl pH 6.8; 2% SDS; 10% glycerol; 12.5 mM EDTA; 50 mM DTT; □-mercaptoethanol; protease inhibitor cocktail) by a 20 min incubation at 95°C and 3 rounds of 30 sec sonication. The protein content of the lysates was evaluated by the Bradford method using the Bio-Rad protein assay kit (Bio-Rad Laboratories).

Western Blot analysis and quantification. Infected MABs and dissected dorsal hippocampi extracts, corresponding to 20 and 30 µg total proteins respectively, were analyzed by Western blotting. Each sample was diluted in SDS-gel loading buffer, boiled for 10 min and centrifuged before loading. Then they were electrophoretically separated onto a 12% SDS-polyacrylamide gel and transferred to nitrocellulose membranes. After blocking in a buffer (PBS-Tween20) containing 5% dried milk, membranes were incubated with the primary antibody in a buffer containing 2.5% dried milk overnight at 4°C. After three washings, incubations were performed with the secondary antibody in buffer/dried milk at room temperature for 1 h. The BDNF protein was revealed using a rabbit anti-BDNF monoclonal antibody (AbCam, dilution 1:1000); GFP using a mouse anti-GFP monoclonal antibody (Roche; 1:1000); actin using a rabbit anti-actin monoclonal

antibody (Sigma, MO, USA; 1:1000). Mouse monoclonal antibodies were revealed using a goat anti-mouse horseradish peroxidase (HRP)-conjugated secondary antibody (Dako, Denmark; dilution 1:1000) and rabbit monoclonal antibodies by a swine anti-rabbit HRP-conjugated secondary antibody (Dako; dilution 1:3000). The immunocomplexes were detected using the ECL Western blot detection kit (GE Healthcare, NJ, USA) and ChemiDoc XRS (Bio-rad) for electronic blot pictures. Quantification was performed using the Image Lab software (Biorad).

Results

HSV-1 amplicon plasmid generation

We developed two silencing strategies to down-regulate BDNF protein level. The first strategy, called "antisense", target and degrade the cytoplasmic mRNA pool of BDNF. For this strategy, the rat BDNF cDNA is expressed in a head to tail, complementary manner to the endogenous BDNF mRNA, in order to induce its degradation through the mechanism of RNA interference (Fig. 1A). The amplicon plasmid (pAM2-BDNF-antisense-GFP) and vector (BDNF-antisense-GFP) we generated express both the mRNA for eGFP and the antisense BDNF mRNA. The second strategy, based on the Convergent Transcription (CT) technology, repress the BDNF gene at transcription level. In this vector (CT-BDNF-GFP), the BDNF cDNA is inserted between two cytomegalovirus (CMV) promoters oriented in opposing directions (Fig. 1B), and the resulting convergent transcription elicits down-regulation of the BDNF gene transcription through chromatin remodeling associated with epigenetic silencing marks (Gullerova et al., 2012). We also generated a control amplicon plasmid and vector (named GFP amplicon vector), which possessed only the GFP reporter

cassette (Fig. 1C). Following the cloning steps, large purified stocks of these 3 amplicon vectors were produced. The titer of each stock was 9.4×10^8 t.u./ml, 1.05×10^9 t.u./ml and 1.05×10^7 t.u./ml, respectively for BDNF-antisense-GFP, CT-BDNF-GFP and GFP amplicon vectors. The BDNF-antisense-GFP and CT-BDNF-GFP amplicon vectors contain more than 20 copies of the silencing cassette. In principle, hosting many copies of the silencing cassette is an optimal choice for efficient knock-down of the expression of the target gene. As described, we produced each amplicon vectors with a GFP expression cassette for monitoring the infection in cells and animals.

***In vitro* validation**

The next step was to evaluate the effects of each amplicon vectors against BDNF *in vitro.* In order to study their efficiency to repress the BDNF expression, we infected BDNF-expressing mesoangioblast (MABs) cells with BDNF-antisense-GFP or CT-BDNF-GFP amplicon vectors at a multiplicity of infection (MOI) of 5. Controls cells were infected with the GFP amplicon vector or not infected. The infection of cells with BDNF-antisense-GFP or CT-BDNF-GFP amplicon vectors was confirmed by GFP fluorescence, as shown in Fig. 2A and Fig. 2E. We examined pro-BDNF protein levels for 96 hours after infection using western blot analysis. MABs cells infected with the BDNF-antisense-GFP amplicon vector displayed lower pro-BDNF levels beginning 24 h post infection as compared with cells not infected or cells infected with the GFP amplicon control vector. The decrease of pro-BDNF protein levels was even more prominent at the following time-points, and became essentially complete 94 h after the infection (Fig. 2D). The same experiment was performed using the CT-BDNF-GFP amplicon vector and, again, we observed a nearly complete cancellation of pro-BDNF expression from MAB cells at 96 h after the injection (Fig. 2G). However, time-course differed in that the decline in pro-BDNF protein levels

occurred more slowly than with BDNF-antisense-GFP (Fig. 2H). These results indicate that, *in vitro*, both amplicon vector, BDNF-antisense-GFP and CT-BDNF-GFP, produce a highly efficient knock-down of pro-BDNF levels. Thus, both vectors were elected for *in vivo* testing.

***In vivo* validation**

We first explored the toxicity of the amplicon vectors after direct injection in the rat hippocampus. To this aim, we injected 5×10^5 t.u. of either vector in a volume of 1 □l in the right hippocampus dentate gyrus area of naïve rats and, 5 days after injection, examined gliosis, microcytosis and neuronal loss using GFAP, IBA-1 immunohistochemestry and neurotrace staining, respectively. Administration of the BDNF-antisense-GFP or of the CT-BDNF-GFP amplicon vectors did not alter the morphology of the hippocampus (Fig. 3). The density of GFAP-positive cells in the injected hippocampus compared was similar to that of the non-injected contralateral hippocampus, i.e. there was no indication of reactive astrocytosis (Fig. 3). Similar to GFAP cells, the density of IBA-1 positive cells was comparable in both the ipsilateral and the contralateral hippocampus, indicating absence of reactive microgliosis (Fig. 3). Finally, neuronal density, as measuerd using the NeuroTrace staining, was also not altered after injection of either amplicon vector (Fig. 3). Taken together, these data suggest that treatment with amplicon vectors do not induce an overt damage when directly injected in the brain.

Next, we tested the biological efficiency for down-regulation of BDNF protein levels. To this aim, we decided employ the pilocarpine model. Intra-peritoneal injection of pilocarpine in rodents provokes generalized seizures leading to a status epilepticus (SE), which drives a massive increase in BDNF levels in the hippocampus (Binder et al., 2001).

To test the efficiency of amplicon vectors, we injected them in the right dorsal hippocampus, 5 days before pilocarpine administration, and animals were then killed at 3 different time points: 3 h (peak of pilocarpine-induced increase in BDNF mRNA levels; Binder et al., 2001; Mudò et al., 1996), 6 h (peak of pilocarpine-induced increase in BDNF protein levels; Elmer et al., 1998) and 24 h after onset of SE. Rats were injected either with the control GFP, the BDNF-antisense-GFP or the CT-BDNF-GFP vector at 2 doses, 1×10^4 or 5×10^5 t.u. Amplicon vector injections into the dorsal hippocampus produced expression of GFP in infected cells (Fig. 4A for BDNF-antisense-GFP) at the site of injection, whereas a negligible number of positive cells was observed contralateral to injection under this experimental conditions. We therefore decided to use the contralateral dorsal hippocampus as an internal control. Pro-BDNF expression was measured by western blotting and the signal was normalized to □-actin. The control GFP amplicon vector did not produce any effect. The low dose (1×10^4 t.u.) of the BDNF-antisense-GFP amplicon vector exhibited a robust reduction of pro-BDNF protein levels at all time points (Fig. 4B). This effect appeared to be dose-dependent, because the high dose let to an even greater effect (data not shown). Different from the antisense strategy, only a small, non significant reduction (about 10%) in pro-BDNF protein levels was observed in low dose (1×10^4 t.u.) CT-BDNF-GFP injected hippocampi (Fig. 4B), even if GFP immunofluorescence confirmed the infection. The high dose of vector also proved ineffective in knocking down pro-BDNF levels (data not shown). Thus, the CT-BDNF-GFP amplicon vector cannot induce heterochromatin to a sufficient level to prevent transactivation in vivo, whereas the BDNF-antisense amplicon vector proves effective in knocking down efficiently pro-BDNF protein levels.

The model system we employed for analysis of BDNF knock down permits an initial evaluation of the behavioral implications. Knocking down BDNF overexpression

only in part of one hippocampus cannot be expected to produce robust behavioral effects in a model in which a pro-convulsant agent is administered systemically. However, we observed that animals treated with BDNF-antisense-GFP entered convulsive SE later then those treated with the control GFP amplicon vector (Fig. 5A). Moreover, whereas the infusion of both BDNF-antisense-GFP and CT-BDNF-GFP amplicon vectors per se did not produce over signs of behavioral toxicity, because all animals were apparently well after the surgery and in the following days, the percentage of animals that died after pilocarpine administration was higher in the high dose BDNF-antisense group (Fig. 5B). Thus, even knocking down BDNF expression in a portion of a single hippocampus seems sufficient to elicit significant behavioral effects.

Discussion

In this study, we generated two conceptually different amplicon vectors to locally knock down the levels of BDNF: a classical antisense approach and an approach based on convergent transcription. The main finding was that, whereas both approaches proved highly efficient in vitro, only the former (antisense) provided robust results in the in vivo settings of status epilepticus-induced BDNF expression in the hippocampus.

HSV-1-based amplicon particles were generated following a recently described method that produces relatively high titers of vector stocks with reduced amounts of helper virus (Epstein, 2009). The need of helper is a major limitation of the amplicon approach, and is therefore very important to reduce it (ideally, to completely eliminate it). The advantages of the amplicon approach are however significant. In particular, worth of note is the fact that the amplicon genome does not express HSV-1 replication functions,

offering the opportunity to package very large transgenic sequences: it is possible to transduce more than 110 kb of foreign DNA in a single particle (Epstein, 2005). Since this amount of space must all be filled in the helper capsid, small transgenes are repeated in concatameters, with a number of repeats that will depend on the size of the original amplicon plasmid (Kwong & Frenkel, 1984; Boehmer & Lehman 1997). In the present study, the produced BDNF-antisense-GFP and CT-BDNF-GFP amplicon vectors contained more than 20 copies of the BDNF silencing cassette. Many copies of the BDNF cassette can be expected to ensure a particularly efficient knock down of the protein of interest.

HSV-1 amplicon vectors also share many useful features of the HSV-1 parent virus (Wang and Fraefel, 2002), like the ability to infect a broad range of dividing and non-dividing host cells, including neurons. HSV amplicon vectors allow efficient infection of many neuronal types, with transgene expression over an extended period of time without demonstrable side effects (Oehmig et al., 2004).

We compared two conceptually different strategies for knocking down BDNF gene expression using amplicon vectors, the classical antisense strategy and the convergent transcription strategy. The former is based on the technique of RNA interference (RNAi) that was first discovered in Caenorhabditis elegans (Wang and Barr, 2005). RNAi is a gene silencing mechanism in which a double-stranded RNA (dsRNA) molecule is generated that directs the specific degradation of the corresponding target mRNA (Kavi et al., 2008). The BDNF-antisense-GFP amplicon targets and degrades the cytoplasmic mRNA pool of BDNF through the mechanism of RNA interference: expression of the transgene leads to formation of sense RNA-antisense RNA hybrids in the cytosol and thereby degrades and/or prevents translation of pro-BDNF mRNA. The second strategy that we tested is based on the convergent transcription (CT) technology (Tran et al., 2003) that acts through

nuclear transcriptional gene silencing. In our experimental settings, expression of the transgene leads to repression of BDNF gene transcription at the nuclear level. *In vitro* experiments demonstrated a reliable effect of both amplicon vectors in knocking down pro-BDNF levels. Thus, both silencing amplicon vectors were elected for *in vivo* studies.

To study the effects of amplicon *in vivo*, we decided to employ a status epilepticus model. Epileptogenic stimuli are known to affect the expression of BDNF transcripts in the hippocampus (Timmusk et al., 1993; Chiaruttini et al., 2008). Specifically, pilocarpine leads to increased BDNF mRNA and protein levels peaking respectively 3 and 6 h after onset of status epilepticus (Tongiorgi et al., 2004, Elmer et al., 1998). It is thought that increased BDNF levels play a role in the transformation of a normal brain in epileptic, i.e. in a brain that can spontaneously generate seizures. Indeed, spontaneous seizures begin to occur a few days or weeks after pilocarpine status epilepticus, and in this latency period is associated with plastic changes in the epileptogenic area, including increased neurogenesis, cell death, plastic modifications of synaptic contacts (Pitkanen & Sultula, 2002). BDNF exerts relevant effects upon all of these phenomena. However, it is still unclear what the implications of its increased biosynthesis could be. Strategies to down-regulate the BDNF signal have been reported by many to retard epileptogenesis (Kokaia et al., 1995; Binder et al., 1999; He et al., 2004; Liu et al., 2013), and bath-applied BDNF exacerbates seizure activity in the epileptic hippocampus *in vitro* (Scharfman, 1997; Scharfman et al., 1999). In contrast, the combined supplementation of BDNF and fibroblast growth factor 2 (FGF-2) has been reported to attenuate cellular alterations associated with epileptogenesis and to highly significantly reduce the frequency and severity of spontaneous recurrent seizures (Paradiso et al., 2009; Bovolenta et al., 2010; Paradiso et al., 2011). To dissect out these mechanisms there is a need to develop tools to locally modulate the BDNF signal *in vivo*, in particular to block it.

Therefore, we decided to test the ability of our vectors to down-regulate BDNF expression in the pilocarpine model system. First, in keeping with previous reports (Oehmig et al., 2004), we found that *in vivo* injection of amplicon vectors did not cause obvious toxic effects (cell death) nor significant activation of astrocytes or microglia. Second, and more important, we found that the silencing activity mediated by the BDNF-antisense-GFP amplicon vector was highly significant, even at relatively low doses, whereas the CT-BDNF-GFP amplicon vector did not produce significant reductions in pro-BDNF levels. Why the efficiency of *in vivo* silencing was so different between the two strategies, in spite of the fact that both were equally effective *in vitro*, is difficult to understand. One hypothesis may be that competition with the pilocarpine-induced transactivation of the BDNF gene (the CT-BDNF strategy) is harder than regulation of the cytosolic BDNF mRNA pool (with the BDNF-antisense strategy).

Importantly, the knock down of BDNF levels induced with BDNF-antisense-GFP was sufficient to produce significant behavioral effects, in spite of the fact that it was produced in a part of a single hippocampus and not in the entire epileptogenic area. Moreover, the kind of behavioral results that were obtained are also worth noting, in that they reflect the double-edge pattern of BDNF effects in epileptogenesis. On one hand, consistent with the pro-epileptic effects of BDNF (Kokaia et al., 1995; Binder et al., 1999; He et al., 2004; Liu et al., 2013) we observed an increased latency to onset of status epilepticus in BDNF-antisense-GFP-injected animals. On the other hand, consistent with the neuroprotective role of BDNF (Paradiso et al., 2011) we observed an increased mortality of animals injected with BDNF-antisense-GFP. These initial data must be verified and extended using multiple, bilateral injections ensuring a robust and widespread knock down of BDNF gene expression in the epileptogenic region.

In conclusion, this study demonstrates a reliable effect of amplicon vectors in knocking down gene expression. At variance with the convergent transcription strategy, which is effective only *in vitro*, the BDNF-antisense-GFP amplicon vector proves effective both *in vitro* and *in vivo*, knocking down efficiently BDNF protein levels in the injected hippocampus at different time points. Therefore, the antisense strategy seems a better choice for silencing BDNF expression *in vivo*. This is further supported by the observation that even knocking down BDNF expression in a portion of a single hippocampus is sufficient to elicit significant behavioral effects. Taken together, these data illustrate the broad potential of amplicon vectors as gene transfer tools for silencing gene expression.

Acknowledgements

This work has been supported by a grant from the European Community [FP7-PEOPLE-2011-IAPP project 285827 (EPIXCHANGE)] to MS and HB.

References

Binder DK, Routbort MJ, McNamara JO (1999) Immunohistochemical evidence of seizure-induced activation of trk receptors in the mossy fiber pathway of adult rat hippocampus. J. Neurosci. 19: 4616–4626.

Binder DK, Croll SD, Gall CM, Scharfman HE (2001) BDNF and epilepsy: too much of a good thing? Trends Neurosci 24: 47-53.

Boehmer PE, Lehman IR (1997) Herpes simplex virus DNA replication. Annu Rev Biochem 66: 347-384.

Bovolenta R, Zucchini S, Paradiso B, Rodi D, Merigo F, Navarro Mora G, Osculati F, Berto E, Marconi P, Marzola A, Fabene PF, Simonato M (2010) Hippocampal FGF-2 and BDNF overexpression attenuates epileptogenesis-associated neuroinflammation and reduces spontaneous recurrent seizures. J Neuroinflammation 7:81.

Chao-Chung YS and Becker KG (2003) A genome-wide view of antisense. Nat Biotechnol 21:492.

Chiaruttini C, Sonego M, Baj G, Simonato M, Tongiorgi E (2008) BDNF mRNA splice variants display activity-dependent targeting to distinct hippocampal laminae. Mol Cell Neurosci 37:11–19.

Cohen-Cory S, Kidane AH, Shirkey NJ, Marshak S (2010) Brain- derived neurotrophic factor and the development of structural neu- ronal connectivity. Dev Neurobiol 70:271–288.

Elmer E, Kokaia K, Kokaia M, Carnahan J, Nawa H, Lindvall O (1998) Dynamic changes of brain-derived neurotrophic factor protein levels in the rat forebrain after single and recurring kindling-induced seizures. Neurosci 83: 351-362.

Epstain A (2005) HSV-1-based amplicon vectors: design and applications. Gene Therapy 12:154-158.

Epstein A (2009) HSV-1-derived amplicon vectors: recent technological improvements and remaining difficulties. Mem Inst Osw Cruz 104:399-410.

Fire A, Xu S, Montgomery MK, Kostas SA, Driver SE, Mello CC (1998) Potent and specific genetic interference by double-stranded RNA in Caenorhabditis elegans. Nature 391: 806–811.

Giordano E, Rendina R, Peluso I and Furia M (2002) RNAi Triggered by Symmetrically Transcribed Transgenes in Drosophila melanogaster. Genetics 160:637-648.

Gullerova M, Proudfoot NJ (2012) Convergent transcription induces transcriptional gene silencing in fission yeast and mammalian cells. Nat Struct Mol Biol 19: 1193-201.

He XP, Kotloski R, Nef S, Luikart BW, Parada LF, McNamara JO (2004) Conditional deletion of TrkB but not BDNF prevents epileptogenesis in the kindling model. Neuron 43: 31–42.

Kavi HH, Fernandez H, Xie W, Birchler JA (2008) Genetics and biochemistry of RNAi in Drosophila. Curr Top Microbiol Immunol 320:37-75.

Kokaia M, Ernfors P, Kokaia Z, Elmer E, Jaenisch R, Lindvall O (1995) Suppressed epileptogenesis in BDNF mutant mice. Exp. Neurol. 33: 215–224.

Kwong AD, Frenkel N (1984) Herpes simplex virus amplicon: effect of size on replication of constructed defective genomes containing eucaryotic DNA sequences. J Virol 51: 595-603.

Lee NS, Dohjima T, Bauer G, Li H, Li MJ, Ehsani A, Salvaterra P and Rossi J (2002) Expression of small interfering RNAs targeted against HIV-1 rev transcripts in human cells. Nat Biotechnol 20:500-505.

Liu G, Gu B, He XP, Joshi RB, Wackerle HD, Rodriguiz RM, Wetsel WC, McNamara JO

(2013) Transient inhibition of TrkB kinase after status epilepticus prevents development of temporal lobe epilepsy. Neuron 79: 31-8.

Mudò G, Jiang XH, Timmusk T, Bindoni M, Belluardo N (1996) Change in Neurotrophins and Their Receptor mRNAs in the Rat Forebrain After Status Epilepticus Induced by Pilocarpine. Epilepsia 37:198-207.

Oehmig A, Fraefel C, Xandra O, Breakefield (2004) Update on Herpesvirus Amplicon Vectors. Molecular Therapy 10:630-643.

Paradiso B, Marconi P, Zucchini S, Berto E, Binaschi A, Bozac A, Buzzi A, Mazzuferi M, Magri E, Navarro Mora G, Rodi D, Su T, Volpi I, Zanetti L, Marzola A, Manservigi R, Fabene PF, Simonato M (2009) Localized delivery of fibroblast growth factor-2 and brain-derived neurotrophic factor reduces spontaneous seizures in an epilepsy model. Proc Natl Acad Sci U S A 106: 7191-6.

Paradiso B, Zucchini S, Su T, Bovolenta R, Berto E, Marconi P, Marzola A, Navarro Mora G, Fabene PF, Simonato M (2011) Localized overexpression of FGF-2 and BDNF in hippocampus reduces mossy fiber sprouting and spontaneous seizures up to 4 weeks after pilocarpine-induced status epilepticus. Epilepsia 52: 572-8.

Paul CP, Good PD, Winer I and Engelke DR (2002) Effective expression of small interfering RNA in human cells. Nat Biotechnol 20:505-508.

Pitkänen A, Sutula TP (2002) Is epilepsy a progressive disorder? Prospects for new therapeutic approaches in temporal-lobe epilepsy. Lancet Neurol 1: 173-81.

Scharfman HE (1997) Hyperexcitability in combined entorhinal/hippo- campal slices of adult rat after exposure to brain-derived neurotrophic factor. J. Neurophysiol. 78: 1082–1095.

Scharfman HE, Goodman JH, Sollas AL (1999) Actions of brain-derived neurotrophic factor in slices from rats with spontaneous seizures and mossy fiber sprouting in the

dentate gyrus. J. Neurosci. 19: 5619–5631.

Shendure J and Church GM (2002) Computational discovery of sense- antisense transcription in the human and mouse genomes. Genome Biol 3:RESEARCH0044.

Shi H, Djikeng A, Mark T, Wirtz E, Tschudi C and Ullu E (2000) Genetic interference in Trypanosoma brucei by heritable and induc- ible double-stranded RNA. Rna 6:1069-1076.

Simonato M, Tongiorgi E, Kokaia M (2006) Angels and demons: neurotrophic factors and epilepsy. Trends Pharmacol Sci 27: 631-638.

Simonato M, Zucchini S (2010) Are the neurotrophic factors a suitable therapeutic target for the prevention of epileptogenesis? Epilepsia 51(Suppl 3):48-51.

Timmusk T, Palm K, Metsis M, Reintam T, Paalme V, Saarma M, Persson H (1993) Multiple promoters direct tissue-specific expres- sion of the rat BDNF gene. Neuron 10:475–489.

Tongiorgi E, Armellin M, Giulianini PG, Bregola G, Zucchini S, Paradiso B, Steward O, Cattaneo A, Simonato M (2004) Brain- derived neurotrophic factor mRNA and protein are targeted to dis- crete dendritic laminas by events that trigger epileptogenesis. J Neurosci 24:6842–6852

Tran N, Cairns MJ, Dawes IW, Arndt GM (2003) Expressing functional siRNAs in mammalian cells using convergent transcription. BMC Biotech. 3:21

Wang J, Tekle E, Oubrahim H, Mieyal JJ, Stadtman ER and Chock PB (2003) Stable and controllable RNA interference: Investigating the physiological function of glutathionylated actin. Proc Natl Acad Sci U S A 100:5103-5106.

Wang J, Barr MM (2005) RNA interference in Caenorhabditis elegans. Methods Enxymol 392:36-55.

Wang S, Fraefel C, et al. (2002) HSV-1 amplicon vectors. Methods Enzymol 346:593□/603.

Yoshii A, Constantine-Paton M. 2010. Postsynaptic BDNF-TrkB sig- naling in synapse maturation, plasticity, and disease. Dev Neurobiol 70:304–322.

Figures

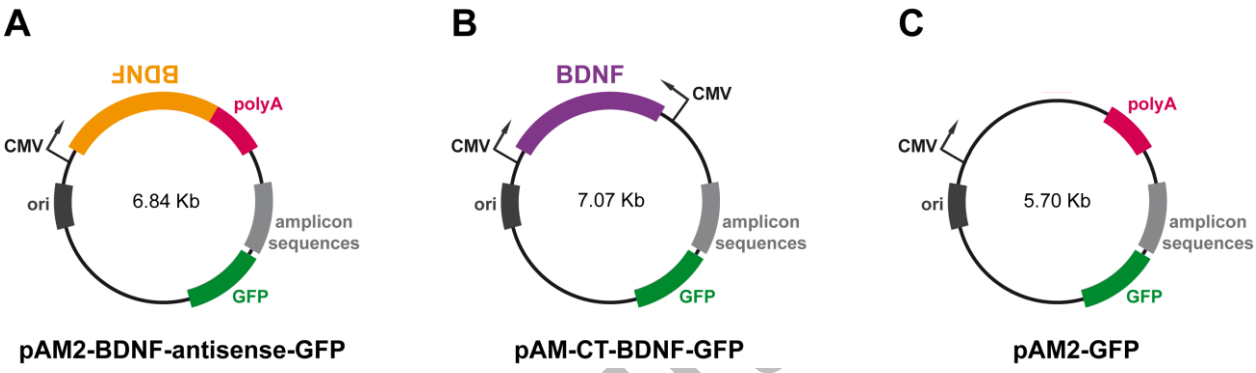

Figure 1. *Structure of the amplicon plasmids.* (A) The pAM2-BDNF-antisense-GFP plasmid (6.84 Kb) results by insertion in antisense orientation of a fragment (1.1 Kb) containing the BDNF sequence and a poly-A tail. (B) In the pAM-CT-BDNF-GFP plasmid (7.07 Kb), the BDNF sequence (1.1 Kb) is inserted in convergent transcription, between two CMV promoters. (C) The control plasmid, pAM2-GFP plasmid (5.70 Kb).

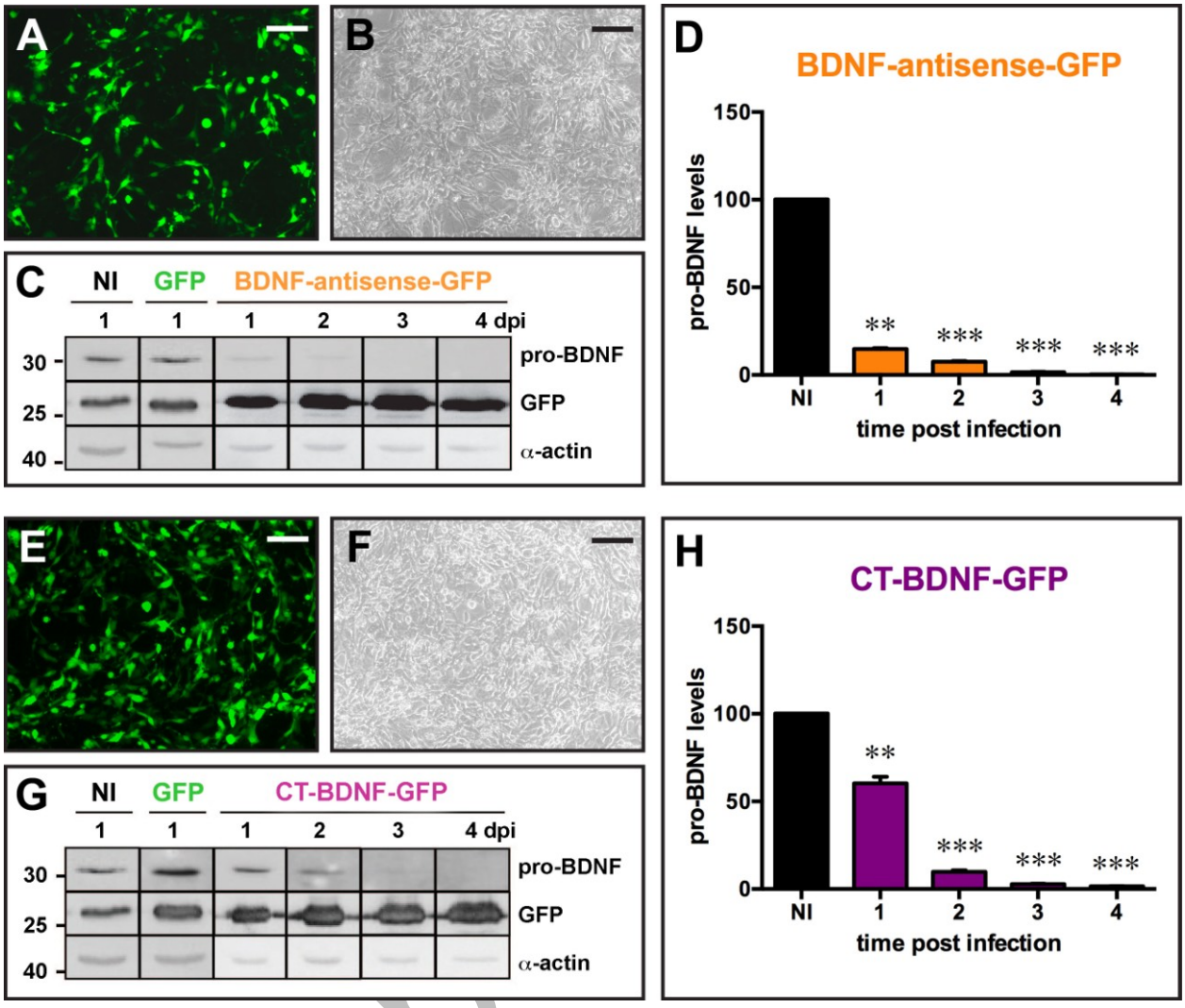

Figure 2. *In vitro validation of the amplicon vectors.* (A to D) Infection of mesoangioblast (MABs) constitutively expressing BDNF with the BDNF-antisense-GFP amplicon vector at MOI 5. Infection of the cells with amplicon vectors was confirmed by GFP fluorescence (A) and GFP detection on western blot (C). Pro-BDNF expression was analyzed by western blot in the 4 days following infection. The pro-BDNF signal was normalized to □-actin for quantification (D). (E to H) Infection of MABs with the CT-BDNF-GFP amplicon vector at MOI 5. Infection of the cells was confirmed by GFP fluorescence (E) and GFP detection on western blot (G). Pro-BDNF expression was analyzed by western blot in the 4 days following infection. The pro-BDNF signal was normalized to actin for quantification (H). * $p<0.05$, **$P<0.01$, ***$p<0.001$: Anova and post-hoc Dunnett test. Horizontal bar in panels A, B, E and F = 25 μm.

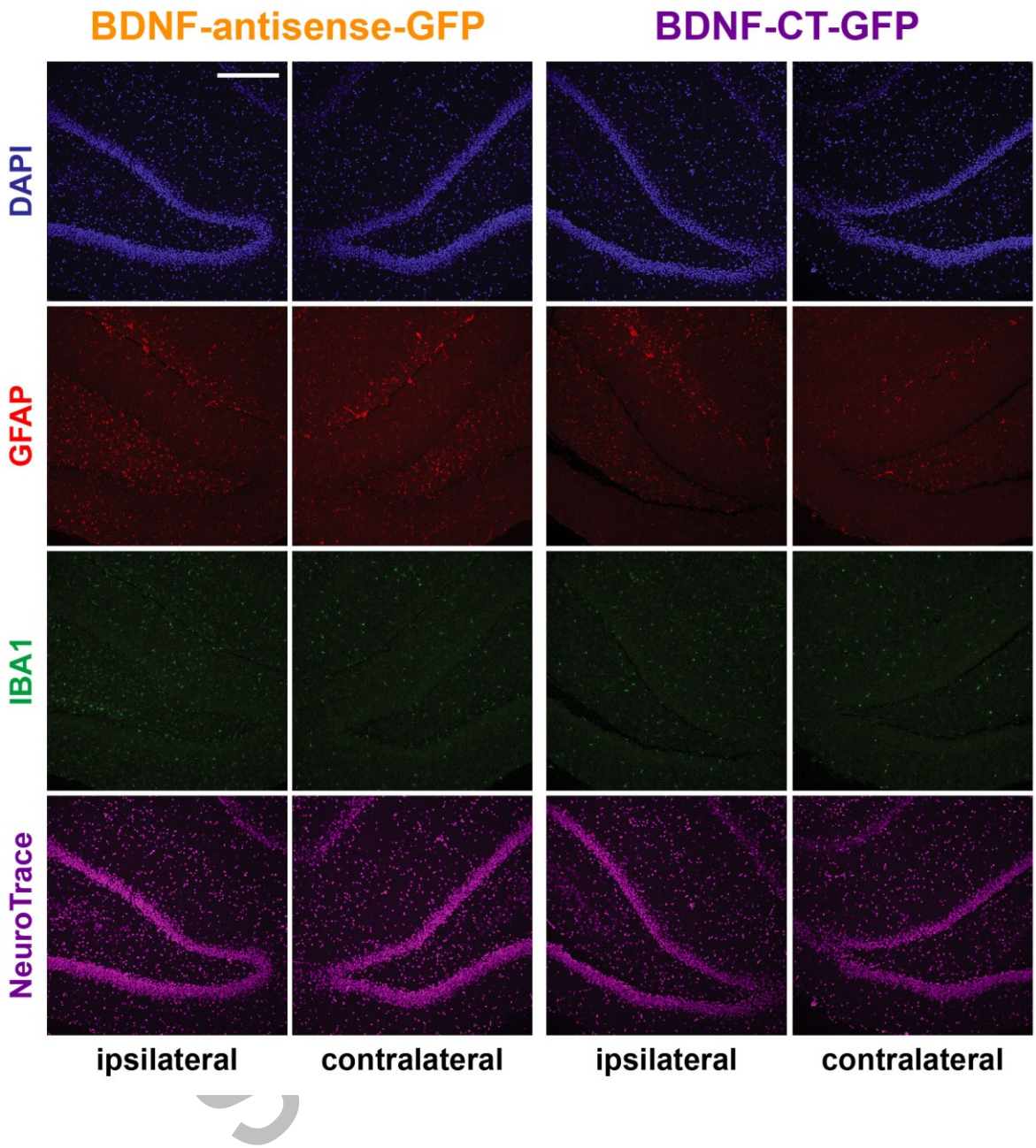

Figure 3. *Absence of overt amplicon vector-induced toxicity after injection in the dorsal hippocampus*. Dentate gyrus (DG) of the dorsal hippocampus injected (ipsilateral) and noninjected (controlateral) with BDNF-antisense-GFP amplicon vector (A) or with CT-BDNF-GFP amplicon vector (B). Nuclei are marked by DAPI in blu, GFAP-positive astrocytes in red, IBA-1-positive microglia in green and neuronal nuclei are laveled by NeuroTrace in magenta. Horizontal bars = 100 μm.

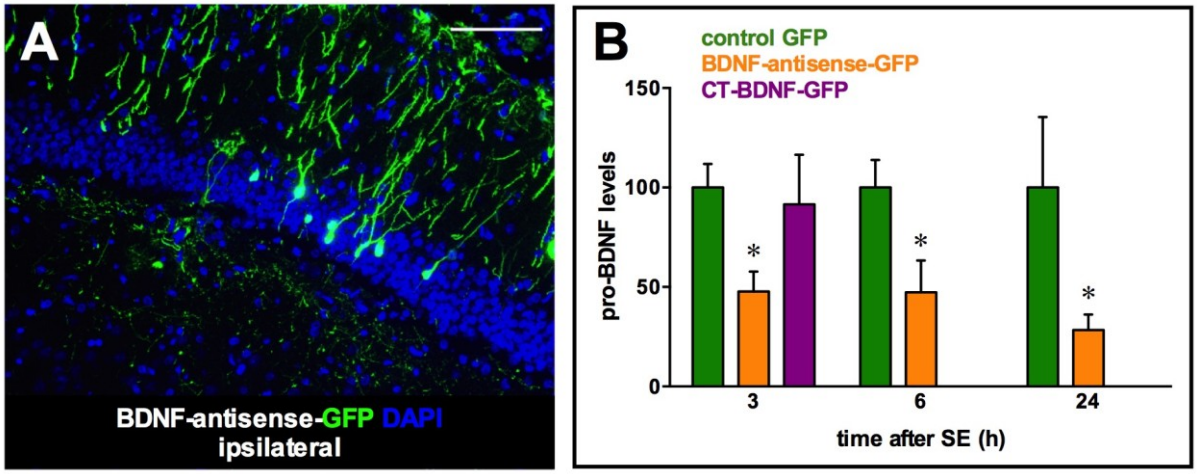

Figure 4. *Transgene expression following injection of amplicon vectors in the right hippocampus at different time points after pilocarpine-induced status epilepticus.* (A) Representative GFP immunofluorescence in the dorsal hippocampus of a rat injected with the BDNF-antisense-GFP amplicon vector. (B) Quantification of the pro-BDNF signal, normalized to α-actin, 3, 6 and 24 h after pilocarpine status epilepticus induced 5 days after injection of the amplicon vectors in the right dorsal hippocampus. * $p<0.05$, ANOVA and post-hoc Dunnett test. Horizontal bar in A = 25 μm.

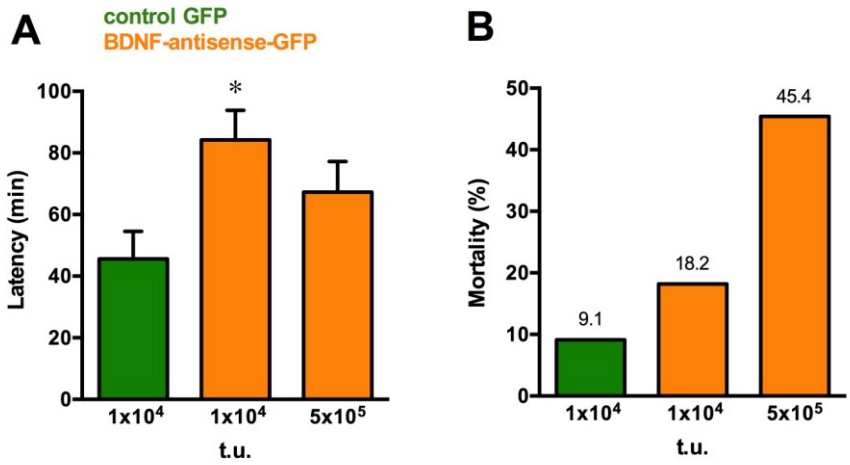

Figure 5. (A) Time to enter convulsive status epilepticus following administration of the different dose of BDNF-antisense-GFP vector. * $p<0.05$, ANOVA and post-hoc Dunnett test. (B) Mortality of pilocarpine-treated animals injected with the different dose of BDNF-antisense-GFP amplicon vector.

2.4 SEIZURE-SUPPRESSANT EFFECT OF ENCAPSULATED BDNF-PRODUCING CELLS IN A RAT MODEL OF TEMPORAL LOBE EPILEPSY

Seizures-suppressant effect of encapsulated BDNF-producing cells in a rat model of temporal lobe epilepsy

Falcicchia C.[1,2], Emerich D.F.[2], Tornøe J.[4], Wahlberg L.U.[2,4] and Simonato M.[1,3]

[1] *Department of Medical Science, Section of Pharmacology, Neuroscience Center, University of Ferrara and National Institute of Neuroscience, Ferrara, Italy;*
[2] *NsGene Inc., Ballerup, Denmark;*
[3] *Laboratory of Technologies for Advanced Therapy (LTTA), Technopole of Ferrara, Ferrara, Italy;*
[4] *NsGene A/S, Providence, RI, USA.*

Running title:

BDNF-producing cells for epilepsy

Corresponding author:

Chiara Falcicchia
Department of Medical Sciences, Section of Pharmacology
University of Ferrara
Via Fossato di Mortara 17-19
44121 Ferrara, Italy
Tel: (+39) 0532 455345
Fax: (+39) 0532 455205
e-mail address: chiara.falcicchia@unife.it

Abstract

Brain-derived neurotrophic factor (BDNF) is a potential therapeutic target for temporal lobe epilepsy, but evaluation of its potential is complicated by difficulties in its delivery. Here, we describe the effect on epileptic seizures of encapsulated cell biodelivery (ECB) devices filled with genetically modified human cells engineered to release BDNF. Encapsulated cells can survive long-term in the host tissue and ensure continued release of the therapeutic molecule. Moreover, they hold the advantage of being a reversible treatment. These devices, bilaterally implanted in the hippocampus, significantly decreased the frequency of spontaneous seizures in rats made chronically epileptic after pilocarpine-induced status epilepticus, whereas animals implanted with empty devices or with devices containing parental ARPE-19 cells displayed identical seizure frequency and severity as those completely untreated. Thus, ECB device-mediated long-term supplementation of BDNF in the epileptic tissue may represent a valid strategy to control spontaneous seizures.

Keywords

BDNF, ECB devices, hippocampus, epilepsy

Introduction

One third of the epilepsies are refractory to medical treatment and, therefore, it is highly needed to find new therapies acting with mechanisms that are different from those of the drugs currently in use (Simonato et al., 2014). In this sense, neurotrophic factors like brain-derived neurotrophic factor (BDNF) may represent interesting candidates, because an extensive literature demonstrates their involvement in each of the cellular alterations associated with epileptogenesis: not only do their trophic effects suggest an involvement in cell death, neurogenesis and axonal sprouting, but they also exert effects at the synaptic level, with distinct modulatory actions at excitatory and inhibitory synapses (Simonato et al., 2006).

However, BDNF has been reported to exert contrasting effects in epilepsy, depending on the period in the natural history of the disease (the latent period between and epileptogenic insult and the beginning of spontaneous seizures vs. the chronic epileptic period) and/or on specific alterations in some of its biological properties (biosynthesis, processing, subcellular sites of action, …) and/or on the delivery strategy (direct intracerebral injection, use of viral vectors, …). Thus, the therapeutic potential of BDNF for epilepsy is still controversial (Koyama and Ikegaya, 2005; Kuramoto et al., 2011; Simonato et al., 2006).

Addressing the issue of BDNF therapeutic potential is further complicated by difficulties in its delivery. No traditional small-molecule drug with suitable pharmacokinetics and capable to act as agonist or antagonist at the high-affinity BDNF receptor TrkB has been yet developed. Moreover, delivery strategies based on cell grafts or viral vectors generally provide a relatively short-term treatment whereas, by their very nature, chronic diseases like epilepsy require long-term treatments.

Here, we describe the effect on epileptic seizures of encapsulated cell biodelivery (ECB) devices filled with genetically modified human cells engineered to release BDNF into the host tissue. Encapsulated cells can survive long-term in the host tissue and ensure continued release of the therapeutic molecule (Emerich et al., 2014). Moreover, they hold the advantage of being a reversible treatment (Nikitidou et al., 2013).

Materials and Methods

Cell culture. ARPE-19 cells, a spontaneously immortalized human retinal pigment epithelial cell line, were cultured using standard plating and passaging procedures in T-75 flasks and incubated at 37°C, 90% humidity and 5% CO_2. The growth medium consisted of Dulbecco's modified Eagle's medium (DMEM)/Nutrient Mix serum with Glutamax (Invitrogen Gibco, USA) supplemented with 10% fetal bovine serum (Gibco). Routine culture consisted of feeding the cells every 2-3 days and passaging them at 70-75% confluence. Cells were split at a 1:3 ratio using TrypLE Select (Invitrogen) following dissociation. Briefly, the medium was removed, the TrypLE dissociation enzyme was added to the flask, and cells were allowed to detach for 3-5 minutes. Cells were then harvested, spun down and resuspended in medium. Finally, T-75 flasks were seeded with 437,500 cells (2500 cells/cm^2).

BDNF-secreting cell line establishment. We generated clonal BDNF-secreting ARPE-19 cell lines using the sleeping beauty (SB) transposon expression system. ARPE-19 cells were co-transfected with the plasmid pT2.CAn.hopp.BDNF that contains the entire pre-pro BDNF sequence and the SB vector pCMV-SB-100x. This technology uses an optimized SB transposase (SB100x), which mediates genomic integration of multiple

copies of the transgene inserted between two transposon terminal inverted repeats. The preferred sites for genomic SB integration are palindromic AT repeats, and the insertion site distribution is nearly random. This vector system is capable of stable gene transfer with long-term gene expression. Clones were selected using G418 (Sigma-Aldrich, Germany) and single colonies were isolated and expanded based on their BDNF release levels. Colonies producing high levels of BDNF were further characterized.

Encapuslation of cells in the ECB device. Small devices for cell culture experiments were built as follows: 7 mm long semipermeable polyethersulfone (PES) hollow fibers (Akzo Membrana, Obernburg, Germany), with an inner diameter of 500 µm and a mean molecular weight cut-off of 280 kd, were fitted with a cored poly-vinyl alcohol (PVA) cylindrical foam matrix (Clinicel, Mpact, Eudora, Kansas USA). A load tube was attached to the membrane in one end with ultraviolet-cured acrylic glue, and in the other end it was sealed with the same glue. Prior to filling, ARPE-19-BDNF cells were cultured in growth medium. Cells were dissociated and suspended in Human Endothelial Serum-free medium (HE-SFM; Invitrogen) at a density of 100,000 cell/µl. Five µl of cell solution ($5x10^4$ cells in total) were injected into each device using a custom manufactured automated cell-loading system. Devices were kept in HE-SFM at 37°C and 5% CO_2 for 2-3 weeks prior to surgical implantation. Devices loaded with non-modified ARPE-19 cells or without cells were treated in the same manner and included as negative controls.

***Device verification*.** The amount of BDNF released by each capsule over a 4 h and 24 h incubation period in HE-SFM was measured using the Human BDNF Quantikine ELISA Kit (R&D systems, Minneapolis, USA). Standards and samples were assayed in duplicate according to manufacturer's instructions, and results were expressed in ng BDNF per 4 h or per 24 h.

Animals. The experiments involving animals were conducted in accordance with European Community (EU Directive 2010/63/EU), national and local laws and polices (authorization: D.M. 83/2009-B and D.M. 246/2012-B). Male Sprague-Dawley rats (250-350 g; Harlan, USA) were used for all experiments. They were housed under standard conditions: constant temperature (22-24ºC) and humidity (55- 65%), 12 h light/dark cycle, free access to food and water.

Pilocarpine treatment. Pilocarpine was administered i.p. (340 mg/kg), and the rats' behavior was observed for 3 h thereafter, using the Racine's scale. Within the first hour after injection, all animals developed seizures evolving into recurrent generalized convulsions (status epilepticus, SE). SE was interrupted 3 h after onset by administration of diazepam (10 mg/kg i.p.)

Surgery. Surgery for ECB device implantation was performe 20 days after SE, between two video monitoring sessions (describe below). Rats were anaesthetized using isoflurane (3-4%) and positioned in a stereotaxic frame (Stoelting, Dublin, Ireland). A midline incision was made in the scalp and two bilateral holes drilled through the scull. Devices filled with ARPE-19 BDNF cell (n=10) were bilaterally implanted in hippocampus in vertical position by an implantation cannula mounted to the stereotaxic frame. The implantation coordinates, with respect to bregma, were: AP: -4.8, ML: ±4.6 and DV: -7.0 (Fig. 1). After implantation, the skin was suture closed.

Video monitoring. Video monitoring was performed using Swann 4 channel System (Swann, Santa Fe Springs, California USA). The first video monitoring session was between day 10 and day 20 after SE, i.e. shortly after animals started experiencing spontaneous seizures (Paradiso et al., 2009). The second video monitoring session was after implantation of the ECB-device, between day 25 and day 35 after SE. Seizure severity was scored using the scale of Racine (Racine, 1972): 1, chewing or mouth and

facial movements; 2, head nodding; 3, forelimb clonus; 4, generalized seizure with rearing; 5, generalized seizure with rearing and falling.

Post-experiment device verification. At the end of the experiments, rats were deeply anaesthetized, decapitated and their brains removed. The devices were retrieved and incubated at 37°C in HE-SFM. Media samples for determination of BDNF release were collected the next day.

Immunohistochemistry. Brains were rapidly removed and frozen in 2-methylbutane. Coronal sections (20 μm thick) were cut across the entire hippocampus, and mounted onto polarized slides (Superfrost slides, Diapath-Microstain, Italy). DAPI immunofluorescence was performed on section re-hydrated in distilled water for 5 min. Sections were washed in phosphate-buffered saline (PBS) 1× for 10 min and than stained with 0.0001% DAPI for 15 min, and washed again. Coverslips were mounted using anti fading, water based Gel/Mount (Sigma).

Results

Efficiency of the devices: BDNF release

To verify the efficacy of the devices, we first measured the release of BDNF in the incubation culture media, after filling each ECB device with ARPE-19 BDNF producing cells. Before implantation in the hippocampus, each device was filled with cells, incubated in HE-SFM medium for 2 weeks, then positioned into a well containing 1 ml fresh HE-SFM medium and incubated at 37°C (5% CO2) for 4 or 24 h. BDNF concentrations in the medium were measures using an ELISA assay. Devices were then implanted and the same procedure was repeated within 24 h after explantation at the end of the experiment, i.e.

following 15 days in vivo. Before implantation, the average BDNF concentration in the medium was 23.13±0.71 ng/ml for 4 h and 139.48±5.21 ng/ml for 24 h incubation, while after the explantation it was about three times higher, i.e. 77.17±7,24 and 454.87±47.96 ng/ml, respectively after 4 and 24 h incubation (Fig. 1).

Video monitoring

Pilocarpine administration induced a convulsive status epilepticus (SE) that was interrupted 3 h after onset through the i.p. injection of diazepam. For 2–3 days after SE, animals experienced some occasional, self-limiting generalized seizures and then entered a latency state in which they were apparently well (Curia et al., 2008; Mazzuferi et al., 2010; Paradiso et al., 2009; Soukupova et al., 2014). To verify that the animals employed in this study presented the previously reported epilepsy development and progression, all animals were continuously video monitored between day 10 and day 20 after SE (referred to herein as early chronic period) and between day 25 and 35 after SE (herein late chronic period), to verify frequency, severity and duration of the spontaneous generalized seizures, class 4 or 5 according to the Racine scale (Racine, 1972). Spontaneous seizures occurred in all animals. In early chronic rats, the mean daily frequency of generalized seizures was 1.9±0.2, while it was 2.8±0.1 in late chronic rats; the mean forelimb clonus duration was 34±2 s in the early chronic and 46±1 s in the late chronic group (Fig. 2). These data indicate a progression of the disease.

Twenty days after SE, at the end of the first monitoring epoch, all animals were randomly assigned to four groups: one group was not treated at all (naïve); the second group was bilaterally implanted with empty ECB devices; the third group with two devices filled with parental ARPE-19 cells; the last group with ECB devices filled with ARPE-19-BDNF cells. Animals without any device displayed an average of 2.8±0.1 generalized

seizures per day; similar to these controls, the group of empty devices and the group of animals implanted with ARPE-19 devices presented a mean of daily seizure of 2.9±0.1 and 2.7±0.1 respectively. On the contrary, animals treated with ECB-ARPE-19-BDNF devices displayed only 0.7±0.1 seizures per day (Fig. 3A). No difference in any of the parameters analyzed in this study was observed between the first three groups, and therefore they have been pooled together for statistical analysis and collectively termed "control devices" group. Thus, a highly significant decrease (about 75%) of the frequency of spontaneous seizures was observed between the control group (2.8±0.1 generalized seizures/day) and the treated ARPE-19-BDNF devices animals (Fig. 3A).

The forelimb clonus duration (s), however, was only moderately (yet significantly) decreased in animals implanted with the ARPE-19-BDNF device compared with control groups (36±4 s vs. 46±1 s; Fig. 3B).

Placement of the ECB devices

DAPI staining was performed on sections from brains of all animals to confirm the correct position of the ECB devices in the hippocampus (Fig. 4).

Discussion

In this study we demonstrate that ECB devices filled with ARPE-19 cells modified to secrete high levels of BDNF, when implanted in the hippocampus, significantly decrease the frequency of spontaneous seizures in rats made chronically epileptic. This effect was somewhat unexpected, in that it has been previously reported that a Herpes Simplex vector-mediated supplementation of BDNF in the hippocampus of epileptic rats did not

produce any alteration in spontaneous seizure frequency or severity (Paradiso et al., 2009). However, some major differences exist between this previous paper and the present one: first, the BDNF delivery method differed (endogenous cell infected by the vector producing and secreting BDNF vs. ECB); second, BDNF was expressed together with fibroblast growth factor 2 (FGF-2) by the viral vector; third, the viral vector induced expression of the transgenes (BDNF and FGF-2) only in the dorsal hippocampi, whereas ECB devices were implanted bilaterally and released BDNF in a wider area, mainly in the ventral hippocampus. Thus, the pattern of BDNF supplementation can be expected to be significantly different in the two studies, being more widespread and robust with ECB devices. The concept that sufficiently high levels of BDNF may produce antiseizure effects is in line with the finding that BDNF reduces $GABA_A$ receptor desensitization in the human and in the murine epileptic hippocampus (Palma et al., 2005; 2007).

These findings suggest that ECB devices could potentially be an alternative source for exogenous long-term delivery of BDNF to the hippocampus, and that this strategy can reduce the frequency of generalized seizures. Of course, a limiting factor may be the extent of damage caused by the implant. However, this factor did not prove critical in the present experimental setup, in that animals implanted with empty devices or with devices containing parental ARPE-19 cells displayed identical seizure frequency and severity as those completely untreated. Moreover, in translational terms the impact of damage would be relatively smaller in the much larger human brain.

One difficult issue to solve is the genuine BDNF-dependence of the effects. Unfortunately, no small molecule TrkB antagonist with suitable pharmacokinetics for peripheral administration is currently available, and the ECB device does not allow practical space for intra-hippocampal injection in the entire area where it releases BDNF. However, the effects observed in this study are very likely dependent on BDNF, because

animals treated with parental ARPE-19 cells (not producing BDNF) displayed a daily frequency of seizures comparable to empty devices and not to ARPE-19 BDNF devices.

In conclusion, the present data suggest that BDNF, continuously released in the epileptic hippocampus, reduces the frequency of generalized seizures. Understanding in depth the mechanistic basis of this effect will require further studies. However, this approach may be applied to patients that are selected for surgical resection of the epileptic hippocampus. These patients may undergo implantation of depth electrodes to define the epileptogenic area before surgery. A ECB device may be implanted together with electrodes: if it proved ineffective, it would be removed and the patient would undergo surgery as originally planned; if effective, the patient would have the option of avoiding surgery. Importantly, the ECB technology has been already tested in other neurologic disease, such as Alzheimer's disease, and has demonstrated good safety and tolerability (Tornoe et al., 2012; Eriksdotter-Jonhagen et al., 2012).

Acknowledgements

This work has been supported by a grant from the European Community [FP7-PEOPLE-2011-IAPP project 285827 (EPIXCHANGE)] to MS and LW.

References

Curia G, Longo D, Biagini G, Jones RS, Avoli M (2008) The pilocarpine model of temporal lobe epilepsy. J. Neurosci. Methods 172, 143–157.

Emerich DF, Orive G, Thanos C, Tornoe J, Wahlberg LU (2014) Encapsulated cell therapy for neurodegenerative diseases: From promise to product. Adv. Drug. Deliv. Rev. 67-68: 131-141.

Eriksdotter-Jonhagen M, Linderoth B, Lind G et al. (2012) Encapsulated cell biodelivery of nerve growth factor to the Basal forebrain in patients with Alzheimer's disease. Dement Geriatr Cogn Disord 33:28-38.

Koyama R, Ikegaya Y (2005) To BDNF or not to BDNF: that is the epileptic hippocampus. Neuroscientist 11: 282–287.

Kuramoto S, Yasuhara T, Agari T, Kondo A, Jing M, Kikuchi Y, Shinko A, Wakamori T, Kameda M, Wang F, Kin K, Edahiro S, Miyoshi Y, Date I (2011) BDNF-secreting capsule exerts neuroprotective effects on epilepsy model of rats. Brain Research 1368: 281-289.

Mazzuferi M, Palma E, Martinello K, Maiolino F, Roseti C, Fucile S, Fabene PF, Schio F, Pellitteri M, Sperk G, Miledi R, Eusebi F, Simonato M (2010) Enhancement of GABA(A)-current run-down in the hippocampus occurs at the first spontaneous seizure in a model of temporal lobe epilepsy. Proc. Natl. Acad. Sci. U. S. A. 107, 3180–3185.

Nikitidou L, Torp M, Fjord-Larsen L, Kusk P, Wahlberg LU, Kokaia M (2013) Encapsulated galanin-producing cells attenuate focal epileptic seizures in the hippocampus Epilepsia: 1–8.

Palma E, Spinelli G, Torchia G, Martinez-Torres A, Ragozzino D, Miledi R, and Eusebi F (2005) Abnormal GABAA receptors from the human epileptic hippocampal subiculum microtransplanted to Xenopus oocytes. Proc Natl Acad Sci USA 102:2514-2518.

Palma E, Roseti C, Maiolino F, Fucile S, Martinello K, Mazzuferi M, Aronica E, Manfredi M, Esposito V, Cantore G, Miledi R, Simonato M, Eusebi F (2007) GABAA-current rundown of temporal lobe epilepsy is associated with repetitive activation of GABA(A) "phasic" receptors. Proc Natl Acad Sci USA 104:20944-8.

Paradiso B, Marconi P, Zucchini S, Berto E, Binaschi A, Bozac A, Buzzi A, Mazzuferi M, Magri E, Navarro Mora G, Rodi D, Su T, Volpi I, Zanetti L, Marzola A, Manservigi R, Fabene PF, Simonato M (2009) Localized delivery of fibroblast growth factor-2 and brain- derived neurotrophic factor reduces spontaneous seizures in an epilepsy model. Proc Natl Acad Sci 106: 7191-7196.

Racine RJ (1972) Modification of seizure activity by electrical stimulation. II. Motor seizure. Electroencephalogr Clin Neurophysiol 32:281-294.

Simonato M, Tongiorgi E, Kokaia M (2006) Angels and demons: neurotrophic factors and epilepsy. Trends Pharmacol Sci 27: 631-638.

Simonato M, Brooks-Kayal AR, Engel J Jr, Galanopoulou AS, Jensen FE, Moshé SL, O'Brien TJ, Pitkanen A, Wilcox KS, French JA (2014) The challenge and promise of anti-epileptic therapy development in animal models. Lancet Neurol 13: 949-60.

Soukupova Soukupová M, Binaschi A, Falcicchia C, Zucchini S, Roncon P, Palma E, Magri E, Grandi E, Simonato M (2014) Impairment of GABA release in the hippocampus at the time of the first spontaneous seizure in the pilocarpine model of temporal lobe epilepsy. Exp Neurol. 257: 39-49.

Tornoe J, Torp M, Jorgensen JR et al. (2012) Encapsulated cell-based biodelivery of Meteorin is neuroprotective in the quinolinic acid rat model of neurodegenerative disease. Restor Neurol Neurosci 30: 225-236.

Figures

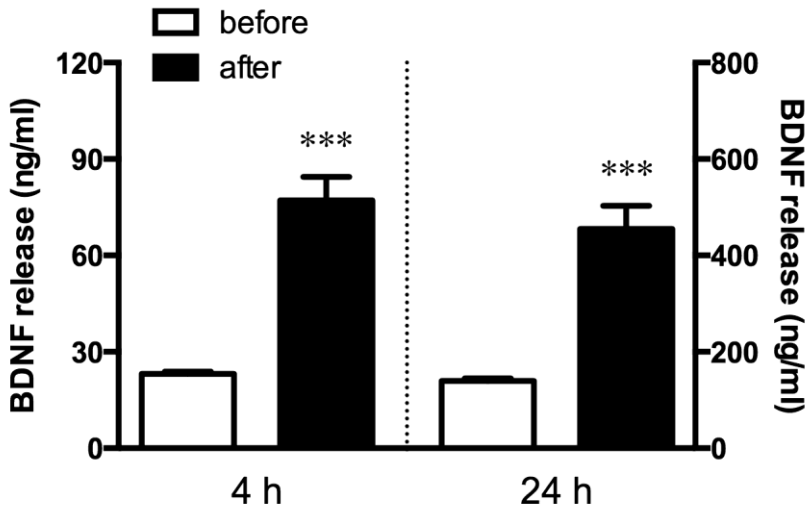

Figure 1. *BDNF release from ECB devices.* Average BDNF release measured by ELISA from ECB devices before the implantation and after the explantation. BDNF release measured per 4 h and 24 h.

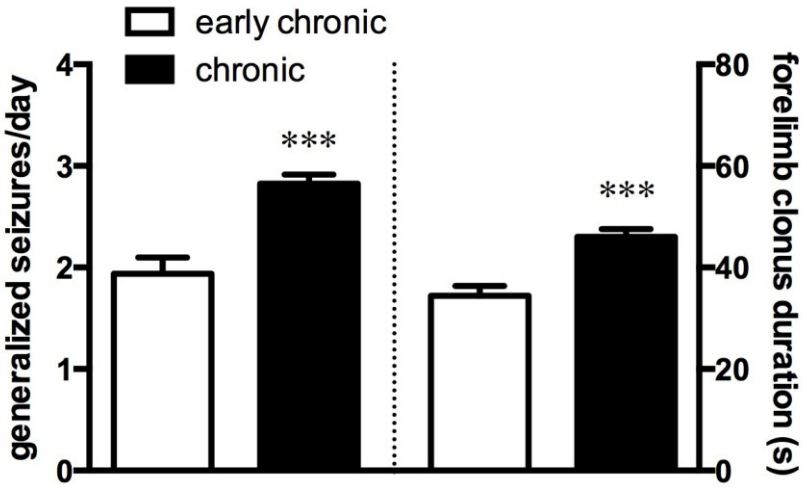

Figure 2. *Behavioral analysis.* Average frequency (left Y axis) and forelimb clonus duration (right Y axis) of spontaneous generalized seizures (class 4 or 5) in the early (day 10-20) and late chronic period (day 25-35) after pilocarpine induced-SE. Data are the means ± SEM of 34 (early chronic) and 15 (chronic). ***<0.001: Student's t-test.

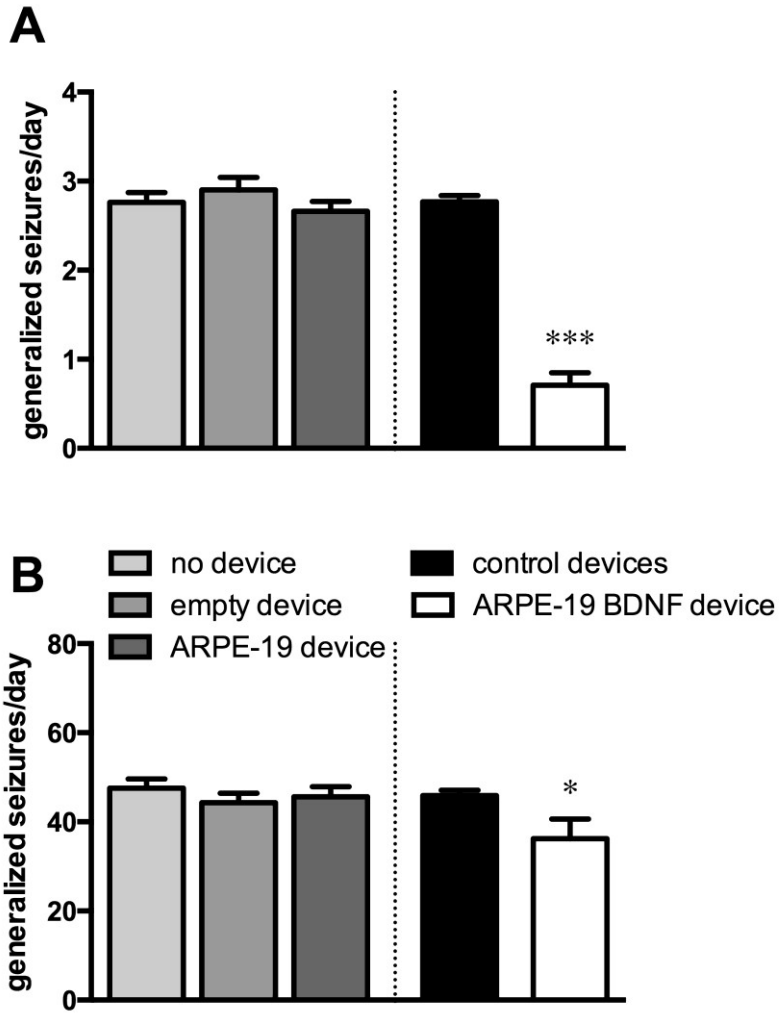

Figure 3. *Behavioral analysis.* Average frequency (A) and duration (B) of spontaneous seizures in the late chronic period (25-35 days after pilocarpine induce-SE). Data are the means ± SEM of 8-10 animals per group. No device: animals not treated with devices; empty device: animals implanted with empty ECB devices; ARPE-19 device: animals implanted with ECB devices filled with parental ARPE-19 cell; ARPE-19 BDNF device: animals implanted with ECB devices filled with ARPE-19 cell secreting BDNF; control: no, empty and ARPE-19 groups pulled together. *<0.05; ***<0.001: Student's t-test for unpaired data.

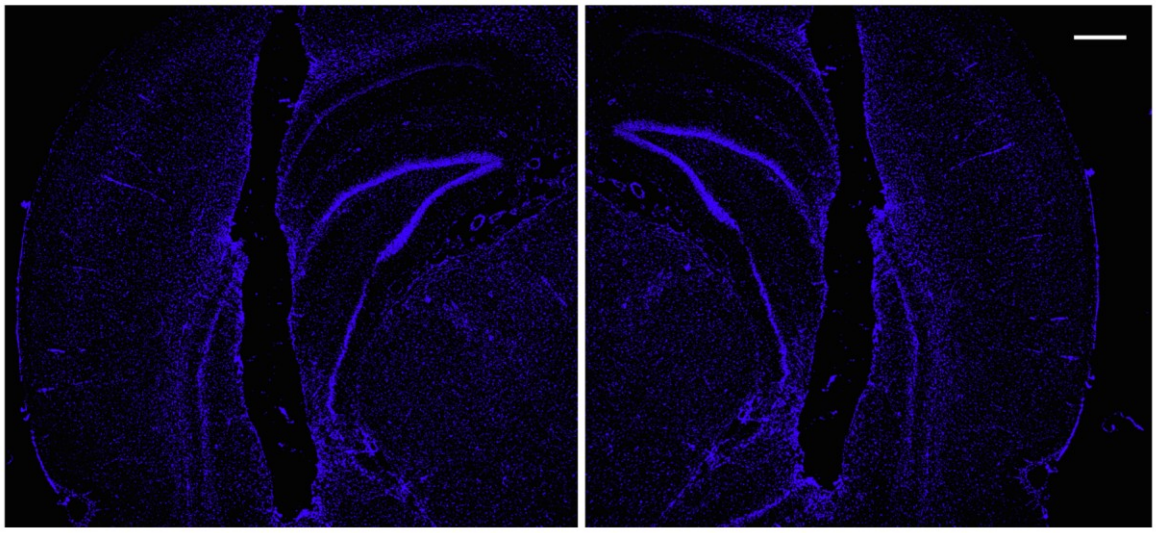

Figure 4. *Placement of ECB devices in the hippocampus.* Representative example of bilaterally implanted ECB devices in the hippocampus. DAPI staining in blue. Horizontal bar = 10 μm.

Chapter 3. GABA

3.1 Impairment of GABA release in the hippocampus at the time of the first spontaneous seizure in the pilocarpine model of temporal lobe epilepsy

Temporal lobe epilepsy (TLE) is associated with profound alterations in the GABA system. Repetitive activation leads to $GABA_A$ receptor desensitization (run-down) in refractory human TLE and in the rat pilocarpine model of TLE (Mazzuferi et al., 2010; Palma et al., 2007). Moreover, TLE is associated with a loss of hippocampal GABAergic interneurons (Drexel et al., 2011; Gill et al., 2010; Kuruba et al., 2011).

These findings suggest an impairment of GABA signaling in the epileptic brain, but the presynaptic counterpart of this phenomenon is still unknown, as the alterations in GABA release have not yet been systematically measured along the natural course of the disease.

This paper aimed at filling this gap by analyzing GABA outflow in the hippocampus at multiple stages of TLE, from the epileptogenic insult (pilocarpine-induced SE) to the chronic period characterized by the spontaneous occurrence of seizures. The data suggest that impaired GABA release in the hippocampus favors the occurrence of spontaneous recurrent seizures and sustains the maintenance of an epileptic state in chronic animals. In contrast, a GABAergic hyper-responsiveness protects from the occurrence of seizures during latency. These events correlate with the loss of GABA interneurons, particularly of parvalbumin and somatostatin positive interneurons.

Experimental Neurology 257 (2014) 39–49

Contents lists available at ScienceDirect

Experimental Neurology

journal homepage: www.elsevier.com/locate/yexnr

Impairment of GABA release in the hippocampus at the time of the first spontaneous seizure in the pilocarpine model of temporal lobe epilepsy

Marie Soukupová [a,b,*], Anna Binaschi [a,b], Chiara Falcicchia [a,b], Silvia Zucchini [a,b,c], Paolo Roncon [a,b], Eleonora Palma [d,e], Eros Magri [f], Enrico Grandi [f], Michele Simonato [a,b,c]

[a] Department of Medical Sciences, Section of Pharmacology, Neuroscience Center, University of Ferrara, Italy
[b] National Institute of Neuroscience, Italy
[c] Laboratory of Technologies for Advanced Therapy (LTTA), Technopole of Ferrara, Italy
[d] Department of Physiology and Pharmacology University of Roma "Sapienza", Italy
[e] IRCCS San Raffaele Pisana, Roma, Italy
[f] Department of Morphology, Surgery and Experimental Medicine, Section of Pathology, University of Ferrara, Italy

ARTICLE INFO

Article history:
Received 20 January 2014
Revised 27 March 2014
Accepted 16 April 2014
Available online 21 April 2014

Keywords:
Temporal lobe epilepsy
Pilocarpine
GABA release
Parvalbumin
Somatostatin

ABSTRACT

The alterations in GABA release have not yet been systematically measured along the natural course of temporal lobe epilepsy. In this work, we analyzed GABA extracellular concentrations (using in vivo microdialysis under basal and high K^+-evoked conditions) and loss of two GABA interneuron populations (parvalbumin and somatostatin neurons) in the ventral hippocampus at different time-points after pilocarpine-induced status epilepticus in the rat, i.e. during development and progression of epilepsy. We found that (i) during the latent period between the epileptogenic insult, status epilepticus, and the first spontaneous seizure, basal GABA outflow was reduced to about one third of control values while the number of parvalbumin-positive cells was reduced by about 50% and that of somatostatin-positive cells by about 25%; nonetheless, high K^+ stimulation increased extracellular GABA in a proportionally greater manner during latency than under control conditions; (ii) at the time of the first spontaneous seizure (i.e., when the diagnosis of epilepsy is made in humans) this increased responsiveness to stimulation disappeared, i.e. there was no longer any compensation for GABA cell loss; (iii) thereafter, this dysfunction remained constant until a late phase of the disease. These data suggest that a GABAergic hyperresponsiveness can compensate for GABA cell loss and protect from occurrence of seizures during latency, whereas impaired extracellular GABA levels can favor the occurrence of spontaneous recurrent seizures and the maintenance of an epileptic state.

Introduction

In temporal lobe epilepsy (TLE), the most frequent epilepsy syndrome in adults, the hippocampal formation often displays distinct neuropathological features, such as neuronal death, neurogenesis, gliosis, axonal sprouting and reorganization of neuronal interconnections. These abnormalities develop in a previously healthy tissue, often after an initial "epileptogenic" event that can produce damage, for example an episode of prolonged, uncontrolled seizures (status epilepticus, SE). Only after a latent period of weeks to years epileptogenic events may be followed by spontaneous recurrent seizures, i.e. by the diagnosis of epilepsy (Pitkanen and Sutula, 2002).

The control of excitability in the mammalian brain, including epileptic hyper-excitability, is largely dependent on the main inhibitory neurotransmitter, γ-aminobutyric acid (GABA). Indeed, many drugs potentiating GABA transmission are effective antiseizure agents (Treiman, 2001). Unfortunately, however, little is known on the dynamic changes in the GABAergic system in natural course of TLE and in its progression toward pharmaco-resistance. In the epileptic tissue, seizures are not generated in a normal circuit but in a profoundly rewired network (Cossart et al., 2005). Only some aspects of the alterations specifically affecting the GABA system have been identified. For example, a substantial loss of glutamic acid decarboxylase (GAD) mRNA-containing (i.e. GABAergic) neurons has been found in the hilus of dentate gyrus (Obenaus et al., 1993) and in the stratum oriens of CA1 (Houser and Esclapez, 1996). Moreover, reduced number of specific GABAergic neurons, including parvalbumin- (Drexel et al., 2011; Kuruba et al., 2011; Pavlov et al., 2011) and somatostatin-positive interneurons (Paradiso et al., 2009; Sperk et al., 1992; Sun et al., 2007), has been found in the epileptic hippocampus. Another interesting alteration is that repetitive activation leads to profound post-synaptic $GABA_A$ receptor desensitization (run-down) in the human epileptic tissue (Ragozzino et al., 2005) and in chronically epileptic rats (Mazzuferi et al., 2010; Palma et al., 2007).

* Corresponding author at: Department of Medical Sciences, Section of Pharmacology, University of Ferrara, Via Fossato di Mortara 17-19, 44121 Ferrara, Italy. Fax: +39 0532 455205.
E-mail address: marie.soukupova@unife.it (M. Soukupová).

http://dx.doi.org/10.1016/j.expneurol.2014.04.014
0014-4886/

The pre-synaptic counterpart of these alterations in the GABA system has not been systematically studied yet. Microdialysis studies in pharmaco-resistant epileptic patients undergoing depth electrode investigation prior to surgery have shown an increased outflow of GABA in the hippocampus in response to seizures, even if this increase was not as dramatic as that of the excitatory neurotransmitters glutamate and aspartate (During and Spencer, 1993; Thomas et al., 2005; Wilson et al., 1996), whereas the basal, interictal GABA outflow was non-significantly reduced in the epileptogenic hippocampus (Pan et al., 2008). For obvious reasons, these works lack stringent controls apart from the apparently non-epileptogenic contralateral hippocampus (During and Spencer, 1993; Thomas et al., 2005) or hippocampus of patients with neo-cortical epilepsy (Pan et al., 2008). Unfortunately, studies in animal models also did not provide insight on this issue, because they revealed transient or non-significant increases in hippocampal GABA outflow during pilocarpine-induced SE (Khongsombat et al., 2008; Meurs et al., 2008; Smolders et al., 1997), but did not yet explore the possible subsequent adaptive changes in GABA neurotransmission.

Here, we used microdialysis to analyze the basal and potassium stimulated GABA outflow in the ventral hippocampus at different time-points after pilocarpine induced SE in the rat. In parallel, we measured the loss of parvalbumin- and somatostatin-expressing GABA interneurons. We found that the loss of GABA neurons is compensated by hyper-responsiveness of the system in the latency period, whereas GABA outflow is dramatically reduced when spontaneous seizures begin to occur.

Materials and methods

Animals

Male Sprague–Dawley rats (250–350 g; Harlan, Italy) were used for all experiments. They were housed under standard conditions: constant temperature (22–24 °C) and humidity (55–65%), 12 h light/dark cycle, free access to food and water. Procedures involving animals and their care were carried out in accordance with European Community (EU Directive 2010/63/EU), national and local laws and polices (authorization: D.M. 83/2009-B and D.M. 246/2012-B). All animals were acclimatized to the microdialysis laboratory conditions for at least 1 h before each experiment and euthanized immediately after the last day of microdialysis by an anesthetic overdose. Rats were killed by decapitation under 1.4% isoflurane anesthesia. The number of animals was kept as small as possible.

Pilocarpine

Rats were randomly assigned to groups that received a single injection of methyl-scopolamine (1 mg/kg, s.c.) 30 min prior to pilocarpine (370 mg/kg, i.p.) or a single injection of methyl-scopolamine 30 min prior to vehicle (0.9% NaCl solution; control animals), and their behavior was observed by experienced researchers for at least 6 h thereafter. Within the first 20–25 min after pilocarpine injection, 83% of the animals developed seizures evolving into recurrent generalized convulsions (status epilepticus, SE). SE was interrupted 3 h after onset by administration of diazepam (20 mg/kg, i.p.). One fourth of the animals that entered SE (i.e. 21% of those administered pilocarpine) died during SE or within 1–2 days. Test and interspersed control animals were then randomly assigned to five experimental groups representing different phases of the natural history of the disease (Fig. 1A): acute phase (24 h after SE), latency (7–9 days after SE), first spontaneous seizure (11 ± 1 days after SE), early chronic (22–24 days after SE, i.e. about 10 days after the first seizure) and late chronic (2 months after SE, i.e. about 50 days after the first seizure). Animals that did not fully recover (i.e. no increase in body weight within the first week) after pilocarpine SE were excluded from the study. Data were collected and processed only from those animals in which the probe was correctly placed, as estimated using a hematoxylin-eosin staining (see below). Experiments were considered completed only when the number of animals in the various groups achieved five or more. In summary: inclusion/exclusion criteria were development of convulsive SE within 1 h after pilocarpine administration; weight gain in the first week after SE; correct positioning of the microdialysis probe.

Analysis and statistics

Convulsive seizures were assessed by 24/24-h video monitoring, performed using a digital video surveillance system DSS1000 (V4.7.0041FD, AverMedia Technologies, USA). Video monitoring was started approximately 6 h after pilocarpine administration (i.e. at the end of direct observation by the researchers – see above) and continued until day 5. For proper identification of the first spontaneous seizure, continuous video-EEG monitoring was started from day 5 after SE until the day of the first spontaneous seizure (Fig. 1A). Video-EEG monitoring (hardware system MP150 and software AcqKnowledge 4.3, all from Biopac, USA) was started at day 5 because, as previously reported (Mazzuferi et al., 2010; Paradiso et al., 2009), we do not observe spontaneous seizures earlier than 8–9 days after pilocarpine administration under the experimental conditions employed in this study. Video-EEG was also performed in the course of microdialysis for assessment of absence of seizures in the 3 h prior to microdialysis and of seizures evoked by high K^+; video-monitoring was also performed in two 2-weeks epochs in the early (days 11–24) and late (days 49–62) chronic phase for assessment of generalized seizure progression (Fig. 1A).

EEG seizures were categorized and measured as periods of paroxysmal activity of high frequency (>5 Hz) characterized by a >3-fold amplitude increment over baseline with progression of the spike frequency that lasted for a minimum of 3 s (Williams et al., 2009). Seizure severity was scored using the scale of Racine (Racine, 1972): 1, chewing or mouth and facial movements; 2, head nodding; 3, forelimb clonus; 4, generalized seizure with rearing; 5, generalized seizure with rearing and falling. Video-EEG analysis was performed by two independent investigators that were blind for the group to which the rats belonged. In case of differential evaluation, data were reviewed together to reach a consensus (Paradiso et al., 2011). In the early and late chronic period, animals were continuously video recorded for two weeks before and during microdialysis, to identify frequency and duration of generalized seizures (class 4 or 5), which were statistically examined using the Student's t-test for unpaired data. The Kruskal-Wallis and post hoc the Dunn's multiple comparison test were used for evaluation of high K^+-evoked seizures.

Microdialysis

Surgery

Under initial ketamine/xylazine (43 and 7 mg/kg, i.p.) anesthesia, rats were secured to a stereotaxic apparatus with the nose bar positioned at +5 mm. Anesthesia was then maintained using isoflurane (1.4% in air; 1.2 ml/min). A 15 mm long guide cannula (MAB 4.15.iC; Agn Tho's, Lidingö, Sweden, outer diameter 500 ± 5 μm) equipped with a dummy cannula (Plastics One, Roanoke, Virginia, USA) and with a recording electrode glued at its outside (0.5 mm longer than the cannula, 0.3 mm in diameter) was implanted into the right ventral hippocampus (A −3.4 mm; L +4.5 mm; P +6.5 mm to bregma; Fig. 1B). A reference electrode was placed on the skull. The guide cannula was fixed to the skull with four stainless screws and methacrylic cement. Rats were allowed 7 days to recover.

In vitro recovery

To optimize the experimental conditions of microdialysis, we estimated the in vitro recovery of GABA when using two perfusion rates and five different home-made or manufactured probes, all of them of 1 mm membrane length. We compared two home-made probes endowed with a polyacrylonitrile membrane (molecular weight cut-

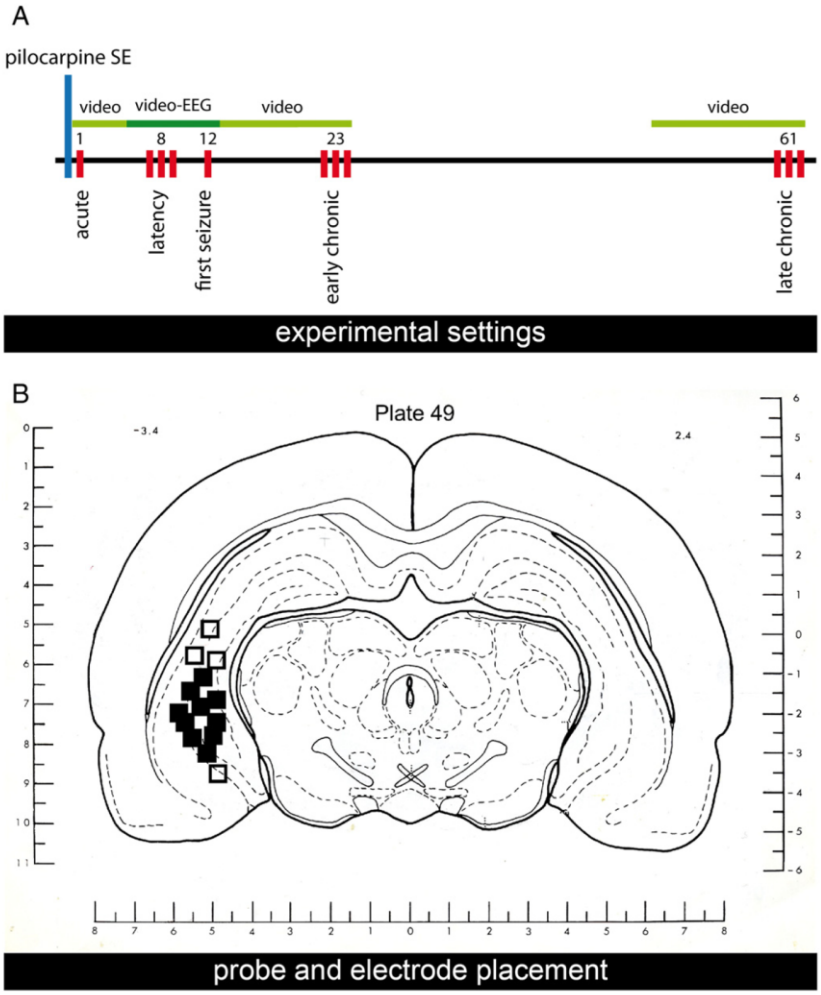

Fig. 1. (A) Schematic diagram of the experiments. Numbers refer to days after SE. The time points of microdialysis experiments are indicated by red bars. See text for details. (B) Schematic illustration of the microdialysis probe positions within the ventral hippocampus. The solid squares (some overlapping) indicate correctly localized probe-electrode tips (n = 25). Open squares indicate incorrectly localized probe-electrode tips in animals not included in the study (n = 4). Coronal brain slices containing the microdialysis probes and recording sites were processed after the experiment for histological analysis. The numbers above the illustration show the distance from bregma (Pellegrino et al. 1979).

off 40 kDa; AN-69, Hospal, Bologna, Italy) or cuprophane membrane (molecular weight cut-off 10 kDa; Hospal) and three manufactured probes endowed either with cuprophane membrane: MAB 4.15.1.Cu (Agn Tho's) and CMA11Cu (CMA, Sweden) or with polyesthersulfone membrane: MAB 4.15.1.PES (Microbiotech/se AB, Sweden). The probes were perfused at rates 2 μl/min or 3 μl/min with a Ringer solution (see the composition below) while placed in a vial containing 2 nmol/ml γ-[2,3-^{3}H(N)]-aminobutyric acid (^{3}H-GABA; PerkinElmer) in Ringer solution. After a 30 min washout period, three 30 min perfusate samples and three equal volume samples of the solution in the vial were collected; 2.5 ml scintillation fluid (Ultima Gold TM, Packard Bioscience) were added and ^{3}H-GABA content was analyzed using a liquid scintillation spectrophotometer (Tri-Carb 2500TR, Packard, Goringhen, Netherlands). The mean recovery (i.e. the mean ^{3}H-GABA content in the perfusate as a percentage of the content in an equal volume of the vial solution) was 10.11 ± 0.67% at a flow rate of 2 μl/min and 4.87 ± 0.22 at 3 μl/min when using the MAB 4.15.1.Cu probe; 9.52 ± 0.68% at a flow rate of 2 μl/min and 4.26 ± 0.62% at 3 μl/min when using the CMA11Cu probe; 6.39 ± 0.22 at a flow rate of 2 μl/min and 6.32 ± 0.84% at 3 μl/min when using the polyacrylonitrile home-made probe; 5.06 ± 0.21% at a flow rate of 2 μl/min and 4.73 ± 0.33 at 3 μl/min when using the MAB 4.15.1.PES probe; and 4.36 ± 0.33% at a flow rate of 2 μl/min and 2.30 ± 0.47 at 3 μl/min when using the home-made cuprophane probe. Therefore, we chose to use the MAB 4.15.1.Cu probes perfused at a flow rate 2 μl/min.

Microdialysis procedure

Twenty-four h before the experiment, rats were briefly anesthetized with isoflurane and a vertical microdialysis probe, endowed with the 1 mm cuprophane dialyzing membrane (MAB 4.15.1.Cu; cut-off 6 kDa; outer diameter 300 ± 5 μm) was inserted in the guide cannula and fixed with modeling clay to the guide cannula support. At the day of the experiment, animals were EEG-monitored to verify absence of seizures for the 3 h preceding the initiation of sample collection. The animals were attached to an EEG hard-wire system and, at the same time, to the microdialysis pump (Univentor, model 864, Malta). The

microdialysis probe was perfused at a flow rate 2 μl/min with a Ringer solution (composition, in mM: $MgCl_2$ 0.85, KCl 2.7, NaCl 148, $CaCl_2$ 1.2) with 0.3% BSA. Starting 1 h after the onset of perfusion, 5 basal samples were collected every 30 min. Stimulation was then applied as a 10 min perfusion with a modified Ringer solution containing 100 mM K^+ (equimolar compensation with Na^+; composition, in mM: $MgCl_2$ 0.85, KCl 100, NaCl 50.7, $CaCl_2$ 1.2, 0.3% BSA). From the onset of stimulation, dialysate samples were collected every 10 min. This stimulation procedure is known to produce a slight elevation in extracellular K^+ concentration near the dialyzing membrane (Largo et al., 1996) and, as a consequence to increase the efflux of several neurotransmitters, including GABA (Aparicio et al., 2004; Marti et al., 2000; Mazzuferi et al., 2005; Takeda et al., 2003). Perfusion of a hippocampal probe with high K^+ is known to evoke seizures in epilepsy models like kindling (Aparicio et al., 2004; Marti et al., 2000; Mazzuferi et al., 2005), thus EEG and behavior were recorded during the all microdialysis session. Routinely, the experiments were repeated for 3 days in 8 h microdialysis sessions, except for the acute phase and first seizure groups, in which a single microdialysis session was performed, respectively 24 h after SE or within 24 h after the first spontaneous seizure (Fig. 1A).

For determination of Ca^{2+} dependency and tetrodotoxin sensitivity of GABA outflow, we used naïve and early chronic rats. In separate microdialysis sessions, all rats were either continuously perfused with a normal Ringer solution; shifted to a perfusion buffer without Ca^{2+} after the third 30-min collection period; or shifted to a perfusion buffer containing 1 μM tetrodotoxina (TTX) after the third 30-min collection period. For characterization of the Ca^{2+} dependency and TTX sensitivity of high K^+-evoked GABA outflow, the animals were perfused with normal Ringer solution, Ringer solution without Ca^{2+} or Ringer with 1 μM TTX during a 10-min stimulation with 100 mM K^+ (as described above).

Chromatography

GABA levels in the dialysate were measured with a high performance liquid chromatograph (HPLC) system comprising a Smartline Pump 1000 solvent delivery module (Knauer, Berlin, Germany), a HT300L autosampler (HTA, Brescia, Italy) and a Smartline Manager 5000 degasser plus system controller unit (Knauer, Berlin, Germany). HPLC was coupled with a RF-551 spectrofluorimetric detector (Shimadzu, Kyoto, Japan). GABA and interfering compounds were separated on a 250 × 4.6 mm, 5 μm particles, EUROSIL bioselect 300A column (LabService Analytica, Italy). The column was protected by a 5 × 4 mm precolumn containing the same packing. The mobile phase was a binary gradient between solution A (0.1 M sodium phosphate, pH 3.0) and solution B (40% 0.1 M sodium phosphate, 30% methanol, 30% acetonitrile, pH 4.0). Precolumn autoderivatization (2 min) and injection were done by the addition of 20 μl of the derivatization mixture containing phthaldialdehyde (Sigma) and 5-mercaptoethanol (Merck), 20:1 (v/v) to 20 μl of dialysate. Elution was carried out at a rate of 0.9 ml/min at a temperature of 22 °C. Chromatograms were recorded 25 min at 345 nm excitation and 455 nm emission wavelengths. GABA retention time was 17.06 min. The method was validated and calibration was performed using standard samples prepared by spiking the Ringer solution and modified Ringer solution with GABA and amino acid standard solution for calibrating amino acid analyzers (Sigma). The sensitivity of the method was 0.16 pmol/20 μl sample according to the ICH Harmonised Tripartite Guideline (2005).

Quantification and statistics

The amounts of GABA in perfusates have been expressed either as absolute values (pmol/10 min) or as percent of basal outflow, as previously described (Mazzuferi et al., 2005). Basal values have been calculated as the mean amount of GABA measured in the last 3 spontaneous (basal) fractions collected before stimulus application. In animals in which multiple microdialysis sessions were performed (i.e. the latency and the two chronic groups), data from the 3 days were averaged to obtain a single estimate for each animal. Time-course curves were expressed in absolute values (pmol/10 min) or as percent of basal values. High K^+-evoked GABA overflow was calculated by subtracting the presumed basal outflow from the total outflow in the samples taken upon stimulus application and in the following 4 samples (5 collection periods, i.e. 50 min). The presumed basal outflow was obtained by interpolation between the samples preceding and following the above-mentioned 5 collection periods containing high K^+-evoked overflow. The % high K^+-evoked outflow was estimated by dividing the sum of the outflow in the samples taken upon stimulus application and in the following 4 by the presumed basal outflow, obtained as described above, and multiplying by 100. To analyze the data, one-way ANOVA and post hoc Dunnett's test ($p < 0.05$ and $p < 0.001$) or Mann–Whitney test (statistical significance at $p < 0.05$) were used, as indicated in the figure legends.

Immunohistochemistry and immunofluorescence

Tissue preparation

Rats were killed 1 h after completion of the microdialysis procedure by decapitation after an anesthetic overdose. Their brains were rapidly removed, immersed in 10% formalin, and paraffin embedded after 48 h. Coronal sections (6 μm thick) were cut across the entire hippocampus, plates 48–52 (Pellegrino et al., 1979) and mounted onto polarized slides (Superfrost slides, Diapath). To standardize the cutting level and to verify the correct probe placement, one section every 10 was used for hematoxylin-eosin staining. These sections were dewaxed (two washes in xylol for 10 min, 5 min in ethanol 100%, 5 min in ethanol 95%, 5 min in ethanol 80%), incubated in Mayer's hematoxylin solution 0.1% (Fluka, 5 min), washed in water (5 min), incubated in alcohol eosin solution 0.5% (Diapath, 2 min) and dehydrated; coverslips were mounted using DPX Mountant for histology (Fluka).

Procedure

Sections were dewaxed and rehydrated as described above. All antigens were unmasked using a commercially available kit (Unmasker, Diapath), according to the manufacturer's instructions. After washing in phosphate buffered saline (PBS), sections were incubated with Triton x-100 (Sigma; 0.3% in PBS 1×, room temperature, 10 min), washed twice in PBS 1×, and incubated with 5% BSA and 5% serum of the species in which the secondary antibody was produced for 30 min. They were incubated in humid atmosphere with the primary antibodies overnight at 4 °C, as follows: parvalbumin 1:100 (mouse monoclonal, Swant), somatostatin-14 1:250 (rabbit polyclonal, Peninsula Laboratories). Detection of parvalbumin was obtained using the biotin-streptavidin system associated with a 3,3-diamino-benzidinetetrahydrochloride (DAB) substrate kit for peroxidase (Dako EnVision Dual Link System HRP, Dako). Somatostatin-14 was detected using a goat anti-rabbit, Alexa Fluor 594-conjugated, secondary antibody (1:1000, Invitrogen) at room temperature for 3 h. After staining the somatostatin-14 sections were washed in PBS, counterstained with 0.0001% 4′,6-diamidino-2-phenylindole (DAPI, Sigma) for 10 min, and washed again. Coverslips were mounted using Shur/Mount (TBS).

Quantification and statistics

The number of parvalbumin or somatostatin positive cells was counted in 500,000 μm^2 frames, in three hippocampal subareas (CA1 including stratum oriens, pyramidale and radiatum; CA3 including stratum oriens, pyramidale, lucidum and radiatum; dentate gyrus, DG, including hilus, stratum granulare and moleculare), every 50th section (that is, one 6 μm thick section every 300 μm) of the left hippocampus, in the region contralateral to the one used for microdialysis. In this way, three sections spanning 0.9 mm of the central part of the hippocampus were evaluated in each animal. Images were acquired using a Leica DFC300 FX video camera mounted on a Leica DMRA2 microscope, captured with a 10× objective, and analyzed in a blinded manner by four investigators, using the program Leica FW 4000. Data obtained from

the multiple sections examined for each rat by the 4 investigators were averaged to obtain a single estimate for each animal. The counts of parvalbumin or somatostatin positive cells have been expressed first as absolute values (number of cells/frame), then as percent of cells in control animals. Data were analyzed using one-way ANOVA and post hoc the Dunnet's test.

Chemicals and solutions

Pilocarpine hydrochloride, scopolamine methylnitrate and xylazine hydrochloride were purchased from Sigma. TTX was purchased from Tocris. All drugs were freshly dissolved in isoosmotic saline solution just before use. Diazepam (Valium®, Roche), ketamine (Ketavet®, InterVet) and isoflurane (IsoFlo®, Esteve Farma) were used in their original fabricated form. 4-Aminobutyric acid, used as standard for chromatography, was from Fluka. Acetonitrile (HPLC grade) and methanol (HPLC grade) were purchased from Sigma. Sodium phosphate dibasic anhydrous (analytical grade) was from Fluka.

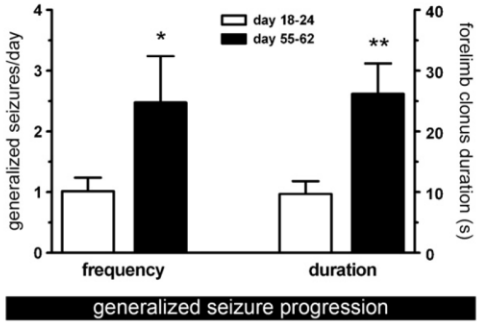

Fig. 2. Behavioral analysis. Average frequency (left Y axis) and forelimb clonus duration (right Y axis) of spontaneous generalized seizures (classes 4 and 5) in the early and late chronic period after pilocarpine induced-SE. Data are the mean ± SEM of 10 (early chronic — open columns) and 6 (late chronic — solid columns) animals per group. *$p < 0.05$ and **$p < 0.01$, Student's t-test for unpaired data.

Results

Video-EEG

To verify that the animals employed in this study present the characteristics of epilepsy development and progression as extensively reported for the pilocarpine model, we performed behavioral and EEG monitoring at specific time points (Fig. 1A). Pilocarpine (370 mg/kg, i.p. 30 min after methyl-scopolamine 1 mg/kg) induced a robust convulsive SE (latency: 25 ± 5 min), which was interrupted after 3 h using diazepam (20 mg/kg, i.p.). For 2–3 days after SE, the animals experienced some occasional, self-limiting generalized seizures (less than 1 min duration) and then entered a latency state in which they were apparently well (Curia et al., 2008; Mazzuferi et al., 2010; Paradiso et al., 2009). Animals that were not killed in the acute group (24 h after SE), after being video-monitored for 5 days, were continuously video-EEG monitored for verification that no spontaneous seizures occurred in the first 9 days, for the latency group, or identification of the first spontaneous seizure, for the first seizure group. The first spontaneous seizure occurred 11.1 ± 0.6 days after SE (mean ± SEM, n = 18). Thereafter, seizures occurred in clusters, as previously described (Goffin et al., 2007; Mazzuferi et al., 2010; Williams et al., 2009), and aggravated in time. In early chronic rats (from 18 to 24 days after SE) the mean daily frequency of generalized (classes 4 and 5) seizures was 1.0 ± 0.2 and the mean forelimb clonus duration was 7.4 ± 1.3 s (mean ± SEM, n = 10), while in late chronic rats (days 55–62 after SE) the mean daily generalized seizure frequency was 2.5 ± 0.5 and the mean forelimb clonus duration 24 ± 3 s (mean ± SEM, n = 6), indicating a progression of the disease (Fig. 2).

During the course of microdialysis experiments, rats were video-EEG monitored to evaluate the response to perfusion of high K^+ in the hippocampus. As shown in Fig. 3, animals in the control, acute and latency groups exhibited partial seizures of class 1 or 2, only rarely severe seizures. More severe seizures appeared to occur with the first spontaneous seizure and in the subsequent stages (time points) of the disease that we examined, but this phenomenon was not statistically significant. It is worth reporting, however, that the response in those animals was apparently distributed in a bi-modal fashion, with a subgroup exhibiting generalized seizures (stage 4 or 5) during high K^+ perfusion, and another subgroup responding with no seizures or non-convulsive seizures only (Fig. 3B). This bi-modal distribution may correlate with the variable vicinity between a cluster of spontaneous seizures and the microdialysis session. Interestingly, the duration of high K^+ evoked seizures was non-significantly reduced in the acute period, i.e. in the post-ictal phase after SE, and then progressively increased in the course of the disease (Fig. 3C).

GABA release

Basal, unstimulated GABA outflow was not significantly altered 24 h after SE, but progressively decreased thereafter, reaching a minimum at the time of the first seizure and then remaining constantly low (about 30% of control values) in the early and late chronic period (control group: 3.26 ± 0.12 pmol/10 min; acute: 2.65 ± 0.47; latency: 1.06 ± 0.19; first seizure: 0.83 ± 0.21; early chronic: 0.89 ± 0.15; late chronic: 0.86 ± 0.29; Fig. 4A). Perfusion with a solution containing high K^+ increased GABA outflow with peak 10 to 20 min after high K^+ perfusion, most likely due to the time needed for accumulation of K^+ in the extracellular spaces around the microdialysis probe (the time course of GABA outflow is shown in absolute values and in percent of basal values in Fig. 4B and C, respectively). Notably, whereas high K^+ perfusion led to a robust increase in GABA outflow in control and latency rats, its effect was very modest in chronic rats. In absolute values, in fact, the net high K^+-evoked GABA overflow was significantly decreased at the time of the first seizure and in chronic animals (Fig. 4D). Probe perfusion with 100 mM K^+ in those animals achieved not even one third of the GABA overflow observed in control, acute and latency rats. However, because of the much lower basal outflow, the effect of high K^+ was proportionally greater during latency (Fig. 4C and E): when expressed as percent of basal levels, GABA overflow was the greatest in latency animals (up to 217 ± 34%), robust in the control (149 ± 5%) and in the acute group (179 ± 12%), and much smaller, about 130%, in all other groups (1st seizure, early and late chronic). These data suggest that the reduced basal outflow of GABA during latency (Fig. 4A) is compensated by a relatively greater stimulus-evoked overflow (Fig. 4C and E), which was similar to the one observed under control conditions in absolute values (Fig. 4D). In contrast, GABA outflow reduction (i.e. impaired extracellular GABA concentrations) in the hippocampus occurs in conjunction with (and may therefore favor) the occurrence of spontaneous recurrent seizures. Importantly, GABA outflow was found reduced also in the subset of animals that responded to high K^+ perfusion with severe seizures (see above), i.e. extracellular GABA concentrations were equally impaired even under conditions when they were expected to be increased (During and Spencer, 1993; Thomas et al., 2005; Wilson et al., 1996). In fact, the high K^+-evoked overflow in chronic animals experiencing generalized seizures was not significantly different ($p > 0.05$, Mann Whitney U test) from the one measured in animals that did not experienced generalized seizures (0.48 ± 0.16 vs. 0.63 ± 0.13 pmol in the convulsive vs. the non-conclusive seizure group).

These alterations in GABA extracellular concentrations were largely Ca^{2+}-dependent and TTX-sensitive. When Ca^{2+} was omitted from the perfusion buffer, the basal GABA outflow gradually declined to 41.3 ±

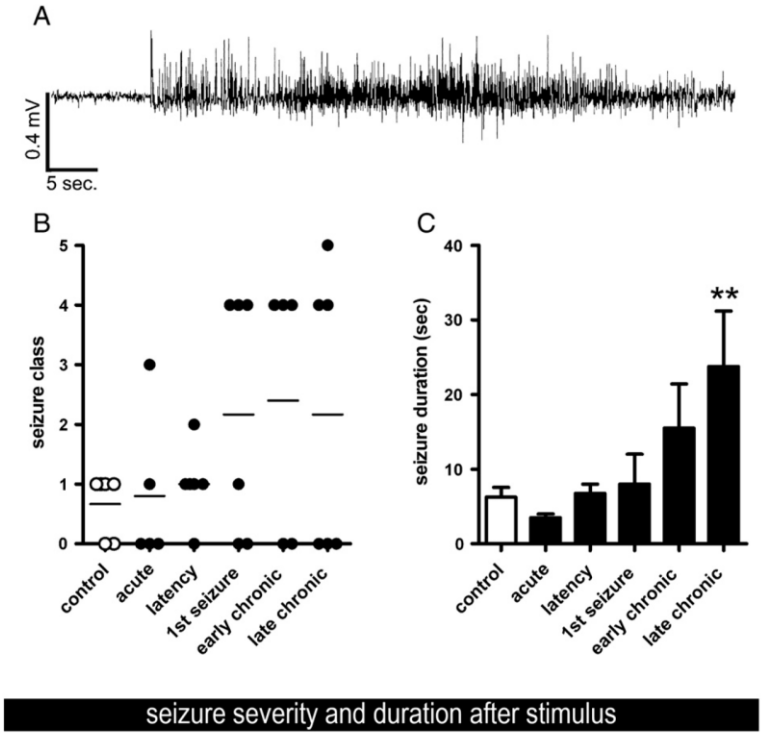

Fig. 3. Seizure activity in response to hippocampal perfusion with a 100 mM K^+ modified Ringer solution for 10 min. (A) Representative seizure evoked by high K^+ perfusion in a late chronic rat. (B) Seizure severity scored according to Racine (1972). (C) EEG-measured single seizure duration during the high K^+ stimulation. After the initial lack of response in rats 24 h after SE the duration of seizures progressively increases and reaches the maximum in late chronic animals. Data are the means ± SEM of 5–6 animals per group. *p < 0.05, Kruskal–Wallis test and post hoc Dunn's test.

5.5% in control animals and to 51.8 ± 6.8% in early chronic rats (Fig. 5). TTX perfusion (1 μM) also decreased the spontaneous efflux of GABA, in control rats to 21.7 ± 5.4% and in early chronic rats to 34.4 ± 11.2% of baseline levels (Fig. 5). Both omission of Ca^{2+} and TTX completely abolished the effect of the high K^+ stimulation (Fig. 5). These data suggest, even if not conclusively demonstrate, a significant contribution of neuronal exocytotic release to the observed epilepsy-associated alterations in GABA outflow.

Loss of GABA interneurons

The dramatic drop in basal, unstimulated GABA release observed beginning at the stage of latency might be caused by a loss of GABA neurons. To explore this possibility, immunohistochemistry and immunofluorescence experiments were performed on the brain of rats at the end of the microdialysis experiments, to estimate the number of parvalbumin and somatostatin-positive cells in the ventral hippocampus. These experiments revealed that the population of parvalbumin-positive cells decreased in the hippocampus of pilocarpine-treated animals. The loss of parvalbumin-positive cells was most rapid and dramatic in the hilus of the dentate gyrus, where it became significant already in the acute phase and further worsened until dropping to less than 10% of control values in the late chronic group (Fig. 6D). The loss of these cells was less dramatic and slower in CA3 (Fig. 6E) and especially in CA1, where it became significant only with the first seizures and did not drop below about 50% of control values (Fig. 6F). The loss of parvalbumin-positive cells that we observed in this study is in line with previously published reports (Andre et al., 2001; Chakir et al., 2006; Kuruba et al., 2011; Pavlov et al., 2011). Furthermore, we observed that the number of somatostatin-positive cells in the hilus of the dentate gyrus also significantly decreased in pilocarpine-treated animals, reaching a minimum (about 50% of control values) in chronic animals (Fig. 7B). No significant variations were observed in the CA1 and CA3 region (data not shown).

Discussion

Main findings

Three key findings emerge from this study: (i) during the epileptogenesis (latent) period, loss of at least some sub-populations of GABA cells is already significant and basal GABA outflow is reduced but the response to high K^+ stimulation proportionally increases; (ii) at the time of the first spontaneous seizure this relatively increased responsiveness to stimulation disappeared; (iii) this dysfunction remains then constant until late phases of the disease.

These findings integrate previous observations, where an increased run-down of the $GABA_A$ current, a sign of impaired responsiveness of $GABA_A$ receptors to stimulation, began in the hippocampus at the time of the first spontaneous seizure (Mazzuferi et al., 2010). Thus, a dramatic impairment of GABA signal appears to take place exactly at the time of the first spontaneous seizure, when both reduced extracellular GABA levels and rapid receptor desensitization are observed. We propose that these phenomena represent a mechanism of transition from latency to spontaneous seizures, i.e., epilepsy. Once established, these maladaptive changes in the GABA system are constantly present in the chronic epileptic condition [see also (Mazzuferi et al., 2010)], arguing that they also underlie maintenance of the disease.

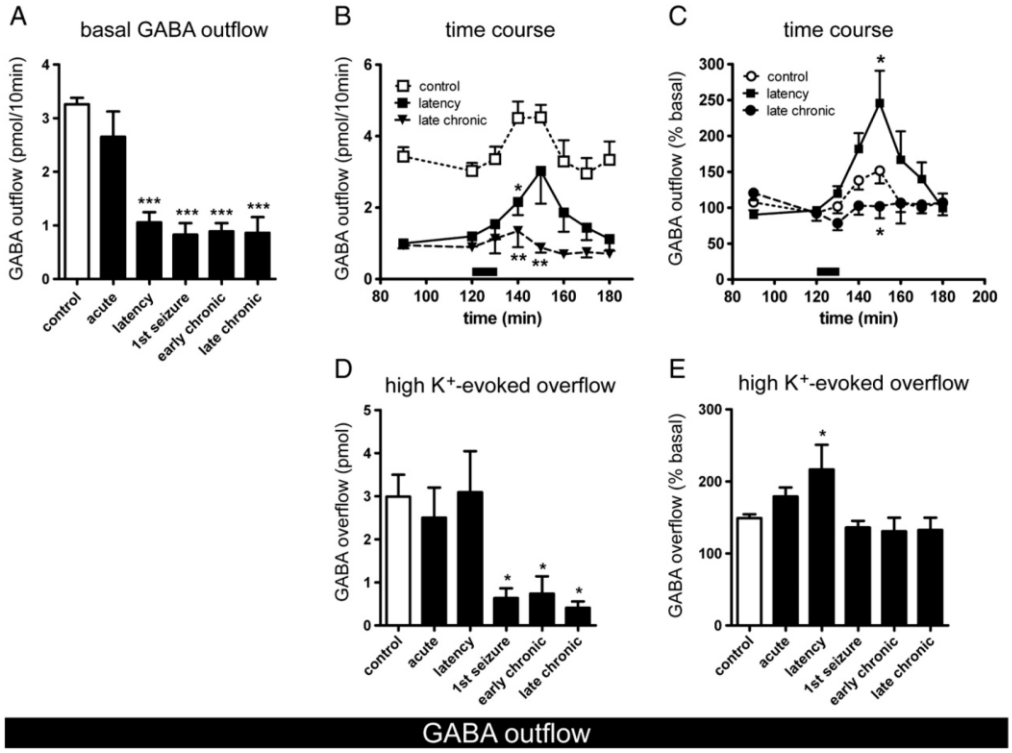

Fig. 4. (A) Spontaneous basal GABA outflow from the hippocampus of control (white column) and pilocarpine-treated (black columns) rats. Under basal conditions, extracellular GABA levels are significantly decreased in the hippocampus of pilocarpine rats, a phenomenon that starts during the latency period and continues at the time of the first spontaneous seizure and in the chronic state. (B) Time course of the effect of 10 min perfusion with 100 mM K^+ (horizontal bar) on GABA outflow from the hippocampus of control (open squares), latency (filled squares) and late chronic rats (filled triangles). In control rats, GABA outflow increases from relatively high basal levels (3.46 ± 0.26 pmol/10 min) to reach 4.53 ± 0.35 pmol/10 min after the stimulus. Animals in the latency period respond to the high K^+ increasing GABA outflow up to 3.03 ± 0.92 pmol/10 min, whereas animals in the late chronic phase react very moderately. For clarity, the profiles in acute, 1st seizure and early chronic animals are not shown. However, the one in acute animals was similar to that in controls and those in 1st seizure and in early chronic animals were similar to that in late chronic. (C) Time course of the effect of 10 min perfusion with 100 mM K + (horizontal bar) on GABA outflow from the hippocampus of control (open circles), latency (filled squares) and late chronic (filled circles) rats. Animals in the latency period respond to the stimulus increasing GABA release up to about 246%, while animals in the late chronic phase do not react at all. For clarity, the profiles in acute, 1st seizure and early chronic animals are not shown. However, the one in acute animals was similar to that in controls and those in 1st seizure and in early chronic animals were similar to that in late chronic. (D) High (100 mM) K^+-evoked GABA overflow from the hippocampus of control (white column) and pilocarpine-treated (black column) rats. Note the dramatic drop in GABA overflow beginning at the time of the first seizure. See Materials and methods for details on the quantification. (E) Effect of 100 mM K^+ perfusion on GABA outflow, expressed as percent of basal release. Data are the means ± SEM of 5–6 rats per group. *$p < 0.05$, ***$p < 0.001$; one-way ANOVA and post hoc Dunnett's test in (A, B and D); Mann–Whitney U test in (C, E).

GABA microdialysis

Microdialysis sampling can provide significant insights into brain function, but has some limitations that should be kept in mind. The first is that the dialysis membrane extends across a relatively wide area, in our case including different hippocampal subfields (not only dentate gyrus but also CA3 and CA1). Thus, the data are an estimate of the GABA extracellular concentrations in all these different subregions. Another relevant limitation is that microdialysis probes reside at distance from the synaptic gap and measure the extracellular concentrations of neurotransmitters, i.e. the result of molecules released into and removed from the extracellular space by neurons, glial cells and other non-neuronal cells. Therefore, measured neurotransmitter levels depend not only on release but also on reuptake. Other factors, like extracellular space volume (which diminishes with age), alterations in the extracellular matrix and environmental factors (for example, tissue damage associated with the probe's insertion and substances entering form the bloodstream) may also influence the measures. Moreover, the relative contribution of neurons and astrocytes to the dialyzed neurotransmitter may be modified by activity. A widely employed strategy to stimulate neurotransmitter release is the elevation of K^+ concentrations in the microdialysis perfusion fluid. Passive diffusion of K^+ across the microdialysis membrane into the tissue will raise extracellular concentrations and induce neuronal depolarization and neurotransmitter release, in principle not only from neurons but also from glia (Stiller et al., 2003).

One way to estimate what part of the dialysate content is of neuronal origin is to establish if the signal fulfills the two classical criteria of neurotransmitter release, Na^+- and Ca^{2+}-dependency, by using TTX and abolishing Ca^{2+} from the perfusion medium. Data generated in this manner should nonetheless be interpreted with caution for GABA, since its release from astrocytes may be also, at least partly, Ca^{2+}-dependent (Lee et al., 2010, 2011).

With specific reference to microdialysis measured GABA, action potential-dependent release from neuronal presynaptic vesicles has been shown to be a major source of the ambient transmitter (Glykys and Mody, 2007). The remaining GABA probably originates from astrocytes (Lee et al., 2010; Yoon et al., 2011) and is released in a non-vesicular manner by reversed plasma membrane transport (Rossi et al., 2003). Indeed, GAT-3, a GABA transporter specifically expressed

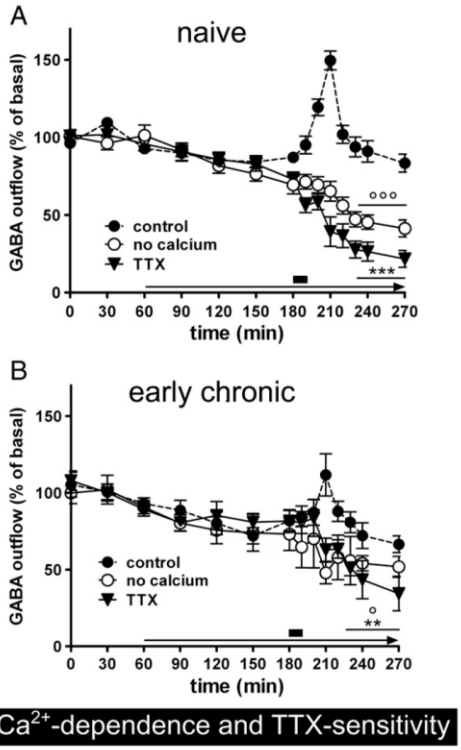

Fig. 5. Ca^{2+}-dependence and TTX-sensitivity of the spontaneous and stimulated GABA outflow from the hippocampus of naïve, non-epileptic, rats (A) and early chronic rats (B) perfused with a normal Ringer solution (solid circles), Ringer without Ca^{2+} (open circles), or a Ringer solution containing 1 μM TTX (triangles). Perfusion of Ringer without Ca^{2+} or with TTX is indicated by an arrow. The 10 min perfusion with high K^+ (black bar) is indicated by a black box above the arrow. Data are presented as a percentage of basal values (average of the three samples preceding Ca^{2+} omission or TTX application) and are the mean ± SEM of 5–6 animals. °p < 0.05, °°°p < 0.001, no calcium vs. respective values in normal Ringer;, **p < 0.01 ***p < 0.001 TTX vs. respective values in normal Ringer; Mann–Whitney U-test.

in astrocytes, has been shown to significantly contribute to the regulation of extracellular GABA levels (Kersante et al., 2013). In the present study, both the basal and the high K^+-evoked GABA outflow from the hippocampus of naïve animals were in the range reported by others (de Groote and Linthorst, 2007; Lasley and Gilbert, 2002; Luna-Munguia et al., 2012; Portelli et al., 2009; Takeda et al., 2003; Tong et al., 2009; Wislowska-Stanek et al., 2008). About 50% of the basal outflow and almost all K^+-evoked GABA overflow were Ca^{2+}-dependent, again in agreement with previous findings (Lasley and Gilbert, 2002). Finally, again similar with our data, the local administration of TTX decreased extracellular GABA to approximately 25% of baseline levels in earlier reports (de Groote and Linthorst, 2007; Kersante et al., 2013).

To our best knowledge, the spontaneous GABA outflow during the development of TLE has never been measured before. Thus far, the attempts to correlate the dynamic changes of extracellular GABA concentrations in the epileptic hippocampus with the occurrence of spontaneous seizures have been limited, and deal with the sole epileptogenic insult (SE). Pilocarpine has been reported to cause a short-lasting (2–3 h) elevation of extracellular GABA concentrations in the hippocampus (Khongsombat et al., 2008; Meurs et al., 2008; Smolders et al., 2004), and no changes were observed at 24 h (Goffin et al., 2007). Whereas previous studies limited measurement of extracellular GABA levels to the first short period after pilocarpine-induced SE, we studied in detail the subsequent phases of the disease, and disclosed a progressive decrease of basal GABA outflow in epileptic animals, initiating during the latency period and reaching a minimum at the time of the first spontaneous seizure. We also observed that the basal GABA outflow than remained steadily low in chronic animals. Data from a microdialysis study in the kindling model support these findings, because a low interictal GABA release was revealed in fully kindled rats (Luna-Munguia et al., 2011). On the other hand, no changes in extracellular GABA levels were observed in chronic rats following intra-hippocampal injection of kainate (Liu et al., 2012). Differences in the epilepsy model (pilocarpine and kindling vs. intra-hippocampal kainate) may account for this discrepancy: one hypothesis could be that the loss of GABAergic cells is less pronounced with the intra-hippocampal kainate procedure employed by Liu et al. (2012).

We also found that GABA outflow from the hippocampus of chronic rats (unlike in control, acute and latency rats) was not significantly increased by high potassium stimulation, in spite of evoking relatively severe seizures. The impaired response to stimulation in epileptic animals begins at the time of the first spontaneous seizure, and is in sharp contrast with a highly increased response during latency. We speculate that this GABAergic hyper-responsiveness during latency contributes to maintain an appropriate inhibitory control and to prevent seizure occurrence despite the significant loss of GABA neurons. In keeping with this idea, (1) high K^+ perfusion evoked short partial seizures during latency but could evoke generalized seizures in chronic animals, i.e. the hippocampus seems less likely to develop seizures during latency; (2) we observed reduction of GABA outflow at the time of the first spontaneous seizure, and the exhaustion of pre-synaptic GABA release has been shown to herald the onset of ictal events in the hippocampal formation in mice (Zhang et al., 2012). Importantly, this exhaustion of pre-synaptic GABA release capacity seems to occur at the same time of the increased post-synaptic $GABA_A$ current rundown, i.e. of $GABA_A$ receptor desensitization (Mazzuferi et al., 2010). Together, these events are expected to lead to a severe impairment of GABA inhibitory control and to strongly favor the occurrence of spontaneous seizures, i.e. lead to the transition from latency to epilepsy.

GABA cell loss

The loss of GABA neurons has been extensively studied in the past and a detailed analysis was beyond the scope of this study. To guesstimate the contribution of cell loss to the observed changes in GABA outflow, however, we studied two classes of GABA interneurons that are known to be particularly vulnerable to epileptogenic insults (namely somatostatin- and parvalbumin-positive interneurons) in the hippocampi of the animals employed for microdialysis. Somatostatin- and parvalbumin-positive cells are estimated to account for about one third of GABA interneurons in the dentate gyrus (Buckmaster and Dudek, 1997).

These cells have been found to be damaged after SE in animal models (Chakir et al., 2006; Drexel et al., 2011; Paradiso et al., 2011). It has been estimated that about 80% of the missing GABAergic neurons in kainate treated rats are somatostatin-positive (Buckmaster and Jongen-Relo, 1999), and that nearly 80% of somatostatin-containing cell in the hilus die following pilocarpine SE in mice (Peng et al., 2013). More limited loss of somatostatin-immunoreactive cells was reported in other models (Buckmaster and Jongen-Relo, 1999; Dinocourt et al., 2003; Gorter et al., 2001). Parvalbumin-positive cells have also been reported to die in various epilepsy models, although in a maybe less dramatic manner compared with those somatostatin-positive (Andre et al., 2001; Gill et al., 2010; Gorter et al., 2001; Marx et al., 2013; Sun et al., 2007). In particular, a progressive reduction of parvalbumin-positive GABAergic neurons in dentate gyrus, CA1 and CA3 was described in the pilocarpine model (Drexel et al., 2011; Knopp et al., 2008; Kuruba et al., 2011; Pavlov et al., 2011).

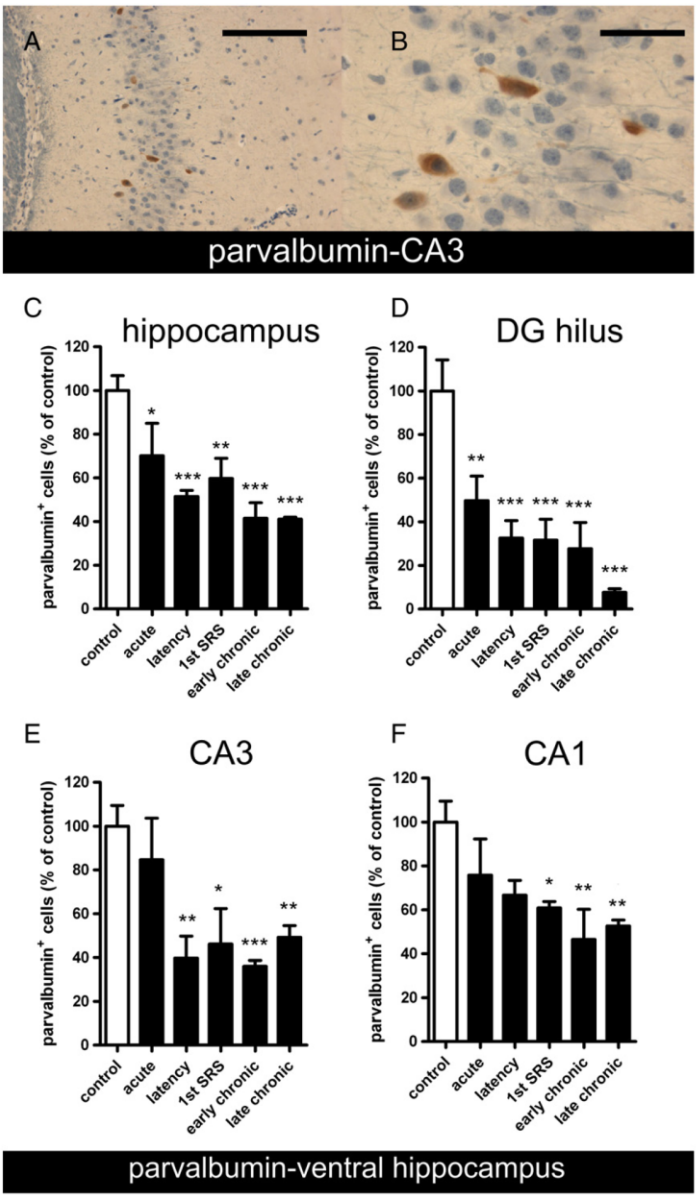

Fig. 6. Parvalbumin positive cell loss at various time points after pilocarpine induced SE. (A) and (B) Representative parvalbumin positive cells (brown — DAB; cell nuclei in blue — hematoxylin) in the CA3 area of a pilocarpine rat during the latency period, 9 days after SE. (B) is a higher magnification of (A). Horizontal bar: 1 mm in (A) and 75 μm in (B). (C-F) Quantification of parvalbumin cells loss in the whole ventral hippocampus (C), hilus of DG (D), CA3 (E) and CA1 (F). Control values are in the white column, values in pilocarpine-treated rats in the black columns. See Materials and methods for details on calculations. Note the rapid loss of parvalbumin positive cells in the hilus of the dentate gyrus early after the SE and the massive loss in late chronic animals (D). The data are the means ± SEM of 5–6 animals per group. *$p < 0.05$, **$p < 0.01$, ***$p < 0.001$ vs. control; one-way ANOVA and post hoc Dunnett's test.

These findings were confirmed in human tissue. The density of parvalbumin- (Andrioli et al., 2007) and of somatostatin-positive interneurons (Sundstrom et al., 2001) in the hippocampal formation was significantly reduced in TLE patients compared with autopsy controls. As in the present study, all above mentioned works rely on immunohistochemical localization of neurochemical markers, and therefore it is difficult to establish whether a loss of immunostaining is due to the actual loss of the particular cell type, or if the marker expression diminished below detection threshold while the cell was still functional. However, double labeling studies with the

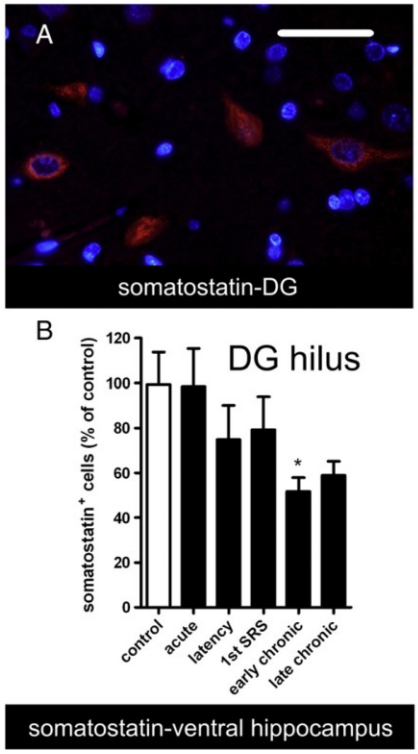

Fig. 7. Somatostatin positive cells loss at various time points after pilocarpine induced SE. (A) Representative somatostatin positive cell (red immunofluorescence) in the hilus of the dentate gyrus of a late chronic animal. Nuclei (DAPI labeled) in blue. Horizontal bar: 75 μm. (B) Quantification of somatostatin-positive cells in the DG hilus. See Materials and methods for details on calculations. Note the significant loss of somatostatin positive interneurons in early chronic animals. No significant change in somatostatin-positive cells was observed in the CA1 and CA3 regions (data not shown). The data are the means ± SEM of 5–6 animals per group. *$p < 0.05$; one-way ANOVA and post hoc Dunnett's test.

neuronal degeneration marker Fluoro-Jade B revealed loss of both somatostatin (Sun et al., 2007) and parvalbumin-expressing interneurons (Huusko et al., 2013) in epilepsy models.

Our findings are in line with those published previously. We found that the number of parvalbumin-positive cells in pilocarpine treated animals reduces gradually during the course of the disease, alongside the decrease in basal GABA outflow. In particular, the loss of parvalbumin-positive neurons was most rapid and advanced in the dentate gyrus, where it became significant already in the acute phase, whereas it was less dramatic and slower in the CA3 and especially in the CA1 region, where it became significant only with the first spontaneous seizure. We also observed that the number of GABAergic somatostatin-positive cells in the hilus of the dentate gyrus also decreased, reaching its minimum in the chronic period.

As mentioned above, however, it should be kept in mind that more than 20 different subtypes of GABA interneurons have been identified in the hippocampus (Tepper et al., 2010) and some of them, in particular calretinin and calbindin-positive interneurons, have been shown to degenerate or even disappear in animal models of TLE (Bouilleret et al., 2000; van Vliet et al., 2004). These findings lend further support to the hypothesis that death of GABA neurons, and the consequently reduced GABA release, in the hippocampus favors (or rather sustains) epileptiform activity.

Conclusions

Speculatively, the present data suggest that a GABAergic hyperresponsiveness may protect from the occurrence of seizures during latency, while impaired GABA release in the hippocampus may favor the occurrence of spontaneous recurrent seizures and the maintenance of an epileptic state. Further studies will be needed to validate this hypothesis, in particular with reference to altered chloride regulation occurring in epilepsy that reduces GABA inhibitory efficacy (Pathak et al., 2007). A better understanding of the (mal)adaptive changes occurring in the GABA system in the natural course of the disease will be important to design rational therapeutic approaches.

Acknowledgments

This study was supported by a grant from the Italian Ministry for the University (Prin 2009, to EP and EG).

References

Andre, V., Marescaux, C., Nehlig, A., Fritschy, J.M., 2001. Alterations of hippocampal GAbaergic system contribute to development of spontaneous recurrent seizures in the rat lithium–pilocarpine model of temporal lobe epilepsy. Hippocampus 11, 452–468.

Andrioli, A., Alonso-Nanclares, L., Arellano, J.I., DeFelipe, J., 2007. Quantitative analysis of parvalbumin-immunoreactive cells in the human epileptic hippocampus. Neuroscience 149, 131–143.

Aparicio, L.C., Candeletti, S., Binaschi, A., Mazzuferi, M., Mantovani, S., Di Benedetto, M., Landuzzi, D., Lopetuso, G., Romualdi, P., Simonato, M., 2004. Kainate seizures increase nociceptin/orphanin FQ release in the rat hippocampus and thalamus: a microdialysis study. J. Neurochem. 91, 30–37.

Bouilleret, V., Loup, F., Kiener, T., Marescaux, C., Fritschy, J.M., 2000. Early loss of interneurons and delayed subunit-specific changes in GABA(A)-receptor expression in a mouse model of mesial temporal lobe epilepsy. Hippocampus 10, 305–324.

Buckmaster, P.S., Dudek, F.E., 1997. Neuron loss, granule cell axon reorganization, and functional changes in the dentate gyrus of epileptic kainate-treated rats. J. Comp. Neurol. 385, 385–404.

Buckmaster, P.S., Jongen-Relo, A.L., 1999. Highly specific neuron loss preserves lateral inhibitory circuits in the dentate gyrus of kainate-induced epileptic rats. J. Neurosci. 19, 9519–9529.

Chakir, A., Fabene, P.F., Ouazzani, R., Bentivoglio, M., 2006. Drug resistance and hippocampal damage after delayed treatment of pilocarpine-induced epilepsy in the rat. Brain Res. Bull. 71, 127–138.

Cossart, R., Bernard, C., Ben-Ari, Y., 2005. Multiple facets of GABAergic neurons and synapses: multiple fates of GABA signalling in epilepsies. Trends Neurosci. 28, 108–115.

Curia, G., Longo, D., Biagini, G., Jones, R.S., Avoli, M., 2008. The pilocarpine model of temporal lobe epilepsy. J. Neurosci. Methods 172, 143–157.

de Groote, L., Linthorst, A.C., 2007. Exposure to novelty and forced swimming evoke stressor-dependent changes in extracellular GABA in the rat hippocampus. Neuroscience 148, 794–805.

Dinocourt, C., Petanjek, Z., Freund, T.F., Ben-Ari, Y., Esclapez, M., 2003. Loss of interneurons innervating pyramidal cell dendrites and axon initial segments in the CA1 region of the hippocampus following pilocarpine-induced seizures. J. Comp. Neurol. 459, 407–425.

Drexel, M., Preidt, A.P., Kirchmair, E., Sperk, G., 2011. Parvalbumin interneurons and calretinin fibers arising from the thalamic nucleus reuniens degenerate in the subiculum after kainic acid-induced seizures. Neuroscience 189, 316–329.

During, M.J., Spencer, D.D., 1993. Extracellular hippocampal glutamate and spontaneous seizure in the conscious human brain. Lancet 341, 1607–1610.

Gill, D.A., Ramsay, S.L., Tasker, R.A., 2010. Selective reductions in subpopulations of GABAergic neurons in a developmental rat model of epilepsy. Brain Res. 1331, 114–123.

Glykys, J., Mody, I., 2007. The main source of ambient GABA responsible for tonic inhibition in the mouse hippocampus. J. Physiol. 582, 1163–1178.

Goffin, K., Nissinen, J., Van, L.K., Pitkanen, A., 2007. Cyclicity of spontaneous recurrent seizures in pilocarpine model of temporal lobe epilepsy in rat. Exp. Neurol. 205, 501–505.

Gorter, J.A., van Vliet, E.A., Aronica, E., Lopes da Silva, F.H., 2001. Progression of spontaneous seizures after status epilepticus is associated with mossy fibre sprouting and extensive bilateral loss of hilar parvalbumin and somatostatin-immunoreactive neurons. Eur. J. Neurosci. 13, 657–669.

Houser, C.R., Esclapez, M., 1996. Vulnerability and plasticity of the GABA system in the pilocarpine model of spontaneous recurrent seizures. Epilepsy Res. 26, 207–218.

Huusko, N., Romer, C., Ndode-Ekane, X.E., Lukasiuk, K., Pitkanen, A., 2013. Loss of hippocampal interneurons and epileptogenesis: a comparison of two animal models of acquired epilepsy. Brain Struct. Funct. http://dx.doi.org/10.1007/s00429-013-0644-1.

ICH Harmonised Tripartite Guideline, 2005. Validation of analytical procedures: text and methodolgy Q2(R1). International Conference of Harmonization of Technical Requirements for Registration of Pharmaceuticals for Human Use. Inter, ICH Global Cooperation Group.

Kersante, F., Rowley, S.C., Pavlov, I., Gutierrez-Mecinas, M., Semyanov, A., Reul, J.M., Walker, M.C., Linthorst, A.C., 2013. A functional role for both -aminobutyric acid (GABA) transporter-1 and GABA transporter-3 in the modulation of extracellular GABA and GABAergic tonic conductances in the rat hippocampus. J. Physiol. 591, 2429–2441.

Khongsombat, O., Watanabe, H., Tantisira, B., Patarapanich, C., Tantisira, M.H., 2008. Acute effects of N-(2-propylpentanoyl)urea on hippocampal amino acid neurotransmitters in pilocarpine-induced seizure in rats. Epilepsy Res. 79, 151–157.

Knopp, A., Frahm, C., Fidzinski, P., Witte, O.W., Behr, J., 2008. Loss of GABAergic neurons in the subiculum and its functional implications in temporal lobe epilepsy. Brain 131, 1516–1527.

Kuruba, R., Hattiangady, B., Parihar, V.K., Shuai, B., Shetty, A.K., 2011. Differential susceptibility of interneurons expressing neuropeptide Y or parvalbumin in the aged hippocampus to acute seizure activity. PLoS One 6, e24493.

Largo, C., Cuevas, P., Somjen, G.G., Martin, R.R., Herreras, O., 1996. The effect of depressing glial function in rat brain in situ on ion homeostasis, synaptic transmission, and neuron survival. J. Neurosci. 16, 1219–1229.

Lasley, S.M., Gilbert, M.E., 2002. Rat hippocampal glutamate and GABA release exhibit biphasic effects as a function of chronic lead exposure level. Toxicol. Sci. 66, 139–147.

Lee, S., Yoon, B.E., Berglund, K., Oh, S.J., Park, H., Shin, H.S., Augustine, G.J., Lee, C.J., 2010. Channel-mediated tonic GABA release from glia. Science 330, 790–796.

Lee, M., McGeer, E.G., McGeer, P.L., 2011. Mechanisms of GABA release from human astrocytes. Glia 59, 1600–1611.

Liu, H.G., Yang, A.C., Meng, D.W., Chen, N., Zhang, J.G., 2012. Stimulation of the anterior nucleus of the thalamus induces changes in amino acids in the hippocampi of epileptic rats. Brain Res. 1477, 37–44.

Luna-Munguia, H., Orozco-Suarez, S., Rocha, L., 2011. Effects of high frequency electrical stimulation and R-verapamil on seizure susceptibility and glutamate and GABA release in a model of phenytoin-resistant seizures. Neuropharmacology 61, 807–814.

Luna-Munguia, H., Meneses, A., Pena-Ortega, F., Gaona, A., Rocha, L., 2012. Effects of hippocampal high-frequency electrical stimulation in memory formation and their association with amino acid tissue content and release in normal rats. Hippocampus 22, 98–105.

Marti, M., Bregola, G., Morari, M., Gemignani, A., Simonato, M., 2000. Somatostatin release in the hippocampus in the kindling model of epilepsy: a microdialysis study. J. Neurochem. 74, 2497–2503.

Marx, M., Haas, C.A., Haussler, U., 2013. Differential vulnerability of interneurons in the epileptic hippocampus. Front. Cell. Neurosci. 7, 167.

Mazzuferi, M., Binaschi, A., Rodi, D., Mantovani, S., Simonato, M., 2005. Induction of B1 bradykinin receptors in the kindled hippocampus increases extracellular glutamate levels: a microdialysis study. Neuroscience 135, 979–986.

Mazzuferi, M., Palma, E., Martinello, K., Maiolino, F., Roseti, C., Fucile, S., Fabene, P.F., Schio, F., Pellitteri, M., Sperk, G., Miledi, R., Eusebi, F., Simonato, M., 2010. Enhancement of GABA(A)-current run-down in the hippocampus occurs at the first spontaneous seizure in a model of temporal lobe epilepsy. Proc. Natl. Acad. Sci. U. S. A. 107, 3180–3185.

Meurs, A., Clinckers, R., Ebinger, G., Michotte, Y., Smolders, I., 2008. Seizure activity and changes in hippocampal extracellular glutamate, GABA, dopamine and serotonin. Epilepsy Res. 78, 50–59.

Obenaus, A., Esclapez, M., Houser, C.R., 1993. Loss of glutamate decarboxylase mRNA-containing neurons in the rat dentate gyrus following pilocarpine-induced seizures. J. Neurosci. 13, 4470–4485.

Palma, E., Roseti, C., Maiolino, F., Fucile, S., Martinello, K., Mazzuferi, M., Aronica, E., Manfredi, M., Esposito, V., Cantore, G., Miledi, R., Simonato, M., Eusebi, F., 2007. GABA(A)-current rundown of temporal lobe epilepsy is associated with repetitive activation of GABA(A) "phasic" receptors. Proc. Natl. Acad. Sci. U. S. A. 104, 20944–20948.

Pan, J.W., Cavus, I., Kim, J., Hetherington, H.P., Spencer, D.D., 2008. Hippocampal extracellular GABA correlates with metabolism in human epilepsy. Metab. Brain Dis. 23, 457–468.

Paradiso, B., Marconi, P., Zucchini, S., Berto, E., Binaschi, A., Bozac, A., Buzzi, A., Mazzuferi, M., Magri, E., Navarro, M.G., Rodi, D., Su, T., Volpi, I., Zanetti, L., Marzola, A., Manservigi, R., Fabene, P.F., Simonato, M., 2009. Localized delivery of fibroblast growth factor-2 and brain-derived neurotrophic factor reduces spontaneous seizures in an epilepsy model. Proc. Natl. Acad. Sci. U. S. A. 106, 7191–7196.

Paradiso, B., Zucchini, S., Su, T., Bovolenta, R., Berto, E., Marconi, P., Marzola, A., Navarro, M. G., Fabene, P.F., Simonato, M., 2011. Localized overexpression of FGF-2 and BDNF in hippocampus reduces mossy fiber sprouting and spontaneous seizures up to 4 weeks after pilocarpine-induced status epilepticus. Epilepsia 52, 572–578.

Pathak, H.R., Weissinger, F., Terunuma, M., Carlson, G.C., Hsu, F.C., Moss, S.J., Coulter, D.A., 2007. Disrupted dentate granule cell chloride regulation enhances synaptic excitability during development of temporal lobe epilepsy. J. Neurosci. 27, 14012–14022.

Pavlov, I., Huusko, N., Drexel, M., Kirchmair, E., Sperk, G., Pitkanen, A., Walker, M.C., 2011. Progressive loss of phasic, but not tonic, GABAA receptor-mediated inhibition in dentate granule cells in a model of post-traumatic epilepsy in rats. Neuroscience 194, 208–219.

Pellegrino, L.J., Pellegrino, A.S., Cushman, A.J., 1979. A Sterotaxic Atlas of the Rat Brain. Plenum Press, New York and London.

Peng, Z., Zhang, N., Wei, W., Huang, C.S., Cetina, Y., Otis, T.S., Houser, C.R., 2013. A reorganized GABAergic circuit in a model of epilepsy: evidence from optogenetic labeling and stimulation of somatostatin interneurons. J. Neurosci. 33, 14392–14405.

Pitkanen, A., Sutula, T.P., 2002. Is epilepsy a progressive disorder? Prospects for new therapeutic approaches in temporal-lobe epilepsy. Lancet Neurol. 1, 173–181.

Portelli, J., Aourz, N., De, B.D., Meurs, A., Smolders, I., Michotte, Y., Clinckers, R., 2009. Intrastrain differences in seizure susceptibility, pharmacological response and basal neurochemistry of Wistar rats. Epilepsy Res. 87, 234–246.

Racine, R.J., 1972. Modification of seizure activity by electrical stimulation. II. Motor seizure. Electroencephalogr. Clin. Neurophysiol. 32, 281–294.

Ragozzino, D., Palma, E., Di, A.S., Amici, M., Mascia, A., Arcella, A., Giangaspero, F., Cantore, G., Di, G.G., Manfredi, M., Esposito, V., Quarato, P.P., Miledi, R., Eusebi, F., 2005. Run-down of GABA type A receptors is a dysfunction associated with human drug-resistant mesial temporal lobe epilepsy. Proc. Natl. Acad. Sci. U. S. A. 102, 15219–15223.

Rossi, D.J., Hamann, M., Attwell, D., 2003. Multiple modes of GABAergic inhibition of rat cerebellar granule cells. J. Physiol. 548, 97–110.

Smolders, I., Van, B.K., Ebinger, G., Michotte, Y., 1997. Hippocampal and cerebellar extracellular amino acids during pilocarpine-induced seizures in freely moving rats. Eur. J. Pharmacol. 319, 21–29.

Smolders, I., Lindekens, H., Clinckers, R., Meurs, A., O'Neill, M.J., Lodge, D., Ebinger, G., Michotte, Y., 2004. In vivo modulation of extracellular hippocampal glutamate and GABA levels and limbic seizures by group I and II metabotropic glutamate receptor ligands. J. Neurochem. 88, 1068–1077.

Sperk, G., Marksteiner, J., Gruber, B., Bellmann, R., Mahata, M., Ortler, M., 1992. Functional changes in neuropeptide Y- and somatostatin-containing neurons induced by limbic seizures in the rat. Neuroscience 50, 831–846.

Stiller, C.O., Taylor, B.K., Linderoth, B., Gustafsson, H., Warsame, A.A., Brodin, E., 2003. Microdialysis in pain research. Adv. Drug Deliv. Rev. 55, 1065–1079.

Sun, C., Mtchedlishvili, Z., Bertram, E.H., Erisir, A., Kapur, J., 2007. Selective loss of dentate hilar interneurons contributes to reduced synaptic inhibition of granule cells in an electrical stimulation-based animal model of temporal lobe epilepsy. J. Comp. Neurol. 500, 876–893.

Sundstrom, L.E., Brana, C., Gatherer, M., Mepham, J., Rougier, A., 2001. Somatostatin- and neuropeptide Y-synthesizing neurones in the fascia dentata of humans with temporal lobe epilepsy. Brain 124, 688–697.

Takeda, A., Hirate, M., Tamano, H., Oku, N., 2003. Release of glutamate and GABA in the hippocampus under zinc deficiency. J. Neurosci. Res. 72, 537–542.

Tepper, J.M., Tecuapetla, F., Koos, T., Ibanez-Sandoval, O., 2010. Heterogeneity and diversity of striatal GABAergic interneurons. Front. Neuroanat. 4, 150.

Thomas, P.M., Phillips, J.P., O'Connor, W.T., 2005. Microdialysis of the lateral and medial temporal lobe during temporal lobe epilepsy surgery. Surg. Neurol. 63, 70–79.

Tong, X., Ratnaraj, N., Patsalos, P.N., 2009. Vigabatrin extracellular pharmacokinetics and concurrent gamma-aminobutyric acid neurotransmitter effects in rat frontal cortex and hippocampus using microdialysis. Epilepsia 50, 174–183.

Treiman, D.M., 2001. GABAergic mechanisms in epilepsy. Epilepsia 42 (Suppl. 3), 8–12.

van Vliet, E.A., Aronica, E., Tolner, E.A., Lopes da Silva, F.H., Gorter, J.A., 2004. Progression of temporal lobe epilepsy in the rat is associated with immunocytochemical changes in inhibitory interneurons in specific regions of the hippocampal formation. Exp. Neurol. 187, 367–379.

Williams, P.A., White, A.M., Clark, S., Ferraro, D.J., Swiercz, W., Staley, K.J., Dudek, F.E., 2009. Development of spontaneous recurrent seizures after kainate-induced status epilepticus. J. Neurosci. 29, 2103–2112.

Wilson, C.L., Maidment, N.T., Shomer, M.H., Behnke, E.J., Ackerson, L., Fried, I., Engel Jr., J., 1996. Comparison of seizure related amino acid release in human epileptic hippocampus versus a chronic, kainate rat model of hippocampal epilepsy. Epilepsy Res. 26, 245–254.

Wislowska-Stanek, A., Hamed, A., Lehner, M., Bidzinski, A., Turzynska, D., Sobolewska, A., Walkowiak, J., Plaznik, A., 2008. Effects of midazolam and buspirone on in vivo concentration of amino acids and monoamine metabolites in the rat hippocampus. Pharmacol. Rep. 60, 209–218.

Yoon, B.E., Jo, S., Woo, J., Lee, J.H., Kim, T., Kim, D., Lee, C.J., 2011. The amount of astrocytic GABA positively correlates with the degree of tonic inhibition in hippocampal CA1 and cerebellum. Mol. Brain 4, 42.

Zhang, Z.J., Koifman, J., Shin, D.S., Ye, H., Florez, C.M., Zhang, L., Valiante, T.A., Carlen, P.L., 2012. Transition to seizure: ictal discharge is preceded by exhausted presynaptic GABA release in the hippocampal CA3 region. J. Neurosci. 32, 2499–2512.

3.2 Loss of cortical GABA terminals in Unverricht-Lundborg disease

Several progressive genetic disorders of the central nervous system can present with seizures as the main clinical symptom. Examples of these disorders are those included in the group of progressive myoclonic epilepsies (PMEs), that are characterized by the occurrence of myoclonus, tonic–clonic seizures and progressive neurological deficit (Berkovic et al., 1993, Lehesjoki and Koskiniemi, 1999, Delgado-Escueta et al., 2001, and Shahwan et al., 2005).

The Unverricht-Lundborg disease (ULD, EPM1) is the most common progressive myoclonic epilepsy and it is associated with a defect of cystatin B (CSTB), a protease inhibitor. We report here the first direct evidence that loss of cortical GABA input occurs in a relevant animal model and in a case of human ULD, leading to a condition of latent hyperexcitability that favors myoclonus and seizures. These findings have direct relevance for understanding of the pathogenic mechanism of ULD and the neurobiological basis of the effect of currently employed drugs.

Neurobiology of Disease 47 (2012) 216–224

Contents lists available at SciVerse ScienceDirect

Neurobiology of Disease

journal homepage: www.elsevier.com/locate/ynbdi

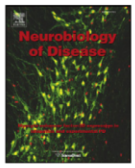

Loss of cortical GABA terminals in Unverricht–Lundborg disease

Andrea Buzzi [a,b], Maia Chikhladze [c], Chiara Falcicchia [a,b], Beatrice Paradiso [a,b,d], Giovanni Lanza [d], Marie Soukupova [a,b], Matteo Marti [a,b], Michele Morari [a,b], Silvana Franceschetti [c], Michele Simonato [a,b,*]

[a] Department of Clinical and Experimental Medicine, Section of Pharmacology and Neuroscience Center, University of Ferrara, Ferrara, Italy
[b] National Institute of Neuroscience, Italy
[c] Division of Neurophysiology and Epileptology, Neurological Institute "C. Besta", Milan, Italy
[d] Department of Experimental and Diagnostic Medicine, Section of Pathology, University of Ferrara, Ferrara, Italy

ARTICLE INFO

Article history:
Received 17 February 2012
Revised 2 April 2012
Accepted 8 April 2012
Available online 17 April 2012

Keywords:
Epilepsy
Myoclonus
GABA
Neurodegeneration
Cortex

ABSTRACT

Unverricht–Lundborg disease (ULD) is the most common progressive myoclonic epilepsy. Its etiology has been identified in a defect of a protease inhibitor, cystatin B (CSTB), but the mechanism(s) by which this defect translates in the clinical manifestations of the disease are still obscure. We tested the hypothesis that ULD is accompanied by a loss of cortical GABA inhibition in a murine model (the CSTB knockout mouse) and in a human case. Cortical GABA signaling has been investigated measuring VGAT immunohistochemistry (a histological marker of the density of GABA terminals), GABA release from synaptosomes and paired-pulse stimulation. In CSTB knockout mice, a progressive decrease in neocortex thickness was found, associated with a prevalent loss of GABA interneurons. A marked reduction in VGAT labeling was found in the cortex of both CSTB knockout mice and an ULD patient. This implicates a reduction in GABA synaptic transmission, which was confirmed in the mouse model as reduction in GABA release from isolated nerve terminals and as loss of electrophysiologically measured GABA inhibition. The alterations in VGAT immunolabeling progressed in time, paralleling the worsening of myoclonus. These results provide direct evidence that loss of cortical GABA input occurs in a relevant animal model and in a case of human ULD, leading to a condition of latent hyperexcitability that favors myoclonus and seizures. These findings contribute to the understanding of the pathogenic mechanism of ULD and of the neurobiological basis of the effect of currently employed drugs.

Introduction

Unverricht–Lundborg disease (EPM1 or ULD; OMIM #254800), an autosomal, recessively inherited disorder, is the most common form of progressive myoclonic epilepsy. Clinical onset occurs between 6 and 16 with stimulus-sensitive myoclonic jerks or, less frequently, with generalized tonic–clonic seizures, which progressively worsens in frequency and severity with age (Kälviäinen et al., 2008). The worsening of myoclonus, which may lead to episodes of status myoclonicus, makes one third of the patients severely incapacitated (Kälviäinen et al., 2008). Neurological findings are initially absent or mild but, in time, signs of cerebellar ataxia, incoordination, tremor, cognitive impairment, emotional liability and depression may become evident (Kälviäinen et al., 2008). Parietal and frontal cerebral atrophy have been documented by MRI studies in late stage patients (Koskenkorva et al., 2009).

ULD is caused by alterations of the cystatin B (CSTB) gene (Lehesjoki et al., 1991, 1993; Pennacchio et al., 1996; Stone et al., 1996; Virtaneva et al., 1996) that encodes a cystein protease inhibitor protecting cells against lysosomal peptidases (Abrahamson et al., 2003). The most common alteration is a dodecamer expansion in the 5′ upstream region that results in a dramatic reduction of CSTB mRNA expression and protein levels (Joensuu et al., 2007; Rinne et al., 2002). The mechanism by which the loss of CSTB leads to ULD is still uncertain. We have shown that hippocampal slices prepared from CSTB knockout (KO) mice are hyperexcitable and that CSTB KOs are more susceptible than wild-type (WT) to kainate-induced tonic–clonic seizures (Franceschetti et al., 2007).

Although these findings provide insight into the mechanism of ULD tonic–clonic seizures, the mechanism of myoclonus, the key symptom of the disease, remains elusive. In the present study, we tested the hypothesis that a loss of neocortical GABA inhibition plays a critical role. Indeed, (i) epileptic myoclonus, including ULD-associated myoclonus, originates in the cortex (Dijk and Tijssen, 2010; Shibasaki, 2006); (ii) transcranial magnetic stimulation in ULD patients evokes cortical hyperexcitability that may depend on reduced inhibition (Canafoglia et al., 2010; Manganotti et al., 2001; Valzania et al., 1999); (iii) a loss of GABA neurons was found in another brain region, the hippocampus, in a model of ULD (Franceschetti et al., 2007); (iv) GABA-acting antiepileptic drugs are effective in ULD treatment. Thus, we first explored cortical GABA neurotransmission in CSTB KO mice by histologically analyzing GABA terminals, measuring GABA release from isolated nerve terminals

* Corresponding author at: Neuroscience Center, University of Ferrara, via Fossato di Mortara 17-19, 44100 Ferrara, Italy. Fax: +39 0532 455205.
E-mail address: michele.simonato@unife.it (M. Simonato).
Available online on ScienceDirect (www.sciencedirect.com).

0969-9961/$ – see front matter © 2012 Elsevier Inc. All rights reserved.
doi:10.1016/j.nbd.2012.04.005

and electrophysiologically evaluating the cortical GABAergic tone. The results provide converging, direct evidence of a loss of cortical GABA input. Translation of these findings to the human disease is not trivial, because human autopsy tissue from ULD patients is very difficult to obtain (Cohen et al., 2011). In this study, however, we managed to have access to a case, which confirmed the findings made in the animal model.

Materials and methods

Animals

129/SvJ-CSTB-deficient (KO) and 129/SvJ WT mice, selected from littermates born from heterozygous breeding pairs, were used for all experiments. Animals were divided in 3 age groups: 3–5, 7–9 and 1113 months old. PCR for genotyping was performed as described by others (Pennacchio et al., 1998). Animals were housed under standard conditions: constant temperature (22–24 °C) and humidity (55–65%), 12 h dark–light cycle, free access to food and water. All procedures were carried out in accordance with guidelines by the European Community and National laws (European Communities Council Directive 86/609/EEC).

Myoclonic behavior was assessed as follows: 0, no myoclonic activity; 1, isolated myoclonic jerk of limbs, head and/or torso; 2, severe myoclonic jerk with jump; 3, myoclonic seizure lasting more than 1 min.

Histology

Mice were killed under deep isoflurane anesthesia. Brains were removed, immersed in 10% formalin for 72 h and then paraffin embedded. Serial sections of 6 μm were cut with a Microtome (Leica RM2125RT, Germany). In all experiments, adjacent sections were used for the different staining procedures.

Hematoxylin–eosin

Sections were dewaxed (2 washes in xylol, 10 min each; 5 min in 100% ethanol, 5 min in 95% ethanol, 5 min in 80% ethanol) and then re-hydrated in distilled water for 5 min. They were stained with hematoxylin (Diapath-Microstain, Italy) for 5 min, rinsed in water, then incubated in eosin (Diapath-Microstain) for 2 min. At the end of the staining procedure, sections were dehydrated in an ethanol series, and coverslips were mounted using xylene-based DPX (Fluka-Sigma-Aldrich, Germany).

VGAT and VGlut immunohistochemistry

VGAT and VGlut immunohistochemistry were performed on sections dewaxed and re-hydrated as above, based on a previously described protocol (Zucchini et al., 2008). In brief: sections were washed in phosphate-buffered saline (PBS) 1× for 10 min; incubated in H_2O_2 0.3% for 15 min at room temperature; rapidly rinsed in distilled water and washed again in PBS 1×. They were then incubated with Ultra-V Block (Lab Vision, Thermo Scientific, USA) for 5 min at room temperature, to block non-specific background. After washing in PBS 1× for 5 min, sections were incubated overnight at 4 °C in a humid chamber in PBS 1× containing a primary antibody against either VGlut1 (rabbit polyclonal; 1:500 dilution; Synaptic Systems, Germany) or VGAT (mouse monoclonal; 1:250 dilution; Synaptic Systems). After rinsing again in PBS 1× for 10 min, sections were incubated for 10 min with a biotinylated secondary antibody (Lab Vision), washed in PBS 1× for 5 min and then incubated in streptavidin peroxidase (Lab Vision) at room temperature for 10 min. Finally, sections were incubated with 3,3-diaminobenzidine tetrahydrochloride (DAB, Sigma) for signal revelation. Coverslips were mounted using Gel mount (Shur mount, Triangle Biomedical Sciences, USA). The specificity of immunohistochemistry was verified in all experiments by controls in which the primary antibody was omitted.

Neu-N immunohistochemistry

Adjacent sections were used to identify neuronal cells (Paradiso et al., 2009). Antigen retrieval was performed at the beginning of the procedure, heating sections in microwave to 98 °C, in a solution of citrate (pH 6.0) (MS-Unmasker, DiaPath, Italy) for 30 min, followed by cooling at room temperature for 20 min. After this step, immunohistochemistry was performed using the same method described for VGAT. The primary antibody directed against Neu-N (Millipore, USA) was a mouse monoclonal diluted 1:100 in PBS 1×.

$GAD_{65–67}$ immunohistochemistry

Other adjacent sections were used for $GAD_{65–67}$ immunohistochemistry, using the procedure described by the manufacturer (Dako, USA) after antigen retrieval (performed as described above for Neu-N). The primary anti-$GAD_{65–67}$ antibody (Millipore) was a rabbit polyclonal diluted 1:200 in PBS 1×. Immunoreaction with the chromogen–substrate-solution (Dako) was carried out for 3 min.

Image capture, data analysis and statistical evaluation

Images were acquired through a camera (Leica DFC300 FX) mounted on an optical microscope (Leica DM RA2) using a 10× objective. Each section was positioned to align the callosum to one border of the field visualized by the camera. Illumination was kept constant throughout the acquisition process. For each section, sensori-motor and temporal cortical areas were analyzed at both symmetrical sides.

Hematoxylin–eosin, Neu-N and $GAD_{65–67}$ images were used for cell counting and quantification of cell density. Cells were counted in 1 mm wide cortical areas, by repeated measures (3 times per section) in 4 regularly spaced sections (one section every 42, that is, one section every 250 μm). Cell density was expressed as mean number of positive cells (hematoxylin-, Neu-N- and $GAD_{65–67}$-positive cells to measure all cells, neurons and GABA interneurons, respectively) per area unit (cells/mm^2). An estimate of the total number of cells in the cortical region under examination was obtained by multiplying the number of positive cells (identified as above) in the 1 mm wide area examined in each section by 42 and summing the 4 resulting counts, obtaining a single value per animal that corresponded to the positive cells in a 1 mm medio-lateral wide and 1 mm antero-posterior long portion of cortex. This value was used for statistical analysis.

For VGAT, densitometric analysis was performed on 1531 × 1144 μm frames (i.e. the entire frame observed through the camera when using a 10× objective), as previously described (Tongiorgi et al., 2004). Each frame was subdivided in 1392 × 1040 pixels. The image was transformed into gray levels, then curves were generated in which each data point represented the average gray level over a line of pixels (200 μm long) at a given distance from the border between callosum and cortex (see boxes in Figs. 3A and B). The average gray level in the last 50 lines of pixels [i.e. in the outer aspect of layer I were, as reported by others (Minelli et al., 2003), no detectable VGAT signal was found] was subtracted from the data obtained in each section, such numbers were the difference between the total signal and background. This signal quantification was repeated 3 times per section in 4 regularly spaced sections per each area (as above). The averages resulting from these multiple estimates were employed for generating curves of signal as a function of distance from callosum. To visually illustrate the differences between WT and KO in VGAT immunoreactivity in the different layers, compensating for the differences in thickness, we also "stretched" the KO curve normalizing the size of each layer to the corresponding layer in WT. For quantification of the signal in the different layers, we measured the average gray level (see Figs. 3A and B).

Analysis was performed using the Image J software (NIH). Statistical evaluation was performed using the Student's *t* test for unpaired data or ANOVA and post-hoc the Newman–Keuls test.

Synaptosomes

Synaptosomes were isolated from the cortices of CSTB KO and WT mice to measure GABA release. Mice were deeply anaesthetized with isoflurane and decapitated. Their cortices were rapidly dissected, weighed, homogenized in ice-cold 0.32 M sucrose buffered at pH 7.4 and then centrifuged for 10 min at 1000 *g* (4 °C). The supernatant was then centrifuged for 20 min at 12000 g (4 °C). Finally, the pellet containing the synaptosomes was resuspended in 5 ml of an oxygenated (95% O_2, 5% CO_2) Krebs solution containing (in mM): NaCl 125, KCl 3, $CaCl_2$ 1.2, $MgSO_4$ 1.2, NaH_2PO_4 1, $NaHCO_3$ 22, glucose 10 (33 °C).

One milliliter aliquots of the suspension (approximately 100 mg protein) were slowly injected into nylon syringe filters (outer diameter 17 mm, 0.45 μm pore size, internal volume of approximately 100 μl; GE, USA), which were then connected to a peristaltic pump. Filters were maintained at 33 °C in a thermostatic bath and superfused at a flow rate of 0.5 ml/min with a preoxygenated Krebs solution. Under these experimental conditions, spontaneous GABA efflux is essentially unaffected by reuptake. Sample collection (every 3 min) was initiated after a 30-min period of filter washout, and consisted of 9 collection periods. Stimulation was applied perfusing a Krebs solution containing high K^+ (20 mM, equimolar substitution of KCl for NaCl) for 90 s, during the 4th collection period. Protein content in each filter was spectrophotometrically analyzed (Novaspec II, Pharmacia LKB, Sweden).

GABA measurement

Endogenous GABA levels in the samples were measured by high performance liquid chromatography (HPLC) coupled to fluorometric detection after precolumn derivatization with o-phthaldialdehyde, as previously described (Sbrenna et al., 1999). A 100 μl aliquot of each sample was placed into a thermostated (5 °C) Triathlon autosampler (Spark Holland, the Netherlands). Thirty-five microliter of o-phthaldialdehyde solution was then added to the sample and 50 μl of the mixture was injected onto a Chromsep (5 mm; C18) analytical column (3 mm internal diameter; 10 cm length; Chrompack, the Netherlands). The column was perfused at a flow rate of 0.48 ml/min with a mobile phase containing 0.1 M sodium acetate, 10% methanol and 2.5% tetrahydrofuran (pH 6.5). To achieve a good separation, a two-step linear gradient of methanol in aqueous sodium acetate buffer was provided by a Beckman 125 pump (Beckman Instruments, USA). Excitation and emission wavelengths of the fluorescence spectrophotometer (FP-2020plus, Jasco, Japan) were set at 370 and 450 nm, respectively. A computer-controlled system (Beckman Gold System) allowed acquisition and analysis of chromatograms. Under our experimental conditions, the retention time for GABA was approximately 17 min. A linear gradient (eluent change to 100% methanol over 1 min and return to 100% eluent 2.5 min later) allowed rapid cleaning of the column after GABA elution. The limit of detection was about 0.5 nM.

Data analysis and statistical evaluation

High K^+-evoked GABA overflow was calculated by subtracting the presumed basal outflow from the total GABA found in the sample at stimulus application and in the following two samples (Muzzolini et al., 1997). The presumed basal outflow was obtained by interpolation between the preceding and the following samples. The overflow was expressed as the percentage of the presumed basal outflow. Statistical evaluation was performed using the Mann–Whitney *U* test.

Electrophysiology

Mice were deeply anesthetized with ether vapors and decapitated. Brains were quickly removed and immersed in cold (3–4 °C) artificial cerebrospinal fluid (aCSF) containing (in mM): NaCl 124, KCl 5, NaH_2PO_4 1.25, $NaHCO_3$ 26, CaCl2 2, $MgSO_4$ 1.25, glucose 10. The solution was bubbled with a 95% O_2 and 5% CO_2 mixture, pH 7.30–7.35. Coronal neocortical slices (400 μm) were cut using a vibratome, transferred to an interface recording chamber and incubated for at least 1 h in oxygenated aCSF. Slices were then superfused continuously at a rate of 1 ml/min with 35 °C aCSF saturated with 95% O_2/5% CO_2.

Glass pipettes filled with aCSF were used to record field potentials and were placed in layers II–III or in layer V. Stimuli were delivered using bipolar stainless steel electrodes that were positioned at the border between layer VI and the white matter beneath the recording electrodes. Synaptic responses were evoked with 0.2 ms pulses of 15–300 A. Before the beginning of each experiment, a complete input–output (I–O) series was performed.

Paired-pulse stimuli (PPS) protocols were performed by applying 50 μs pulses at inter-pulse intervals (IPIs) ranging from 10 to 1000 ms, using stimulus intensities yielding the field potential (FP) amplitude corresponding to about 65% of the maximum. A series of PPS were also applied with a fixed interstimulus interval of 20 ms by consecutively increasing the stimulus intensity until obtaining the maximal response.

Data analysis and statistical evaluation

Data were collected using a Neurodata amplifier (Cygnus Technologies, USA), filtered (upper cut-off frequency: 20 kHz), digitally stored (sample frequency: 10 kHz) and analyzed using a homemade software developed in Matlab language. To compute paired-pulse depression (PPD), the amplitude of the response to the second pulse of the pair was divided by the amplitude of the response to the first pulse in the pair. In pharmacological experiments, comparisons were made between measurements taken immediately before and 20 min after the onset of

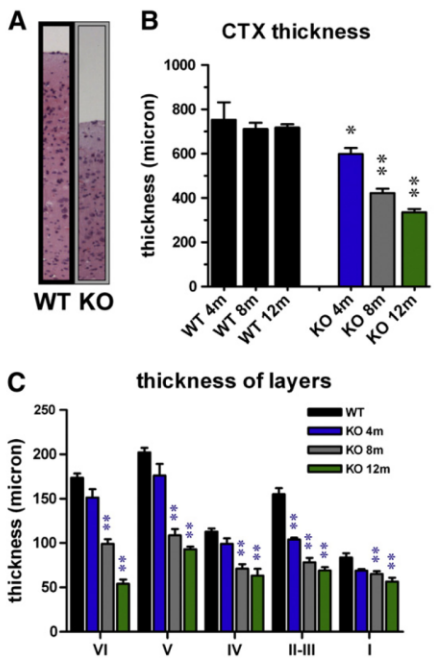

Fig. 1. Thickness of the sensori-motor cortex in WT and CSTB KO mice. (A) Representative hematoxylin–eosin stained cortical sections taken from an 8-month-old WT and an 8-month-old CSTB KO mouse. (B) Quantification of cortical thickness in WT (black bars) and CSTB KO mice (4-month-old: blue bar; 8-month-old: gray bar; 12-month-old: green bar). Data are means ± s.e. of 6 animals per group. ** $P<0.01$ vs. control of the same age, Student's *t* test for unpaired data. (C) Quantification of the thickness of the different cortical layers in WT and CSTB KO mice. Data are means ± s.e. of 6 animals per group. ** $P<0.01$; Student's *t* test for unpaired data.

drug application. Statistical analysis was performed using the Student's *t* test or non-parametric tests, as indicated in the figure legends.

Human samples

ULD human brain samples of the precentral motor cortex were from the Department of Neuropathology at the "C. Besta" Neurological Institute (Milan, Italy). They were from a 50-year-old male ULD patient who died for bronchopneumonia. We employed three controls (36, 57, and 64-year-old males) who died with the same clinical history of bronchopneumonia. These cases were from the Department of Diagnostic and Experimental Medicine, Section of Pathology, University of Ferrara (Italy). All autopsies were performed within 36 h after death. Gross histopathological examination of the brain was always performed, and no evidence for neuropathological alterations, including inflammation or areas of demyelination, was noticed. Each brain was dissected into parts including the precentral gyrus (primary motor cortex) (Heines, 2003). The samples were fixed in 10% buffered formalin and embedded in paraffin.

Seven micrometer thick sections were cut at the microtome, and processed for routine hematoxylin–eosin staining for histological analysis. Immunohistochemistry was performed as described for mouse sections, using an avidin–biotin–peroxidase complex, following the manufacturer's protocol (Ultra Vision Detection System; Lab Vision Corporation). The primary antibody for VGAT was a mouse monoclonal, diluted 1:50 (Synaptic Systems).

Results

Histology in CSTB KO mice

It was known that the thickness of the neocortex is reduced in CSTB KO mice (Pennacchio et al., 1998). Here, we found that this phenomenon progresses with age. In 4-month-old KO mice, we estimated an approximately 20% reduction, that became 40% at 8 months and 55% at 12 (Figs. 1A–B). Thickness was equally reduced in all layers (Fig. 1C).

To verify a correlation with cell loss, we deepened analysis in the 8-month group. First, we estimated the overall cell density and total cell number in the cortex by counting hematoxylin-stained nuclei, and found a slight increase in density that did not compensate for the loss in thickness, such that the overall number of cells was significantly reduced in the KO cortex (Fig. 2A). The density of neurons (measured using Neu-N) and of GABA interneurons (measured using GAD_{65-67}) was unchanged (Figs. 2B–C, left bars), indicating that the increase in overall cell density depended on non-neuronal cells, likely astrocytes and/or microglia, as previously suggested (Franceschetti et al., 2007). Interestingly, the loss of GABAergic interneurons was more pronounced compared with the general loss of neurons (45% vs. 30%, Figs. 2B–C, right bars), indicating that GABA interneurons are more susceptible to damage than other neuronal subtypes.

Therefore, we explored the density of GABAergic innervation using a marker of GABA terminals, the vesicular GABA transporter VGAT (Chaudhry et al., 1998; McIntire et al., 1997) A dramatic decrease in VGAT signal was found in the sensori-motor cortex of 8-month-old CSTB KO mice (Figs. 3A–C), particularly in layers V and VI (Fig. 3D). Similar findings were made in the temporal cortex (Figs. 4A–B). These changes were progressive, since they were much less pronounced in 4-month-old and more severe in 12-month-old KOs (Figs. 3D and 4C–D). We also examined the density of glutamatergic terminals using the VGlut marker (Bellocchio et al., 2000; Takamori et al., 2000a, 2000b): consistent with our findings indicating a more severe damage on GABA interneurons, VGlut immunolabeling was only slightly attenuated in KO mice (Fig. 5).

These progressive histological alterations paralleled with a progressive increase in myoclonic activity. At 4 months, CSTB KO mice rarely displayed severe myoclonus or myoclonic seizures, while these events became increasingly common with age, up to an average of approximately 60 isolated myoclonuses (stage 1 in our scoring system), 10 severe myoclonic events with jumping (stage 2) and 5 myoclonic seizures (stage 3) in 12 h daytime observation at 12 months.

GABA release

Next, we investigated GABA release from isolated neocortical terminals (synaptosomes). While basal, unstimulated, GABA outflow was not different in synaptosomes prepared from 8-month-old CSTB KO and WT mice, high K^+-evoked overflow was significantly reduced in KO animals (Fig. 6), suggesting that the residual nerve terminals in KOs fail to provide a normally efficient response to stimuli.

Electrophysiology

Finally, we performed field potential recordings to examine the functional consequences of the loss of GABA terminals. In slices from both WT and KO mice, field potentials evoked in layers II–III included an early component followed by a prominent late component peaking 4.5–6 ms after the stimulus artifact. Postsynaptic field potentials evoked in layer V were monophasic and peaked around 5 ms. To evaluate I–O curves and paired-pulse stimulation (PPS) profiles, we measured the late component of the field potentials in layers II–III and the peak in layer V. In all layers, the I–O curve reached saturation at similar levels in WT and KO mice (9.3 ± 2.6 and 9.5 ± 2.6 V, respectively). In both layers II–III and V the amplitude of the responses to low intensity stimuli was slightly, but not significantly, larger in KO than in WT animals (Fig. 7).

In layers II–III, PPS protocols performed by stimuli evoking half-maximal responses consistently induced a depression of the second

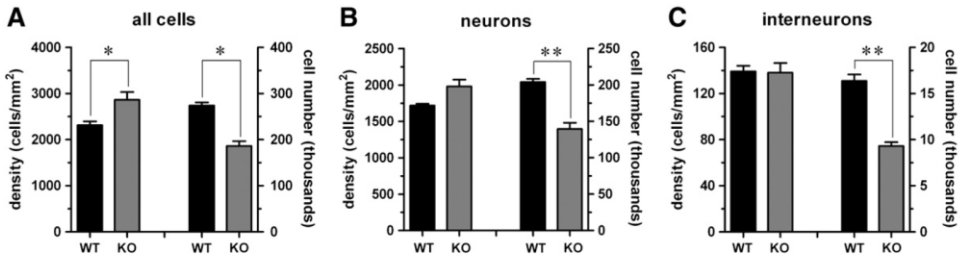

Fig. 2. Cell density and total cell number in the sensori-motor cortex of 8 month-old WT (black bars) and CSTB KO (gray bars) mice. Cell density is expressed as number of cells per area unit (cells/mm^2). The total number of cells was measured in a 1 mm medio-lateral wide and 1 mm antero-posterior long portion of cortex (see Materials and methods for details). (A) Total cells, measured using the hematoxylin–eosin staining. (B) Neuronal cells, measured using Neu-N immunohistochemistry. (C) GABA interneurons, measured using GAD_{65-67} immunohistochemistry. Data are the means ± s.e. of 6 animals per group. * $P<0.05$; Student's *t* test for unpaired data.

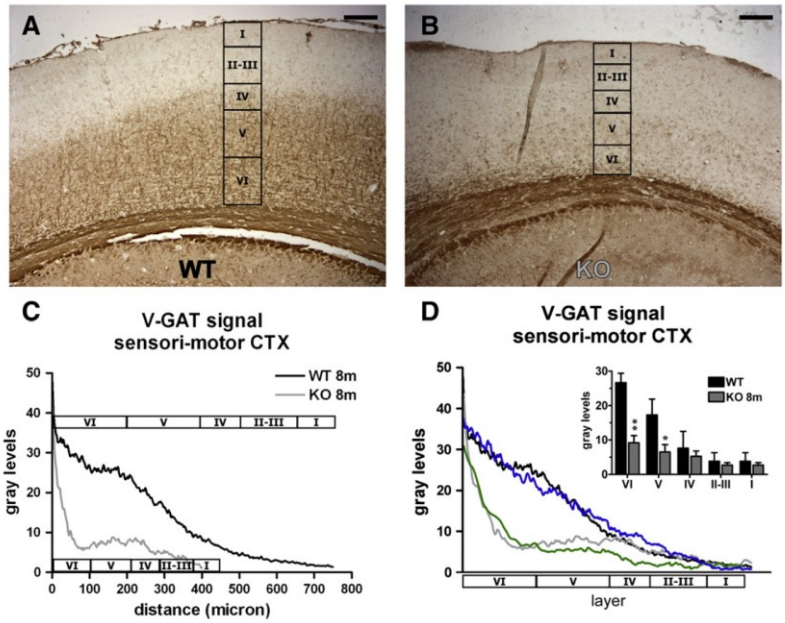

Fig. 3. VGAT immunoreactivity in the sensori-motor cortex of 8-month-old WT and CSTB KO mice. (A) and (B) Representative VGAT immunolabeled cortical sections taken from a WT (A) and a CSTB KO (B) mouse. The boxes indicate examples of the areas employed for densitometric analysis of the entire cortex and of the different layer (I to VI). (C) Densitometric analysis of the VGAT signal, expressed as pixel intensity (0–255 gray levels, 255 = white, 0 = black) as a function of the distance from callosum (μm). Analysis was performed as described in the Materials and methods section. Data are the means ± s.e. of 6 animals per group: WT (black line) and CSTB KO (gray line). (D) Densitometric analysis as in (C), except the thickness of layers in KO animals was normalized to the one in WT, as described in the Materials and methods section. Note the drop in VGAT signal in 8 month-old KO animals (gray line) at layer VI. This phenomenon could not be appreciated in 4 month-old KOs (blue line), while it was even more pronounced in 12 month-old KOs (green line). Positive Insert: average gray levels in the different layers of WT (black bars) and 8 month-old CSTB KO (gray bars). Data are the means ± s.e. of 6 animals per group. * $P<0.05$, ** $P<0.01$; Student's *t* test for unpaired data. Horizontal bars in A and B = 100 μm.

response at each inter-pulse interval (IPI) shorter than 1000 ms in both WT and KO mice. However, the inhibition was significantly smaller in KO mice at IPIs between 10 and 200 ms (Figs. 8A–B). In layer V, depression of the conditioned response was observed in WT mice but not in KO mice (Figs. 8D–E).

To prove that a reduced GABA inhibition accounts for the changes in PPS profiles, we tested the I–O curve of the conditioned response at 20 ms, an IPI at which GABA is the main factor in determining the inhibitory effect (Rozas et al., 2001). In layers II–III, the degree of inhibition of the conditioned responses progressively increased with the stimulus strength in both groups, but was significantly smaller in KO than in WT mice (Fig. 8C). In layer V, the profile of inhibition in WT slices was similar (although less pronounced) to that occurring in layers II–III, whereas inhibition was absent in KO mice (Fig. 8F).

Perfusion with low concentrations of the $GABA_A$ antagonist bicuculline (0.5 μM) was unable to produce significant changes in the amplitude of the field responses in slices obtained from WT mice (Figs. 9A and D). Conversely, it resulted in a significant amplification of the field response in KO slices (Figs. 9B and E), an effect that may be due to reduction of early GABA inhibition occurring simultaneously with the postsynaptic excitatory potential. In the presence of bicuculline, PPS (performed at an intensity adjusted to elicit unconditioned responses with amplitude similar to that measured under control conditions) induced minimal or no changes in depression profile in WT mice, while significantly reducing depression of conditioned responses in KO mice (Figs. 9C and F).

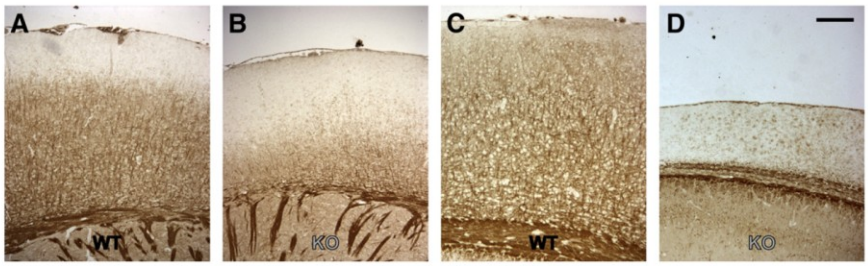

Fig. 4. VGAT immunoreactivity in the temporal cortex of 8-month-old WT and CSTB KO mice: (A) and (B) are representative VGAT immunolabeled cortical sections taken from a WT and a CSTB KO mouse. VGAT immunoreactivity in the sensori-motor cortex of 12-months old WT and CSTB KO mice: (C) and (D) are representative VGAT immunolabeled cortical sections taken from a WT and a CSTB KO mouse. Horizontal bar = 100 μm.

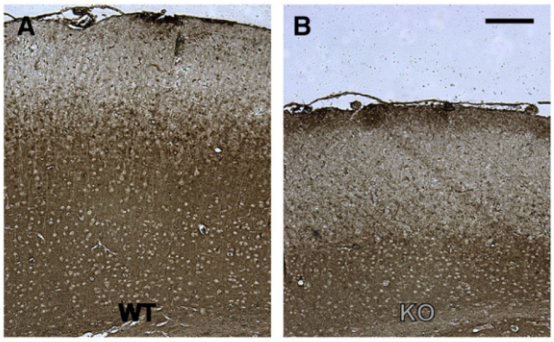

Fig. 5. VGlut immunoreactivity in the sensori-motor cortex of 8-month-old WT and CSTB KO mice: (A) and (B) are representative VGlut immunolabeled cortical sections taken from a WT and a CSTB KO mouse. Horizontal bar = 100 μm.

Case report

To challenge the clinical relevance of these findings, we compared VGAT immunohistochemistry in the post-mortem tissue of an ULD patient and of age and sex matched non-epileptic individuals who died under similar pathological conditions. The pattern of VGAT labeling in controls was very similar to that previously described (Blazquez-Llorca et al., 2010). In all layers, numerous VGAT-positive terminal-like puncta were observed in the neuropil and around unstained neurons. We also observed other previously described patterns of VGAT staining, like chandelier axon terminals forming vertical rows of boutons (DeFelipe et al., 1989). Consistent with mouse data, a great reduction in thickness of the cortex and an obvious, dramatic loss of VGAT labeling was detected in the ULD patient (Fig. 10).

Discussion

Main findings

We found here a highly significant reduction in the VGAT signal in the cortex of both CSTB KO mice and a human case of ULD. This suggests a loss of GABA inhibition, as confirmed in the mouse model by a reduction in paired-pulse depression (PPD) at IPI at which GABA is the main inhibitory factor. In CSTB KO mice, the alterations in VGAT immunolabeling were progressive, paralleling the progression of the disease and the worsening of myoclonus in particular. Altogether,

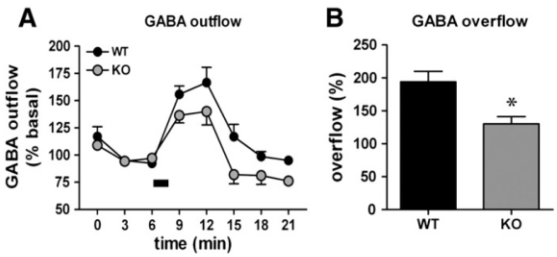

Fig. 6. GABA outflow from synaptosomes prepared from the sensori-motor cortex of 8 month-old WT and CSTB KO mice. (A) GABA fractional outflow as a function of time from synaptosomes of WT (black symbols) and CSTB KO (gray symbols) mice. Data are expressed as percent of the mean outflow in the last basal collection periods before high K+ stimulation (black bar). In absolute values (pmol/mg prot), basal outflow was not significantly different in the two groups. (B) High K+-evoked GABA overflow from synaptosomes of WT (black bar) and CSTB KO (gray bar) mice. Results are expressed as percent of the presumed GABA outflow (see Materials and methods for details). Data are the means ± s.e. of 5 animals per group. * $P<0.05$; Mann–Whitney *U* test.

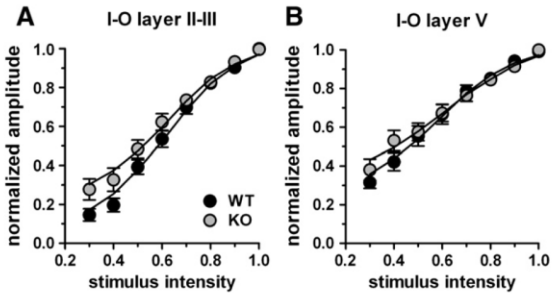

Fig. 7. Input–output (I/O) curves of stimulation of layers II–III (A) and V (B) in WT (black circles) and CSTB KO (gray circles) 8-months old mice. Data are the means ± s.e. of 8 animals per group.

these results support the conclusion that a key factor underpinning the pathological basis of ULD is a loss of cortical GABA signaling which, in time, becomes insufficient to control excitability. This phenomenon may underlie the progressive worsening of the clinical signs of the disease when not controlled by drugs that potentiate the GABA signal.

Findings in CSTB KO mice

We observed a progressive, dramatic thinning of the cortex in CSTB KO mice. This observation extends previous findings in mice demonstrating the loss of thickness but not its progressive nature (Pennacchio et al., 1998) and is consistent with MRI observations in ULD patients (Koskenkorva et al., 2009). Importantly, reduction in cortical thickness in CSTB KO mice associated with a progressive worsening in the frequency and severity of myoclonus. Such correlation is also observed in humans, further validating the CSTB KO mouse as a model of ULD.

The reduced thickness was associated with cell loss but also with increased density of non-neuronal cells. Indeed, the density of astrocytes and microglia has been previously reported to increase in CSTB KOs (Franceschetti et al., 2007; Pennacchio et al., 1998; Shannon et al., 2002). In contrast, CSTB deficiency leads to neuronal loss, maybe due to impaired redox homeostasis (Lehtinen et al., 2009). Interestingly, we observed here a dramatic loss of GAD-positive cells, much more pronounced than that of Neu-N-positive cells, indicating that GABA interneurons may be more susceptible to damage than other neuron subtypes.

This finding prompted a detailed investigation of the cortical GABA synapses. We first measured the density of GABA terminals by using the vesicular GABA transporter VGAT as a marker (Chaudhry et al., 1998; Takamori, 2006), and found a dramatic decrease in the CSTB KO neocortex. This phenomenon likely reflects the loss in GABA interneurons and displayed several distinct features: (i) coherently with the proposal that GABA neurons are particularly vulnerable in the absence of CSTB, it was more pronounced than the loss of glutamatergic terminals measured using the VGlut marker; (ii) it was apparently more pronounced in the deep than in the superficial layers, although electrophysiology (a more sensitive approach) showed that the GABA input was also impaired in the superficial layers; (iii) it was progressive, paralleling other anatomical parameters (loss of cortical thickness and of GABA interneurons) as well as the worsening of the disease (myoclonus).

The loss of GABA-containing vesicles predicted an impairment of the overall secretory capacity. Consistently, depolarization-evoked GABA release from synaptosomes was significantly reduced in CSTB KOs, indicating that the residual terminals cannot provide adequate GABA release in response to incoming depolarizing stimuli.

Neurophysiological experiments also confirmed a defective GABA inhibition. Using the paired-pulse paradigm, which allows detection of widespread alterations in cortical inhibition (Rozas et al., 2001),

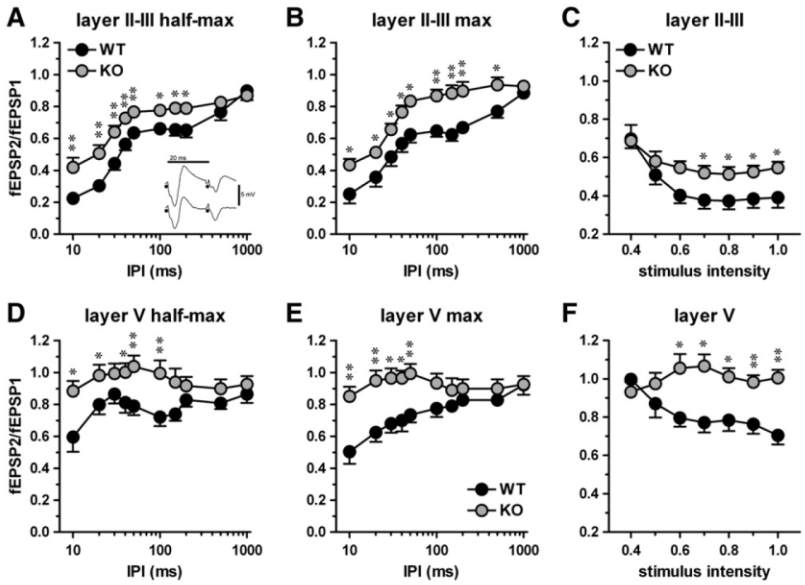

Fig. 8. PP stimulation in neocortical layers. (A) and (B) In layers II–III the conditioned response is consistently depressed up to 1000 ms IPI in both strains, but inhibition is significantly smaller in KO than in WT mice either using half-maximal or maximal stimulus intensities. (D) and (E) In layer V, the depression of the conditioned response is less robust in WT, and essentially absent in KO mice. (C) and (F) Effect of increasing stimulus intensity on PP depression at 20 ms IPI. In layers II–III (C), the depression of the conditioned response increases with the increasing stimulus intensity, but the depression remains significantly lower in KO than in WT slices. In layer V (F), a milder depression of the conditioned response occurs in WT mice, while it is virtually lacking in KO slices. Data are the means ± s.e. of 9–11 animals per group. * $P<0.05$, ** $P<0.01$, Student's *t* test for unpaired data.

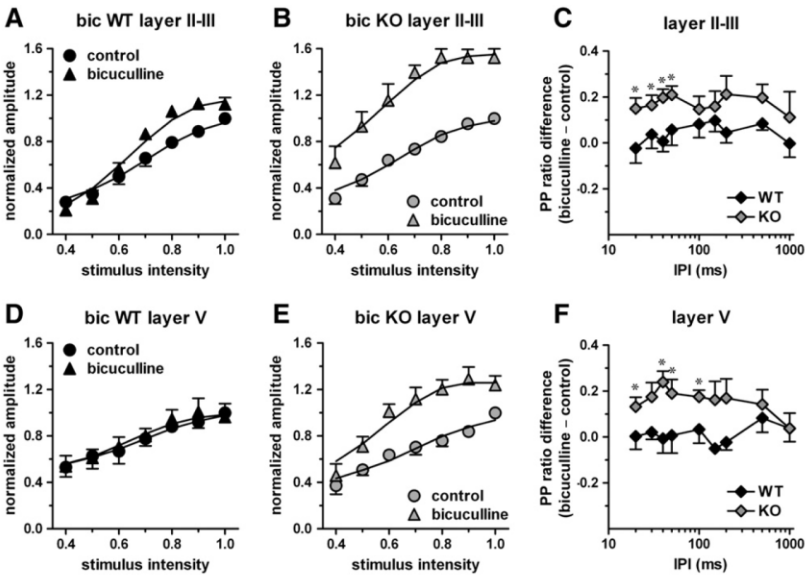

Fig. 9. I–O relationship and PP ratio after mild GABA blockade. The perfusion with 0.5 μM bicuculline induces minimal or no change in the amplitude of field potentials in both layers II–III (A) and V (D) of WT mice, as shown by minimal changes of the I–O relationship. Conversely, the same low bicuculline concentration is sufficient to significantly increase the amplitude of the field potential (FP) due to a partial block of GABA inhibition in KO mice (B and E), as illustrated by a depolarizing shift in the I–O relationship. The difference between PP response ratios measured in layers II–III and V under control condition and in the presence of bicuculline is plotted in the panels (C) and (F). The stimulus intensity was adjusted to elicit unconditioned FP with similar amplitude in the two conditions and resulted in a reduced inhibition in KO mice but in a non-significant change in WT mice. Data are the means ± s.e. of 4 animals per group. * $P<0.05$, Student's *t* test for unpaired data.

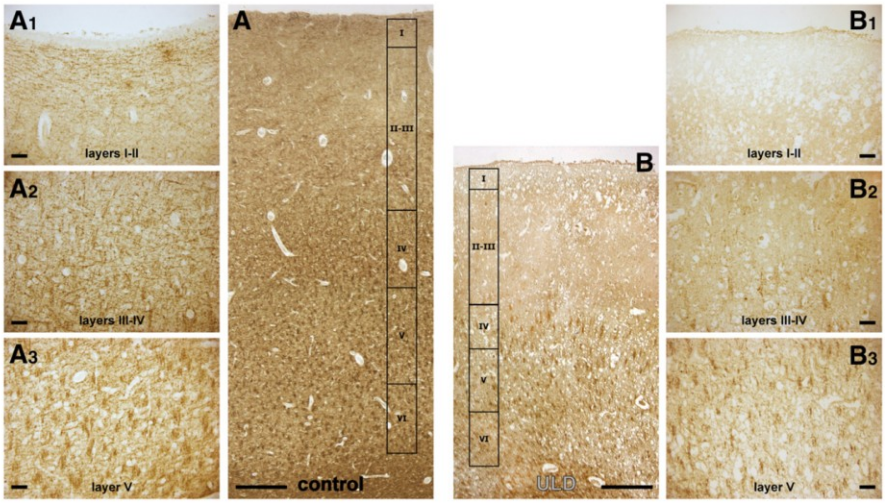

Fig. 10. VGAT immunolabeled sections of precentral motor cortex taken from a representative non-epileptic control (A) and a ULD (B) patient. The boxes indicate of the different layer (I to VI). (A_{1-3}) Higher magnification of layers I–II (A_1), layers II–IV (A_2) and layer V (A_3) in the non-epileptic control. (B_{1-3}) Higher magnification of layers I–II (B_1), layers II–IV (B_2) and layer V (B_3) in the ULD patient. Note the dramatic reduction in thickness and the obvious loss of VGAT-labeled GABA terminals in ULD. Horizontal bars = 1 mm in A and B; 100 μm in A_{1-3} and B_{1-3}.

we found a markedly reduced PPD in neocortical slices obtained from KO compared with WT mice. PPD in extracellular recordings reflects the net effect of excitation and inhibition, thus it cannot unequivocally demonstrate GABA impairment. However, a defective inhibition accounts for similarly impaired PPD in models of chronic epilepsy and acute lesions (Hagemann et al., 1999). Moreover, no significant change was found in field potential amplitude or I–O relationship, suggesting that excitatory transmission was preserved in KO mice.

GABA transmission, significantly shifted the I–O relationship to the left in KO, but not in WT mice. This further supports the notion that GABA inhibition is impaired in KOs because, under these experimental conditions, GABA inhibition occurs together with excitatory postsynaptic responses, which become enhanced when inhibition is weak. The greater reduction of PPD at short IPIs again suggests impaired inhibition in KOs, because this results from a greater disinhibition when the PP protocol is performed in the presence of low concentration bicuculline.

The reduced inhibition of the conditioned response at ≈20 ms IPIs in KO mice further supports a defective GABA signaling, because PPD mostly depends on $GABA_A$ receptors at these IPIs (Rozas et al., 2001). In the cortex, GABA activates fast, $GABA_A$ receptor-mediated IPSCs peaking at 20-30 ms and slower, $GABA_B$ receptor-mediated IPSCs peaking considerably later (Alger and Nicoll, 1982). In KO mice, inhibition was also defective at longer IPIs, suggesting that $GABA_B$ function is also impaired. In keeping with these data, evaluation of cortical inhibition, performed in ULD patients by matching paired magnetic stimuli delivered to motor cortex or paired sensory and magnetic stimuli, indicate a reduced $GABA_A$ and, to a lesser extent, $GABA_B$ dependent cortical inhibition (Badawy et al., 2010; Canafoglia et al., 2010; Manganotti et al., 2001). The loss of GABAergic terminals observed in this study suggests that these phenomena arise from an overall reduction in the synaptic availability of GABA and not from alterations at receptor level.

Implications for human ULD

Are these findings relevant for the human disease? To tackle this question, we analyzed VGAT immunoreactivity in the post-mortem brain of an ULD patient, in comparison with three matching non-epileptic cases. Note that autopsy tissue from these patients is very difficult to obtain, and previous human neuropathological studies of ULD are limited (Cohen et al., 2011; Haltia et al., 1969; Koskiniemi et al., 1974). In the ULD specimen we examined, not only the thickness of the cortex was obviously reduced, consistent with MRI findings (Koskenkorva et al., 2009), but also VGAT immunoreactivity was dramatically reduced, consistent with our data in CSTB KO mice. These findings support the notion that a loss of cortical GABA terminals occurs in humans with ULD and, thus, that the GABAergic control is impaired. The data also suggest that the underlying pathology progresses even if the treatment with antiepileptic drugs symptomatically controls the disease: in fact, in spite of an effective treatment, this patient presented pathological features (decreased cortical thickness, loss of GABA terminals) typical of the natural evolution of the untreated disease.

VGAT immunoreactivity does not allow establishing whether neurodegeneration affects a specific subpopulation of cortical GABA interneurons, because VGAT is the only vesicular transporter of GABA and appears to be present in every GABA terminal (Takamori, 2006). Based on morphology, however, it seems likely that the principal GABA interneurons (basket and chandelier cells) are lost with their nerve endings.

ULD has now a better prognosis than in the past, even when presenting with a progressive and disabling myoclonus (Lehesjoki and Koskiniemi, 1999). This improved prognosis results from the pharmacological treatments applied in the last years. Initially, treatment was attempted using sodium channel blockers. These drugs prevent high frequency firing, a characteristic of many GABA interneurons. In light of the present findings, their clinical failure can now be interpreted as being due to the impairment of GABA interneuron residual activity. The first choice drug for ULD is now valproate, which increases GABA synaptic levels by inhibiting its catabolism, and the alternative choice are the benzodiazepines, which allosterically potentiate GABA action on $GABA_A$ receptors (Sigel and Buhr, 1997). The present findings provide a strong rationale for using these drugs, which potentiate the residual GABA signal.

In conclusion, we report here the first direct evidence that loss of cortical GABA input occurs in a relevant animal model and in a case of human ULD, leading to a condition of latent hyperexcitability that favors myoclonus and seizures. These findings have direct relevance for understanding of the pathogenic mechanism of ULD and the neurobiological basis of the effect of currently employed drugs.

Acknowledgments

This work has been supported by grants from the Fondazione Mariani ([project R-07-63], "Neurodegenerazione ed epilessia: studio del modello murino della mioclono-epilessia progressiva di Unverricht–Lundborg") to SF and MS. The authors are grateful to Dr. G. Giaccone for providing the human ULD case and to S. Spinello for technical support (Department of Neuropathology, "C. Besta" Institute, Milan, Italy).

References

Abrahamson, M., et al., 2003. Cystatins. Biochem. Soc. Symp. 179–199.
Alger, B.E., Nicoll, R.A., 1982. Pharmacological evidence for two kinds of GABA receptor on rat hippocampal pyramidal cells studied in vitro. J. Physiol. (Lond) 328, 125–141.
Badawy, R.A.B., et al., 2010. Can changes in cortical excitability distinguish progressive from juvenile myoclonic epilepsy? Epilepsia 51, 2084–2088.
Bellocchio, E.E., et al., 2000. Uptake of glutamate into synaptic vesicles by an inorganic phosphate transporter. Science 289, 957–960.
Blazquez-Llorca, L., et al., 2010. GABAergic complex basket formations in the human neocortex. J. Comp. Neurol. 518, 4917–4937.
Canafoglia, L., et al., 2010. Short and long interval cortical inhibition in patients with Unverricht–Lundborg and Lafora body disease. Epilepsy Res. 89, 232–237.
Chaudhry, F.A., et al., 1998. The vesicular GABA transporter, VGAT, localizes to synaptic vesicles in sets of glycinergic as well as GABAergic neurons. J. Neurosci. 18, 9733–9750.
Cohen, N.R., et al., 2011. New neuropathological findings in Unverricht–Lundborg disease: neuronal intranuclear and cytoplasmic inclusions. Acta Neuropathol. 121, 421–427.
DeFelipe, J., et al., 1989. Visualization of chandelier cell axons by parvalbumin immunoreactivity in monkey cerebral cortex. Proc. Natl. Acad. Sci. U. S. A. 86, 2093–2097.
Dijk, J.M., Tijssen, M.A.J., 2010. Management of patients with myoclonus: available therapies and the need for an evidence-based approach. Lancet Neurol. 9, 1028–1036.
Franceschetti, S., et al., 2007. A pathogenetic hypothesis of Unverricht–Lundborg disease onset and progression. Neurobiol. Dis. 25, 675–685.
Hagemann, G., et al., 1999. Effects of tetanus toxin on functional inhibition after injection in separate cortical areas in rat. Brain Res. 818, 127–134.
Haltia, M., et al., 1969. Neuropathological studies in three Scandinavian cases of progressive myoclonus epilepsy. Acta Neurol. Scand. 45, 63–77.
Heines, D.E., 2003. Neuroanatomy. An atlas of structures, sections and systems. Lippincott Williams and Wilkins, Philadelphia, PA, USA.
Joensuu, T., et al., 2007. Cystatin B: mutation detection, alternative splicing and expression in progressive myclonus epilepsy of Unverricht–Lundborg type (EPM1) patients. Eur. J. Hum. Genet. 15, 185–193.
Kälviäinen, R., et al., 2008. Clinical picture of EPM1-Unverricht–Lundborg disease. Epilepsia 49, 549–556.
Koskenkorva, P., et al., 2009. Motor cortex and thalamic atrophy in Unverricht–Lundborg disease: voxel-based morphometric study. Neurology 73, 606–611.
Koskiniemi, M., et al., 1974. Progressive myoclonus epilepsy: a clinical and histopathological study. Acta Neurol. Scand. 50, 307–332.
Lehesjoki, A.E., Koskiniemi, M., 1999. Progressive myoclonus epilepsy of Unverricht–Lundborg type. Epilepsia 40 (Suppl. 3), 23–28.
Lehesjoki, A.E., et al., 1991. Localization of a gene for progressive myoclonus epilepsy to chromosome 21q22. Proc. Natl. Acad. Sci. U. S. A. 88, 3696–3699.
Lehesjoki, A.E., et al., 1993. Localization of the EPM1 gene for progressive myoclonus epilepsy on chromosome 21: linkage disequilibrium allows high resolution mapping. Hum. Mol. Genet. 2, 1229–1234.
Lehtinen, M.K., et al., 2009. Cystatin B deficiency sensitizes neurons to oxidative stress in progressive myoclonus epilepsy, EPM1. J. Neurosci. 29, 5910–5915.
Manganotti, P., et al., 2001. Hyperexcitable cortical responses in progressive myoclonic epilepsy: a TMS study. Neurology 57, 1793–1799.
McIntire, S.L., et al., 1997. Identification and characterization of the vesicular GABA transporter. Nature 389, 870–876.
Minelli, A., et al., 2003. Postnatal development of the vesicular GABA transporter in rat cerebral cortex. Neuroscience 117, 337–346.
Muzzolini, A., et al., 1997. Characterization of glutamate and [^{3}H]D-aspartate outflow from various in vitro preparations of the rat hippocampus. Neurochem. Int. 31, 113–124.
Paradiso, B., et al., 2009. Localized delivery of fibroblast growth factor-2 and brain-derived neurotrophic factor reduces spontaneous seizures in an epilepsy model. Proc. Natl. Acad. Sci. U. S. A. 106, 7191–7196.
Pennacchio, L.A., et al., 1996. Mutations in the gene encoding cystatin B in progressive myoclonus epilepsy (EPM1). Science 271, 1731–1734.
Pennacchio, L.A., et al., 1998. Progressive ataxia, myoclonic epilepsy and cerebellar apoptosis in cystatin B-deficient mice. Nat. Genet. 20, 251–258.
Rinne, R., et al., 2002. Reduced cystatin B activity correlates with enhanced cathepsin activity in progressive myoclonus epilepsy. Ann. Med. 34, 380–385.
Rozas, C., et al., 2001. Developmental inhibitory gate controls the relay of activity to the superficial layers of the visual cortex. J. Neurosci. 21, 6791–6801.
Sbrenna, S., et al., 1999. L-glutamate and gamma-aminobutyric acid efflux from rat cerebrocortical synaptosomes: modulation by kappa- and mu- but not delta- and opioid receptor like-1 receptors. J. Pharmacol. Exp. Ther. 291, 1365–1371.
Shannon, P., et al., 2002. Neuropathological changes in a mouse model of progressive myoclonus epilepsy: cystatin B deficiency and Unverricht–Lundborg disease. J. Neuropathol. Exp. Neurol. 61, 1085–1091.
Shibasaki, H., 2006. Neurophysiological classification of myoclonus. Neurophysiol. Clin. 36, 267–269.
Sigel, E., Buhr, A., 1997. The benzodiazepine binding site of $GABA_A$ receptors. Trends Pharmacol. Sci. 18, 425–429.
Stone, N.E., et al., 1996. Construction of a 750-kb bacterial clone contig and restriction map in the region of human chromosome 21 containing the progressive myoclonus epilepsy gene. Genome Res. 6, 218–225.
Takamori, S., 2006. VGLUTs: "exciting" times for glutamatergic research? Neurosci. Res. 55, 343–351.
Takamori, S., et al., 2000a. Identification of a vesicular glutamate transporter that defines a glutamatergic phenotype in neurons. Nature 407, 189–194.
Takamori, S., et al., 2000b. Immunoisolation of GABA-specific synaptic vesicles defines a functionally distinct subset of synaptic vesicles. J. Neurosci. 20, 4904–4911.
Tongiorgi, E., et al., 2004. Brain-derived neurotrophic factor mRNA and protein are targeted to discrete dendritic laminas by events that trigger epileptogenesis. J. Neurosci. 24, 6842–6852.
Valzania, F., et al., 1999. Facilitation of rhythmic events in progressive myoclonus epilepsy: a transcranial magnetic stimulation study. Clin. Neurophysiol. 110, 152–157.
Virtaneva, K., et al., 1996. Progressive myoclonus epilepsy EPM1 locus maps to a 175-kb interval in distal 21q. Am. J. Hum. Genet. 58, 1247–1253.
Zucchini, S., et al., 2008. FGF-2 overexpression increases excitability and seizure susceptibility but decreases seizure-induced cell loss. J. Neurosci. 28, 13112–13124.

Chapter 4. CONCLUSIONS

4.1 OVERALL CONCLUSION AND FUTURE PERSPECTIVES

Expanding the knowledge of NTFs is important, because data on their biology and their implication in the pathogenesis of neurodegenerative diseases, including epilepsy, are insufficient. Also, improvements are needed to deliver these molecules selectively in the lesion area.

In this thesis, we explored new technologies to better understand the role of BDNF in epilepsy, by developing and validating innovative strategies to modulate the BDNF signal within the epileptic focus. Whilst on the one hand we developed tools (amiplicon vectors) to silence BDNF expression *in vivo*, on the other we tested the effects of a continuous administration of BDNF in the epileptic hippocampus by using ECB devices.

Some aspects of the present findings are worthy of note. First, the data support the consolidated hypothesis that BDNF can exert contrasting effect in the epileptic brain, depending on the experimental settings and on the stage of progression of the disease. Second, the implantation of the ECB devices was performed under conditions that are perfectly compatible with the clinical situation: chronic patients with surgically-treatable TLE that are planned to undergo a two-step surgery (implantation of recording electrodes, then removal of the epileptogenic area) may be an ideal population to clinically test this approach because the ECB device might be implanted together with the electrodes and, should it prove ineffective, it could be removed and the patient could undergo surgery as originally planned. Third, the results are promising not only in epileptic field, but also for other neurodegenerative diseases or to test other NTFs.

A detailed analysis of the mechanisms of action was behind the scope of this thesis. The present data, however, prompt future studies in which a more refined modulation of BDNF levels is achieved, for example by using amplicon vectors designed to up and down regulate the different splice variants of BDNF mRNA. We plan to investigate these fascinating and challenging possibilities in the future.

References

Abubakr A, Wambacq I (2008) **Long-term outcome of vagus nerve stimulation therapy in patients with refractory epilepsy.** *J Clin Neurosci 15:127-129.*

Acharya JN (2002) **Recent advances in epileptogenesis.** *Curr Scie 82: 679-688.*

American Epilepsy Society Basic Science Committee And The International League Against Epilepsy Working Group On Recommendations For PreclinicalEpilepsy Drug Discovery. Galanopoulou AS1, Buckmaster PS, Staley KJ, Moshé SL, Perucca E, Engel J Jr, Löscher W, Noebels JL, Pitkänen A, Stables J, White HS, O'Brien TJ, Simonato M (2012) **Identification of new epilepsy treatments: issues in preclinical methodology.** *Epilepsia 253: 571-582.*

Ardesch JJ, Buschman HP, Wagener-Schimmel LJ, van der Aa HE, Hageman G (2007) **Vagus nerve stimulation for medically refractory epilepsy: a long-term follow-up study.** *Seizure 16: 579-585.*

Arida RM, Scorza FA, Peres CA, Cavalheiro EA (1999) **The course of untreated seizures in the pilocarpine model of epilepsy.** *Epilepsy Res 34: 99-107.*

Ashok K Shetty (2014) **Hippocampal injury-induced cognitive and mood dysfunction, altered neurogenesis, and epilepsy: Can early neural stem cell grafting intervention provide protection?** *Epilepsy & Behavior 38:117-124.*

Barret GL and Bartlett PF (1994) **The p75 nerve growth factor receptor mediates survival or death depending on the stage of sensory neuron development.** *Proc Natl Acad Sci USA 91:6501-6505.*

Berkovic SF, Andermann F, Carpenter S, Wolfe LS (1986) **Progressive myoclonus epilepsies: specific causes and diagnosis.** *N Engl J Med 315: 296-305.*

Berkovic SF, Cochius J, Andermann E, Andermann F (1993) **Progressive myoclonus epilepsies: clinical and genetic aspects.** *Epilepsia 34: 19–30.*

Ben-Ari Y (2006) **Seizures beget seizures: the quest for GABA as a key player.** *Crit Rev Neurobiol.18: 135-144.*

Ben-Ari Y and Dudek FE (2010) **Primary and secondary mechanisms of epileptogenesis in the temporal lobe: there is a before and an after.** *Epilepsy Currents 10: 118-125.*

Bhowmik M, Khanam R, Saini N, Vohora D (2014) **Activation of AKT/GSK3β pathway by TDZD-8 attenuates kainic acid induced neurodegeneration but not seizures in mice.** *NeuroToxicology 46: 44-52.*

Biagini G, Baldelli E, Longo D, Pradelli L, Zini I, Rogawski MA, Avoli M (2006) **Endogenous neurosteroids modulate epileptogenesis in a model of temporal lobe epilepsy.** *Exp Neurol 201: 519–24.*

Biervert C, Schroeder BC, Kubisch C, Berkovic SF, Propping P, Jentsch TJ, Steinlein OK (1998) **A potassium channel mutation in neonatal human epilepsy.** *Science 279: 403-406.*

Binder DK, Routbort MJ, McNamara JO (1999) **Immunohistochemical evidence of seizure-induced activation of trk receptors in the mossy fiber pathway of adult rat hippocampus.** *J. Neurosci. 19: 4616–4626.*

Binder DK and Scharfman HE (2004) **Brain-derived neurotrophic factor.** *Growth Factors 22: 123–131.*

Blümcke I, Schewe JC, Normann S, Brüstle O, Schramm J, Elger CE, Wiestler OD *(2001)* ***Increase of nestin-immunoreactive neural precursor cells in the dentate gyrus of pediatric patients with early onset temporal lobe epilepsy.*** *Hippocampus 11: 311-321.*

Blümcke I, Thom M, Aronica E, Armstrong DD, Bartolomei F, Bernasconi A, Bernasconi N, Bien CG, Cendes F, Coras R, Cross JH, Jacques TS, Kahane P, Mathern GW, Miyata H, Moshé SL, Oz B, Özkara Ç, Perucca E, Sisodiya S, Wiebe S, Spreafico R (2013) **International consensus classification of hippocampal sclerosis in temporal lobe epilepsy: a Task Force report from the ILAE Commission on Diagnostic Methods.** *Epilepsia. 54: 1315-1329.*

Boehmer PE, Lehman IR (1997) **Herpes simplex virus DNA replication.** *Annu Rev Biochem 66: 347-384.*

Bothwell M (1995) **Functional interactions of neurotrophins and neurotrophin receptors.** *Annu Rev Neurosci 18: 223-53.*

Bucci C, Alifano P and Cogli L (2014) **The Role of Rab Proteins in Neuronal Cells and in the Trafficking of Neurotrophin Receptors.** *Membranes 4: 642-677.*

Buckmaster PS, Dudek FE (1997) **Neuron loss, granule cell axon reorganization, and functional changes in the dentate gyrus of epileptic kainate-treated rats.** *J Comp Neurol 385: 385–404.*

Butte MJ (2001) **Neurotrophic factor structures reveal clues to evolution, binding, specificity, and receptor activation.** *Cell. Mol. Life Sci. 58: 1003-1013.*

Canossa M, Griesbeck O, Berninger B, Campana G, Kolbeck R, Thoenen H (1997) **Neurotrophin release by neurotrophins: implications for activity-dependent neuronal plasticity.** *Proc Natl Acad Sci USA 94: 13279-13286.*

Carter BD, Kaltschmidt C, Kaltschmidt B, Offenhäuser N, Böhm-Matthaei R, Baeuerle PA, Barde YA (1996) **Selective activation of NF-kappa B by nerve growth factor through the neurotrophin receptor p75.** *Science 272: 542-545.*

Cavalheiro EA, Leite JP, Bortolotto ZA, Turski WA, Ikonomidou C, Turski L (1991) **Long-term effects of pilocarpine in rats: structural damage of the brain triggers kindling and spontaneous recurrent seizures.** *Epilepsia 32: 778–82.*

Chao MV (2003) **Neurotrophins and their receptors: a convergence point for many signalling pathways.** *Nat. Rev Neurosci.4: 299-309.*

Chiaruttini C, Sonego M, Baj G, Somonato M, Tongiorgi E (2008) **BDNF mRNA splice variants display activity-dependent targeting to distinct hippocampal laminae.** *Mol.Cell.Neurosci. 37: 11-19.*

Conner JM, et al (1997) **Distribution of brain-derived neurotrophic factor (BDNF) protein and mRNA in the normal adult rat CNS: evidence for anterograde axonal transport.** *J Neurosci 17: 2295–2313.*

Cossart R, Bernard C, Ben-Ari Y (2005) **Multiple facets of GABAergic neurons and synapses: multiple fates of GABA signaling in epilepsies.** *Trends Neurosci. 28: 108-115.*

Crespel A, Coubes P, Rousset MC, Brana C, Rougier A, Rondouin G, Bockaert J, Baldy-Moulinier M, Lerner-Natoli M (2002) **Inflammatory reactions in human medial temporal lobe epilepsy with hippocampal sclerosis.** *Brain Res 952: 159-169.*

Croll SD, Suri C, Compton DL, Simmons MV, Yancopoulos GD, Lindsay RM, Wiegand SJ, Rudge JS, Scharfman HE (1999) **Brain-derived neurotrophic factor transgenic mice exhibit passive avoidance deficits, increased seizure severity and in vitro hyper-excitability in the hippocampus and entorhinal cortex.** Neuroscience 93: 1491–1506.

Cross DJ, Cavazos JE (2009) **Circuitry reorganization, regeneration, and sprouting. In Schwartzkroin PA.** *Encyclopedia of basic epilepsy research: 1148–1154.*

Curia G, Longo D, Biagini G, Jones RS, Avoli M (2008) **The pilocarpine model of temporal lobe epilepsy.** *J Neurosci Methods 172: 143-57.*

Curtis R, Adryan KM, Stark JL et al. (1995) **Differential role of the low affinity neurotrophin receptor (p75) in retrograde axonal transport of the neurotrophins.** *Neuron 14: 1201–1212.*

Dalby NO and Mody I (2001) **The process of epileptogenesis: a pathophysiological approach.** *Curr Opin Neurol 14: 187-92.*

Dechant G and Barde YA (1997**) Signaling through the neurotrophin receptor p75NTR.** *Curr Opin Neurobiol 7: 413-418.*

Deiss LP, Chou J, Frenkel N (1986) **Functional domains within the a sequence involved in the cleavage-packaging of herpes simplex virus DNA.** *J Virol 59: 605-618.*

Delgado-Escueta AV, Ganesh S, Yamakawa K (2001) **Advances in the genetics of progressive myoclonus epilepsy.** *Am. J. Med. Genet 106: 129–138.*

Drexel M, Preidt AP, Kirchmair E, Sperk G (2011) **Parvalbumin interneurons and calretinin fibers arising from the thalamic nucleus reuniens degenerate in the subiculum after kainic acid-induced seizures.** *Neuroscience 189: 316-329.*

Duncan JS (2007) **Epilepsy surgery.** *Clin Med* 7:137-142.

Dudek FE, Li-Rong Shao (2004) **Mossy Fiber Sprouting and Recurrent Excitation: Direct Electrophysiologic Evidence and Potential Implications.** *Epilepsy Curr. 4: 184-187.*

Eide FF, Vining ER, Eide BL, Zang K, Wang XY, Reichardt LF (1996) **Naturally occurring truncated TrkB receptors have dominant inhibitory effects on brain-derived neurotrophic factor signaling.** *J. Neurosci.16: 3123–3129.*

Elkabes S, DiCicco-Bloom EM, Black IB (1996) **Brain microglia/macrophages express neurotrophins that selectively regulate microglial proliferation and function.** *J Neurosci 15: 2508-2521.*

Emerich DF, Winn SR (2004) **Neuroprotective effects of encapsulated CNTF-producing cells in a rodent model of Huntington's disease are dependent on the proximity of the implant to the lesioned striatum.** *Cell Transplant. 13: 253-259.*

Emerich DF, Orive G, Thanos C, Tornoe J, Wahlberg LU. (2014) **Encapsulated cell therapy for neurodegenerative diseases: From promise to product.** *Adv. Drug. Deliv. Rev. 67-68: 131-141.*

Engel J Jr. (2006) **ILAE classification of epilepsy syndromes.** *Epilepsy 70: 5-10.*

Epstain A (2005) **HSV-1-based amplicon vectors: design and applications.** *Gene Therapy 12: 154-158.*

Epstein A (2009) **HSV-1-derived amplicon vectors: recent technological improvements and remaining difficulties.** *Mem Inst Osw Cruz 104: 399-410.*

Escayg A, MacDonald BT, Meisler MH, Baulac S, Huberfeld G, An-Gourfinkel I, Brice A, LeGuern E, Moulard B, Chaigne D, Buresi C, Malafosse A (2000) **Mutations of SCN1A, encoding a neuronal sodium channel, in two families with GEFS+2.** *Nat Genet 24: 343-345.*

Fisher RS, van Emde Boas W, Blume W, Elger C, Genton P, Lee P, Engel J, Jr. (2005) **Epileptic seizures and epilepsy: definitions proposed by the International League Against Epilepsy (ILAE) and the International Bureau for Epilepsy (IBE)**. *Epilepsia 46: 470-472.*

Freund TF, Buzsáki G (1996) **Interneurons of the hippocampus.** *Hippocampus 6: 347-470.*

Fujikawa DG (1996) **The temporal evolution of neuronal damage from pilocarpine-induced status epilepticus.** *Brain Res 725: 11-22.*

Fujikawa DG, Itabashi HH, Wu A, Shinmei SS (2000) **Status epilepticus-induced neuronal loss in human without systemic complications or epilepsy.** *Epilepsia 41: 981-991.*

Gill DA, Ramsay SL, Tasker RA (2010**) Selective reductions in subpopulations of GABAergic neurons in a developmental rat model of epilepsy.** *Brain Res 1331:114-123.*

Goffin K, Nissinen J, Van Laere K, Pitk¨anen A (2007) **Cyclicity of spontaneous recurrent seizures in pilocarpine model of temporal lobe epilepsy in rat.** *Exp Neurol 205: 501-505.*

Gong C, Wang TW, Huang HS, Parent JM (2007) **Regulates Neuronal Progenitor Migration in Intact and Epileptic Hippocampus.** *J. Neurosci. 8: 1803-1911.*

Götz R, Köster R, Winkler C, Raulf F, Lottspeich F, Schartl M, Thoenen H (1994) **Neurotrophin-6 is a new member of the nerve growth factor family.** *Nature 372: 266-269.*

He XP, Kotloski R, Nef S, Luikart BW, Parada LF, McNamara JO (2004) **Conditional deletion of TrkB but not BDNF prevents epileptogenesis in the kindling model.** *Neuron 43: 31–42.*

Hennigan A, O'Callaghan RM, Kelly AM (2007) **Neurotrophins and their receptors: roles in plasticity, neurodegeneration and neuroprotection.** *Biocheical Soc. Trans. 35: 424-427.*

Hirtz D, Thurman DJ, Gwinn-Hardy K, Mohamed M, Chaudhuri AR, Zalutsky R. (2007) **How common are the ''common'' neurologic disorders?** *Neurology 68: 326–337.*

Houser CR and Esclapez M (1996) **Vulnerability and plasticity of the GABA system in the pilocarpine model of spontaneous recurrent seizures.** *Epilepsy Res 26: 207-218.*

Huang EJ, Reichardt LF (2003) **Trk receptors: Roles in neuronal signal transduction.** *Annu. Rev. Biochem.72: 609–642.*

Huang B, Tabata Y, Gao JQ (2012) **Mesenchymal stem cells as therapeutic agents and potential targeted gene delivery vehicle for brain diseases.** *J Control. Release 162: 464-473.*

Kaplan DR, Miller FD (2000**) Neurotrophin signal transduction in the nervous system.** *Curr. Opin. Neurobiol.10: 381–391.*

Kobow K, Blumcke I (2011) **The methylation hypothesis: do epigenetic chromatin modifications play a role in epileptogenesis?** Epilepsia 52: 15–19.

Kobow K, Auvin S, Jensen F, Loscher W, Mody I, Potschka H, Prince D, Sierra A, Simonato M, Pitkanen A, Nehlig A, Rho JM (2012) **Finding a better drug for epilepsy: Antiepileptogenesis targets.** *Epilepsia 53: 1868-1876.*

Kokaia M, Ernfors P, Kokaia Z, Elmer E, Jaenisch R, Lindvall O (1995) **Suppressed epileptogenesis in BDNF mutant mice.** *Exp. Neurol. 33: 215–224.*

Kotsopoulos IA, van Merode T, Kessels FG, de Krom MC, Knottnerus JA (2002) **Systematic review and meta-analysis of incidence studies of epilepsy and unprovoked seizures.** *Epilepsia 43: 1402-1409.*

Koyama R, Ikegaya Y (2005) **To BDNF or not to BDNF: that is the epileptic hippocampus.** *Neuroscientist 11: 282–287.*

Kralic JE, Ledergerber DA, Fritschy KM (2005) **Disruption of the neurogenic potential of the dentate gyrus an a mouse model of temporal lobe epilepsy with focal seizures.** *European Journal of Neuroscience 22: 1916-1927.*

Kullander K, Carlson B, Hallbook F (1997) **Molecular phylogeny and evolution of the neurotrophins from monotremes and marsupials.** *J Mol Evol. 45: 311-321.*

Kuramoto S, Yasuhara T, Agari T, Kondo A, Jing M, Kikuchi Y, Shinko A, Wakamori T, Kameda M, Wang F, Kin K, Edahiro S, Miyoshi Y, Date I (2011) **BDNF-secreting capsule exerts neuroprotective effects on epilepsy model of rats.** *Brain Research 1368: 281-289.*

Kuryatov A, Gerzanich V, Nelson M, Olale F, Lindstrom J (1997) **Mutation causing autosomal dominant nocturnal frontal lobe epilepsy alters Ca^{2+} permeability, conductance, and gating of human alfa4beta2 nicotinic acetylcholine receptors.** *J Neurosci 17: 9035-9047.*

Kuruba R, Hattiangady B, Shetty AK (2009) **Hippocampal neurogenesis and neural stem cells in temporal lobe epilepsy.** *Epilepsy Behav 14: 65-73.*

Kuruba R, Hattiangady B, Parihar VK, Shuai B, Shetty AK (2011) **Differential susceptibility of interneurons expressing neuropeptide Y or parvalbumin in the aged hippocampus to acute seizure activity.** *PLoS. One. 6: e24493.*

Kwan P and Brodie MJ (2000) **Early identification of refractory epilepsy.** *N Engl J Med 342: 314-319.*

Kwong AD, Frenkel N (1984) **Herpes simplex virus amplicon: effect of size on replication of constructed defective genomes containing eucaryotic DNA sequences.** *J Virol 51: 595-603.*

Labar D, Nikolov B, Tarver B, Fraser R (1998) **Vagus nerve stimulation for symptomatic generalized epilepsy: a pilot study.** *Epilepsia 39: 201-205.*

Lee R, Kermani P, Teng KK, Hempstead BL (2001) **Regulation of cell survival by secreted proneurotrophins.** *Science 294: 1945–1948.*

Lehesjoki AE, Koskiniemi M (1999) **Progressive myoclonus epilepsy of Unverricht–Lundborg type.** *Epilepsia 40: 23–28.*

Lei L and Parada F (2007) **Transcriptional regulation of Trk family neurotrophin receptors.** *Cell Mol. Life Sci. 64: 522-532.*

Lemos T and Cavalheiro EA (1995) **Suppression of pilocarpine-induced status epilepticus and the late development of epilepsy in rats.** *Exp Brain Res 102: 423-428.*

Lindvall O, Wahlberg LU (2008) **Encapsulated cell biodelivery of GDNF: a novel clinical strategy for neuroprotection and neuroregeneration in Parkinson's disease?** *Exp.Neurol.209: 82-88.*

Liu QR et al. (2005) **Human brain derived neurotrophic factor (BDNF) genes, splicing patterns, and assessments of associations with substance abuse and Parkinson's disease.** *Am. J. Med. Genet. B Neuropsychiatr. Genet.134: 93–103.*

Liu QR, Lu L, Zhu XG, Gong JP, Shaham Y, Uhl GR (2006) **Rodent BDNF genes, novel promoters, novel splice variants, and regulation by cocaine.** *Brain Res 10667:1-12.*

Liu Z, Nagao T, Desjardins GC, Gloor P, Avoli M (1994) **Quantitative evaluation of neuronal loss in the dorsal hippocampus in rats with long-term pilocarpine seizures.** *Epilepsy Res 17: 237-247.*

Loeb DM, Stephens RM, Copeland T, Kaplan DR, Greene LA *(1994)* **A Trk nerve growth factor (NGF) receptor point mutation affecting interaction with phospholipase C-γ1 abolishes NGF-promoted peripherin induction but not neurite outgrowth.** *J Biol Chem 269: 8901-8910.*

Lukasiuk K, Dabrowski M, Adach A, Pitkanen A (2006) **Epileptogenesis-related genes revisited.** *Prog Brain Res 158: 223-241.*

Makkerh JP, Ceni C, Auld DS, Vaillancourt F, Dorval G, Barker PA (2005) **P75 neurotrophin receptor reduces ligand-induced Trk receptor ubiquitination and delays Trk receptor internalization and degradation.** *EMBO Rep. 6: 936–941.*

Marchi N, Angelov L, Masaryk T, Fazio V, Granata T, Hernandez N, Hallene K, Diglaw T, Franic L, Najm I, Janigro D (2007a) **Seizure-promoting effect of bloodbrain barrier disruption.** *Epilepsia 48: 732-742.*

Marchi N, Oby E, Batra A, Uva L, De Curtis M, Hernandez N, Van Boxel-Dezaire A, Najm I, Janigro D (2007b) **InVivo and InVitro Effects of Pilocarpine: Relevance to Ictogenesis.** *Epilepsia 48: 1934-1946.*

Marks W.J., Bartus R.T., Siffert J., Davis C.S.,Lozano A., Boulis N.,VitekJ., Stacy M., Turner D., Verhagen L., Bakay R., Watts R., Guthrie B., Jankovic J, Simpson R., Tagliati M., Alterman R., Stern M., Baltuch G., Starr P.A., Larson P.S., Ostrem J.L., Nutt J., Kieburtz K., Kordower J.H., Olanow C.W. (2010) **Gene delivery of AAV2-neurturin for Parkinsin's disease: a double-blind, randomized, controlled trial.** *Lancet Neutol. 9: 1164-1172.*

Mathern GW, Babb TL, Mischel PS, Vinters HV, Pretorius JK, Leite JP, Peacock WJ. (1996) **Childhood generalized and mesial temporal epilepsies demonstrate different amounts and patterns of hippocampal neuron loss and mossy fiber synaptic reorganization.** *Brain 119: 965–987.*

Mazzuferi M, Palma E Martinello K, Maiolino F, Roseti C, Fucile S, Fabene PF, Schio F, Pellitteri M, Sperk G, Miledi R, Eusebi F, Simonato M (2010) **Enhancement of GABA(A)-current run-down in the hippocampus occurs at the first spontaneous seizure in a model of temporal lobe epilepsy.** *Proc Natl Acad Sci USA 107: 3180-3185.*

McAllister A, Katz L, Lo D (1999) **Neurotrophins and synaptic plasticity**. *Annual Review of Neuroscience 22: 295–318.*

McDonald NQ, Lapatto R, Murray-Rust J, Gunning J, Wlodawer A, Blundell TL (1991) **New protein fold revealed by a 2.3-Å resolution crystal structure of nerve growth factor.** *Nature 354: 411-414.*

McHugh JD, Delanty N (2008) **Epidemiology and classification of epilepsy: gender comparisons.** *Int Rev Neurobiol 83: 11-26.*

McNamara JO (1999) **Emerging insights into the genesis of epilepsy.** *Nature 399: A15-22.*

Merlio JP, et al (1993) **Increased production of the trkB protein tyrosine kinase receptor after brain insults.** *Neuron 10: 151–164.*

Milby AH, Halpern CH, Baltuch GH (2008) **Vagus nerve stimulation for epilepsy and depression.** *Neurotherapeutics 5: 75-85.*

Mowla, SJ, Pareek S, Farhadi HF, Petrecca K, Fawcett JP, Seidah NG, Morris SJ, Sossin WS, Murphy RA (1999) **Differential sorting of nerve growth factor and brain-derived neurotrophic factor in hippocampal neurons.** *J. Neurosci. 19: 2069–2080.*

Mowla, S. J. et al. (2001) **Biosynthesis and post-translational processing of the precursor to brain-derived neurotrophic factor.** *J. Biol. Chem. 276: 12660–12666.*

Murray PS, Holmes PV (2011) **An pverview of Brain-Derived Neurotrophic Factor and implication for Excitotoxic Vulnerability in the Hippocampus.** *Int. J. Pept Vol. 2011.*

Nadler JV (2009) **Axon sprouting and epilepsy. In Schwartzkroin PA (Ed.) Encyclopedia of basic epilepsy research.** *Elsevier Academic Press, San Diego, pp. 1143–1148.*

Neal EG, Chaffe H, Schwartz RH, Lawson MS, Edwards N, Fitzsimmons G, Whitney A, Cross JH (2008) **The ketogenic diet for the treatment of childhood epilepsy: a randomised controlled trial.** *Lancet Neurol 7: 500-506***.**

Nikitidou L, Torp M, Fjord-Larsen L, Kusk P, Wahlberg LU, Kokaia M (2013) **Encapsulated galanin-producing cells attenuate focal epileptic seizures in the hippocampus.** *Epilepsia: 1–8.*

Obenaus A, Esclapez M, Houser CR (1993) **Loss of glutamate decarboxylase mRNA-containing neurons in the rat dentate gyrus following pilocarpine-induced seizures.** *J.Neurosci. 13: 4470-4485.*

Oberheim NA, Tian GF, Han X, Peng W, Takano T, Ransom B, Nedergaard M (2008) **Loss of Astrocytic Domain Organization in the Epileptic Brain.** *J. Neurosci 13: 3264-3276.*

Orive G, Anitua E, Pedraz JL, Emerich DF. (2009) **Biomaterials for promoting brain protection, repair and regeneration.** *Nat. Rev. Neurosci. 10: 682-692.*

Palma E, Torchia G, Limatola C, Trettel F, Arcella A, Cantore G, Di Gennaro G, Manfredi M, Esposito V, Quarato PP, Miledi R, Eusebi F (2005) **BDNF modulates GABAA receptors microtrans- planted from the human epileptic brain to Xenopus oocytes.** *Proc. Natl. Acad. Sci. U. S. A. 102: 1667–1672.*

Palma E, Roseti C, Maiolino F, Fucile S, Martinello K, Mazzuferi M, Aronica E, Manfredi M, Esposito V, Cantore G, Miledi R, Simonato M, Eusebi F (2007) **GABA(A)-current**

rundown of temporal lobe epilepsy is associated with repetitive activation of GABA(A) "phasic" receptors. *Proc. Natl. Acad. Sci. USA 104: 20944-20948.*

Paradiso B, Marconi P, Zucchini S, Berto E, Binaschi A, Bozac A, Buzzi A, Mazzuferi M, Magri E, Navarro Mora G, Rodi D, Su T, Volpi I, Zanetti L, Marzola A, Manservigi R, Fabene PF, Simonato M (2009) **Localized delivery of fibroblast growth factor-2 and brain- derived neurotrophic factor reduces spontaneous seizures in an epilepsy model.** *Proc Natl Acad Sci 106: 7191-7196.*

Parent JM, Tada E, Fike JR, Lowenstein DH (1999) **Inhibition of dentate granule cell neurogenesis with brain irradiation does not prevent seizure-induced mossy fiber synaptic reorganization in the rat.** *J Neurosci. 19: 4508-4519.*

Parent JM, Jessberger S, Gage FH, Gong C (2007) **Is neurogenesis reparative after status epilepticus?** *Epilepsia 48(suppl 8): 69–71.*

Pawson T, Nash P (2000) **Protein-protein interactions define specificity in signal transduction.** *Genes Dev.14: 1027–1047.*

Peltola J, Laaksonen J, Haapala AM, Hurme M, Rainesalo S, Keränen T (2002) **Indicators of inflammation after recent tonic-clonic epileptic seizures correlate with plasma interleukin- 6 levels.** *Seizure 11: 44-46.*

Phillips HA, Scheffer IE, Crossland KM, Bhatia KP, Fish DR, Marsden CD, Howell SJL, Stephenson BP, Tolmie J, Plazzi G, Eeg-Olofsson O, Singh R, Lopes-Cendes I, Andermann E, Andermann F, Berkovic SF, Mulley JC (1998) **Autosomal dominant nocturnal frontal-lobe epilepsy: genetic heterogeneity and evidence for a second locus at 15q24.** *Am J Hum Genet 63: 1108-1116.*

Pitkänen A, Nissinen J, Lukasiuk K, Jutila L, Paljarvi L, Salmenpera T, Karkola K, Vapalahti M, Ylinen A (2000) **Association between the density of mossy fiber sprouting and seizure frequency in experimental and human temporal lobe epilepsy.** *Epilepsia 41: S24–S29.*

Pitkänen A, Sutula TP (2002) **Is epilepsy a progressive disorder? Prospects for new therapeutic approaches in temporal-lobe epilepsy.** *Lancet Neurol. 1: 173-181.*

Pitkänen A and Lukasiuk K (2009) **Molecular and cellular basis of epileptogenesis in symptomatic epilepsy.** *Epilepsy & Behavior 14: 16–25.*

Pitkänen A (2010) **Therapeutic approaches to epileptogenesis-hope on the horizon.** *Epilepsia 51: 2–17.*

Pitkänen A and Lukasiuk K (2011) **Mechanisms of epilpetogenesis and potential treatment targets.** *Lancet Neurol. 10: 173-186.*

Racine RJ (1972) **Modification of seizure activity by electrical stimulation. II. Motor seizure.** *Electroencephalogr Clin Neurophysiol 32:281-294.*

Ragozzino D, Palma E, Di Angelantonio S, Amici M, Mascia A, Arcella A, Giangaspero F, Cantore G, Di Gennaro G, Manfredi M, Esposito V, Quarato PP, Miledi R, Eusebi F (2005) **Rundown of GABA type A receptors is a dysfunction associated with human drug-resistant mesial temporal lobe epilepsy.** *Proc. Natl. Acad. Sci. USA 102: 15219-15223.*

Reibel S, Larmet Y, Le BT, Carnahan J, Marescaux C, Depaulis A (2000a) **Brain-derived neurotrophic factor delays hippocampal kindling in the rat.** *Neuroscience 100: 777–788.*

Ribak CE, Tran PH, Spigelman I, Okazaki MM, Nadler JV (2000**) Status epilepticus-induced hilar basal dendrites on rodent granule cells contribute to recurrent excitatory circuitry.** *J Comp Neurol 428: 240-253.*

Roux PP, Colicos MA, Barker PA, Kennedy TE (1999) **p75 neurotrophin receptor expression is induced in apoptotic neurons after seizure.** *J Neurosci 19: 6887-6896.*

Roux PP, Barker PA (2002). **Neurotrophin signaling through the p75 neurotrophin receptor.** *Prog. Neurobiol. 67: 203–233.*

Rubin L.L, Staddon J.M. (1999) **The cell biology of the blood-brain barrier.** *Ann. Rev. Neurosci. 22: 11-28.*

Sakas DE, Korfias S, Nicholson CL, Panourias IG, Georgakoulias N, Gatzonis S, Jenkins A (2007) **Vagus nerve stimulation for intractable epilepsy: outcome in two series combining 90 patients.** *Acta Neurochir Suppl. 97: 287-291.*

Sanchez RM, Koh S, Rio C (2001) **Decreased glutamate receptor 2 expression and enhanced epileptogenesis in immature rat hippocampus after perinatal hypoxia-induced seizures.** *J Neurosci 21: 8154-8163.*

Santhakumar V, Aradi I, Soltesz I (2005) **Role of mossy fiber sprouting and mossy cell loss in hyperexcitability: a network model of the dentate gyrus incorporating cell types and axonal topography.** *J Neurophysiol 93: 437–453.*

Scharfman HE (1997) **Hyperexcitability in combined entorhinal/hippocampal slices of adult rat after exposure to brain-derived neurotrophic factor.** *J. Neurophysiol. 78: 1082–1095.*

Scharfman HE, Goodman JH, Sollas AL (1999) **Actions of brain-derived neurotrophic factor in slices from rats with spontaneous seizures and mossy fiber sprouting in the dentate gyrus.** J. *Neurosci. 19: 5619–5631.*

Scharfman HE, Sollas AL, Smith KL, Jackson MB, Goodman JH (2002b) **Structural and functional asymmetry in the normal and epileptic rat dentate gyrus.** *J. Comp. Neurol. 454: 424–439.*

Schroeder BC, Kubisch C, Stein V, Jentsch TJ (1998) **Moderate loss of function of cyclic-AMP-modulated KCNQ2/KCNQ3 K+ channels causes epilepsy.** *Nature 396: 687-690.*

Segal M (1998) **Synaptic activation of a cholinergic receptor in rat hippocampus.** *Brain Res 452: 79-86.*

Shahwan A, Farrell M, Delanty N (2005) **Progressive myoclonic epilepsies: a review of genetic and therapeutic aspects.** *Lancet Neurol. 4: 239–248.*

Shapiro LA, Korn MJ, Ribak CE (2005) **Newly generated dentate granule cells from epileptic rats exhibit elongated hilar basal dendrites that align along GFAP-immunolabeled processes.** *Neuroscience 136: 823-831.*

Sierra-Paredes G, Sierra-Marcuno G (2007) **Extrasynaptic GABA and glutamate receptors in epilepsy.** *CNS Neurol Disord Drug Targets 6: 288-300.*

Simonato M, Tongiorgi E, Kokaia M (2006) **Angels and demons: neurotrophic factors and epilepsy.** *Trends Pharmacol Sci 27: 631-638.*

Singh NA, Charlier C, Stauffer D, DuPont BR, Leach RJ, Melis R, Ronen GM, Bjerre I, Quattlebaum T, Murphy JV, McHarg ML, Gagnon D, Rosales TO, Peiffer A, Anderson VE, Leppert M (1998) **A novel potassium channel gene, KCNQ2, is mutated in an inherited epilepsy of newborns.** *Nat Genet 18: 25-29.*

Sng JC, Taniura H, Yoneda Y (2006) **Histone modifications in kainate-induced status epilepticus.** *Eur J Neurosci 23: 1269–1282.*

Spaete RR, and Frenkel N (1982) **The herpes simplex virus amplicon: A new eucaryotic defective-virus cloning-amplifying vector.** *Cell 30: 295–304.*

Spaete RR, Frenkel N (1985) **The herpes simplex virus amplicon: analyses of cis-acting replication functions.** *Proc Natl Acad Sci USA 82: 694-698.*

Spigelman I, Yan X-X, Obenaus A, Lee EY, Wasterlain CG, Ribak CE (1998) **Dentate granule cells form novel basal dendrites in a rat model of temporal lobe epilepsy.** *Neuroscience 86: 109-120.*

Steinlein OK, Magnusson A, Stoodt J, Bertrand S, Weiland S, Berkovic SF, Nakken KO, Propping P, Bertrand D (1997) **An insertion mutation of the CHRNA4 gene in a family with autosomal dominant nocturnal frontal lobe epilepsy.** *Hum Mol Genet 6: 943-948.*

Sun C, Mtchedlishvili Z, Bertram EH, Erisir A, Kapur J (2007) **Selective loss of dentate hilar interneurons contributes to reduced synaptic inhibition of granule cells in an electrical stimulation-based animal model of temporal lobe epilepsy.** *J.Comp Neurol. 500: 876-893.*

Sutula T (2002) **Seizure-Induced Axonal Sprouting: Assessing Connections Between Injury, Local Circuits, and Epileptogenesis.** *Epilepsy Curr.2: 86-91.*

Tatarewicz SM, Wei X,Gupta S, Masterman D, Swanson SJ, Moxness MS. (2007) **Development of a maturing T-cell-mediated immune response in patients with idiopathic Parkinson's disease receiving r-metHuGDNF via continuous intraputaminal infusion.** *J. Cli. Immunol. 27: 620-627.*

Tessarollo L, Tsoulfas P, Martin-Zanca D, Gilbert DJ, Jenkins NA, Copeland NG, Parada LF (1993) **TrkC, a receptor for neurotrophin-3, is widely expressed in the developing nervous system and in non-neuronal tissues.** *Development 118: 463-475.*

Thom M, Eriksson S, Martinian L, Caboclo LO, McEvoy AW, Duncan JS, Sisodya SM. (2009) **Temporal lobe sclerosis associated with hippocampal sclerosis in temporal lobe epilepsy: neuropathological features.** *J Neuropathol Exp Neurol 68: 928-938.*

Treiman DM (2001) **GABAergic mechanisms in epilepsy.** *Epilepsia 42:8-12.*

Turski WA, Cavalheiro EA, Schwarz M, Czuczwar SJ, Kleinrok Z, Turski L (1983) **Limbic seizures produced by pilocarpine I rats: behavioral, electroencephalographic and neuropathological study.** *Behav Brain Res 9: 315-335.*

Van Gassen KL, de Wit M, Koerkamp MJ, Rensen MG, van Rijen PC, Holstege FC, Lindhout D, de Graan PN (2008) **Possible role of the innate immunity in temporal lobe epilepsy.** *Epilepsia 49: 1055-1065.*

Veliskova J (2006) **Behavioural characterization of seizures in rats.** In: Pitkänen A, Schwartzkroin PA, Moshè SL, editors. *Models of seizures and epilepsy. Burlington: Elsevier Academic Press 601-611.*

Vezzani A, Friedman A, Dingledine RJ (2013) **The role of inflammation in epileptogenesis.** *Neuropharmacology 69: 19-24.*

Villanueva V, Carreno M, Herranz Fernandez JL, Gil-Nagel A (2007) **Surgery and electrical stimulation in epilepsy: selection of candidates and results.** *Neurologist 13: S29-37.*

Wallace RH, Wang DW, Singh R, Scheffer IE, George AL Jr, Phillips HA, Saar K, Reis A, Johnson EW, Sutherland GR, Berkovic SF, Mulley JC (1998) **Febrile seizures and generalized epilepsy associated with a mutation in the Na^+-channel beta1 subunit gene SCN1B.** *Nature Genet 19: 366-370.*

Werner FM, Covenas R (2011) **Classical neurotransmitters and neuropeptides involved in generalized epilepsy: a focus on antiepileptic drugs.** *Curr Med Chem 18: 4933-4948.*

Wilde GJ, Pringle AK, Sundstrom LE, Mann DA, Iannotti F (2000) **Attenuation and augmentation of ischaemia-related neuronal death by tumour necrosis factor-alpha in vitro.** *Eur J Neurosc. 12: 3863-3870.*

World Health Organization, International Bureau of Epilepsy & International League Against Epilepsy. (2005) **Atlas Epilepsy Care in the world 2005**.

World Health Organization. (2010) **World Health Organization International Bureau for Epilepsy: Epilepsy in the WHO European region: fostering epilepsy care in Europe**.

World Health Organization (2012) **Fact Sheet n.999**

Xu B, Michalski B, Racine RJ, Fahnestock, M (2004) **The effects of brain-derived neurotrophic factor (BDNF) administration on kindling induction, Trk expression and seizure-related morphological changes.** *Neuroscience 126: 521–531.*

Yang S, Liu ZW, Wen L, Qiao HF, Zhou WX, Zhang YX (2005) **Interleukin-1beta enhances NMDA receptor-mediated current but inhibits excitatory synaptic transmission.** *Brain Res 1034: 172-179.*